**USAAMRDL TECHNICAL REPORT 71-47**

# EVALUATION OF THE UH-1D/H HELICOPTER CRASHWORTHY FUEL SYSTEM IN A CRASH ENVIRONMENT

By

Richard L. Cook
Donald E. Goebel

November 1971

## EUSTIS DIRECTORATE
## U. S. ARMY AIR MOBILITY RESEARCH AND DEVELOPMENT LABORATORY
## FORT EUSTIS, VIRGINIA

CONTRACT DAAJ02-69-C-0030
DYNAMIC SCIENCE ENGINEERING OPERATIONS
A DIVISION OF MARSHALL INDUSTRIES
PHOENIX, ARIZONA



Approved for public release; distribution unlimited.

Best
Available
Copy

## DISCLAIMERS

The findings in this report are not to be construed as an official Department of the Army position unless so designated by other authorized documents.

When Government drawings, specifications, or other data are used for any purpose other than in connection with a definitely related Government procurement operation, the United States Government thereby incurs no responsibility nor any obligation whatsoever; and the fact that the Government may have formulated, furnished, or in any way supplied the said drawings, specifications, or other data is not to be regarded by implication or otherwise as in any manner licensing the holder or any other person or corporation, or conveying any rights or permission, to manufacture, use, or sell any patented invention that may in any way be related thereto.

Trade names cited in this report do not constitute an official endorsement or approval of the use of such commercial hardware or software.

## DISPOSITION INSTRUCTIONS

Destroy this report when no longer needed. Do not return it to the originator.

**DEPARTMENT OF THE ARMY**
**U. S. ARMY AIR MOBILITY RESEARCH & DEVELOPMENT LABORATORY**
**EUSTIS DIRECTORATE**
**FORT EUSTIS, VIRGINIA 23604**

This report was prepared by Dynamic Science (The AvSER Facility), a Division of Marshall Industries, under the terms of Contract DAAJ02-69-C-0030. The technical monitors for this program were Mr. R. E. Bywaters and Mr. H. W. Holland of the Safety and Survivability Division.

The purpose of this effort was to evaluate the effectiveness of the UH-1D/H crashworthy fuel system when subjected to a severe but survivable crash environment. The various components which make up the crashworthy fuel system were previously tested individually to qualify them as crashworthy; however, they had never been tested assembled as a system. Results of the full-scale tests showed that with a few exceptions, the fuel system performed as designed during impacts on irregular terrain.

The conclusions and recommendations contained in this report are concurred in by this Directorate. Further research and development will be continued in an effort to optimize crashworthy fuel systems for Army aircraft.

**Project 1F162203A529**
**Contract DAAJ02-69-C-0030**
**USAAMRDL Technical Report 71-47**
**November 1971**

# EVALUATION OF THE UH-1D/H HELICOPTER CRASHWORTHY FUEL SYSTEM IN A CRASH ENVIRONMENT

Final Report

Dynamic Science 1520-71-15

By

Richard L. Cook
Donald E. Goebel

Prepared by

Dynamic Science Engineering Operations
A Division of Marshall Industries
Phoenix, Arizona

for

EUSTIS DIRECTORATE
U. S. ARMY AIR MOBILITY RESEARCH AND DEVELOPMENT LABORATORY
FORT EUSTIS, VIRGINIA

Unclassified
Security Classification

**DOCUMENT CONTROL DATA - R & D**

(Security classification of title, body of abstract and indexing annotation must be entered when the overall report is classified)

| | |
|---|---|
| 1. ORIGINATING ACTIVITY (Corporate author)<br>Dynamic Science Engineering Operations<br>A Division of Marshall Industries<br>Phoenix, Arizona | 2a. REPORT SECURITY CLASSIFICATION<br>Unclassified<br>2b. GROUP |

3. REPORT TITLE

EVALUATION OF THE UH-1D/H HELICOPTER CRASHWORTHY FUEL SYSTEM IN A CRASH ENVIRONMENT

4. DESCRIPTIVE NOTES (Type of report and inclusive dates)

Final Report

5. AUTHOR(S) (First name, middle initial, last name)

Richard L. Cook
Donald E. Goebel

| | | |
|---|---|---|
| 6. REPORT DATE<br>November 1971 | 7a. TOTAL NO. OF PAGES<br>180 | 7b. NO. OF REFS<br>None |
| 8a. CONTRACT OR GRANT NO.<br>DAAJ02-69-C-0030<br>b. PROJECT NO.<br>1F162203A529<br>c.<br>d. | 9a. ORIGINATOR'S REPORT NUMBER(S)<br>USAAMRDL Technical Report 71-47<br>9b. OTHER REPORT NO(S) (Any other numbers that may be assigned this report)<br>Dynamic Science 1520-71-15 | |

10. DISTRIBUTION STATEMENT

Approved for public release; distribution unlimited.

| | |
|---|---|
| 11. SUPPLEMENTARY NOTES | 12. SPONSORING MILITARY ACTIVITY<br>Eustis Directorate, U. S. Army Air Mobility Research and Development Laboratory, Fort Eustis, Virginia |

13. ABSTRACT

The primary objective of the program was to obtain empirical data to evaluate the effectiveness of the UH-1D/H helicopter crash-resistant fuel system when subjected to a severe but survivable crash environment. These data would reveal any specific weaknesses which still remain in the system that would cause a serious fire hazard. Since the performance of the various system components is the key to the effectiveness of the system, the evaluation of these components was the secondary objective of the program.

The program began with a series of static and dynamic component tests and terminated with three full-scale drop tests. The full-scale tests consisted of one vertical (free fall) drop test and two tests conducted by guiding the vehicle down an inclined cable. The two inclined impact tests not only tested the aircraft fuel system but demonstrated a unique testing procedure which saw its first use in this program.

The results of the full-scale tests showed that, with the exception of a few weak links, the fuel system performs as designed during impacts on irregular terrain. These weaknesses were restricted to ancillary hardware and attachments rather than the fuel tanks themselves. Under most conditions they do not indicate a high probability of catastrophic fire, but, with minor modifications, this hazard potential could be greatly reduced.

DD FORM 1 NOV 65 1473 REPLACES DD FORM 1473, 1 JAN 64, WHICH IS OBSOLETE FOR ARMY USE.

Unclassified
Security Classification

Unclassified

Security Classification

| 14 KEY WORDS | LINK A ROLE | LINK A WT | LINK B ROLE | LINK B WT | LINK C ROLE | LINK C WT |
|---|---|---|---|---|---|---|
| Crashworthy Fuel System | | | | | | |
| UH-1D/H Helicopter | | | | | | |
| Full-Scale Crash Testing | | | | | | |
| Static and Dynamic Component Testing | | | | | | |

Unclassified

Security Classification

12078-71

## SUMMARY

The primary objective of the program was to obtain empirical data to evaluate the effectiveness of the UH-1D/H helicopter crash-resistant fuel system when subjected to a severe but survivable crash environment. These data would reveal any specific weaknesses which still remain in the system that would cause a serious fire hazard. Since the performance of the various system components is the key to the effectiveness of the system, the evaluation of these components was the secondary objective of the program.

The program began with a series of static and dynamic component tests and terminated with three full-scale drop tests. The full-scale tests consisted of one vertical (free fall) drop test and two tests conducted by guiding the vehicle down an inclined cable.

The results of the full-scale tests showed that, with the exception of a few weak links, the fuel system performs as designed during impacts on irregular terrain. These weaknesses were restricted to ancillary hardware and attachments rather than the fuel tanks themselves. Under most conditions they do not indicate a high probability of catastrophic fire, but, with minor modifications, this hazard potential could be greatly reduced.

## CONTENTS

## CONTENTS (CONTD)

CONTENTS (CONTD)

## ILLUSTRATIONS

## ILLUSTRATIONS (CONTD)

## ILLUSTRATIONS (CONTD)

ILLUSTRATIONS (CONTD)

## ILLUSTRATIONS (CONTD)

## ILLUSTRATIONS (CONTD)

## TABLES

## INTRODUCTION

This report documents a test program conducted over the past several years to evaluate the effectiveness of a crashworthy fuel system designed for the UH-1D/H helicopter. The program began with static and dynamic component tests of fuel system hardware, including frangible retainers, self-sealing breakaway valves, check valves, and crash-resistant hose end fittings, and concluded with the full-scale crash testing of two UH-1D/H helicopters equipped with a crashworthy fuel system.

The primary objective of the full-scale tests was to determine the integrity of the UH-1D/H crashworthy fuel system and its components under severe but survivable crash conditions, with secondary importance being given to considerations such as accelerations and structural deformation. To achieve this objective, a plan was formulated and followed that first provided detailed test data on the performance of the various individual components of the fuel system. These component data, after detailed analysis and interactive evaluation, were then compared with system performance data obtained from full-scale crash simulations. After the component and system data comparison, detailed analyses were made to provide ultimate performance characteristics and to identify any latent weaknesses which could negate the overall system effectiveness.

The component tests were conducted both statically and dynamically using standard laboratory testing equipment for the static tests and a drop tower for the dynamic tests.

The first of the three full-scale tests was made by hoisting the helicopter to a predetermined height directly above an impact area and releasing it. The second and third full-scale tests were accomplished by guiding the helicopters down a guide cable stretched taut at a 45-degree incline. Ground protrusions used to test the fuel system in the vertical drop were attached to the bottom of the test vehicle. Protrusions (rocks and stumps) imbedded in the ground provided the surface environment for the inclined impact tests. The test vehicles were instrumented for acceleration and pressure data, and high-speed photographic coverage was used to measure and document the deflections of the system.

After each test, a step-by-step damage analysis on all pertinent parts of the system was made. Photographic records were made of the damaged portions of the fuel system as they were disassembled and analyzed for cause of failure and potential hazard to the total system. All failures were viewed in

the light of their actual or potential hazard, including interaction with such factors as ignition sources and exposure of the occupiable area to a potential fire.

Although only two helicopters were supplied for testing, three tests were conducted because of a malfunction of the mechanism used for the first inclined impact test. Fortunately, the damage incurred on impact did not affect the fuel system, permitting a second test to be made on the same helicopter.

## COMPONENT TESTS

This section summarizes the numerous tests conducted on fuel system components. The test methodology and detailed results are contained in Appendixes I through VI.

Some of the components tested were developmental prototypes and not actual UH-1D/H hardware. Their inclusion in the program was a means of determining critical base performance data in certain areas. The test results are highly relevant to the crashworthiness of the UH-1D/H and other aircraft.

Some of the designs discussed herein possess features which have already been superseded by more efficient designs, brought about by changes recommended earlier during component testing. For the most part, the reader will be edified more by the results of testing certain concepts and principles shown herein than by the details of the configurations themselves.

### HOSE AND HOSE END-FITTING COMBINATIONS

Appendix I presents the methodology and results of a series of static tests conducted on MIL-H-58089 hose and hose end-fitting combinations.

In order to improve the crashworthiness of the UH-1 fluid lines, it was deemed necessary to replace numerous rigid fuel and oil lines with flexible lines conforming to MIL-H-58089. The replacement lines were stainless-steel, braid-covered lines that greatly resist puncture, shear, and tensile forces in an accident. The weak point in the hose assembly is the attachment of the end fitting to the hose, or, in the case of elbow fittings in a bending mode, the fitting itself.

The objective of this series of 81 tests was to determine the failure method(s) and ultimate separation load(s) for various hose and hose end-fitting combinations which had not been previously tested.

### NINETY-DEGREE ELBOW-TYPE TANK-TO-LINE BREAKAWAY VALVE

Appendix II presents the methodology and results of a series of static and dynamic tests conducted on an elbow-type breakaway self-sealing valve.

The objective of this series of 11 tests was to evaluate the functional characteristics of the breakaway self-sealing valve during the loading conditions anticipated in an upper-limit survivable crash of a UH-1D/H helicopter.

TANK-TO-LINE BREAKAWAY VALVES

Appendix III presents the methodology and results of static and dynamic tests on tank interconnects and tank-to-line connectors.

The objective of this series of five tests was to evaluate the crashworthy functional characteristics of a cell-to-line self-sealing valve during the most likely loading conditions anticipated in an upper-limit survivable crash.

CHECK VALVES

Appendix IV presents the methodology and results of a series of static and dynamic tests conducted on two sizes of check valves supplied by one manufacturer and one size of check valve supplied by another manufacturer. The valves were being considered for use at locations where the auxiliary systems join the main fuel system and at a position inside the tanks of the UH-1B and C helicopters.

The objective of the series of 12 tests was to determine: (1) the strength of the valves, (2) the manner of failure of the valves or their attached components, and (3) the performance of the valves under loading representative of the crash environment.

FRANGIBLE RETAINERS

Appendix V presents the methodology and results of a series of dynamic tests performed on frangible retainers proposed for use in attaching fuel cells to airframe structure. Figure 1 shows a typical design before and after dynamic testing. The frangible action is obtained by bending of the clips and/or failure of the rivets.

The objective of this series of 19 tests was to evaluate the functional characteristics of the frangible retainers under dynamic test conditions. The dynamic tests were designed to subject the retainers to what were estimated to be the three most extreme loading conditions experienced during actual crash conditions.

SOCKET-HEAD FRANGIBLE SCREWS

Appendix VI presents the methodology and results of a series of static tests performed on frangible screws. The UH-1 retrofit program created a requirement for a frangible method of attaching the fuel cells to the airframe structure to reduce

Figure 1. Frangible Retainer Before and After Testing (Bending Load Application).

the loading on the fuel cell in the crash environment. One method of providing this feature utilizes frangible aluminum screws which will break under crash loading and release the tank and fitting from the aircraft structure.

Earlier frangible screw concepts utilized a hexagonal bolt head which was very susceptible to mishandling due to excessive torque application or confusion with standard steel bolts. For this reason, a frangible screw incorporating a socket head was designed and tested.

The objective of this series of 26 tests was to evaluate the functional characteristics of socket-head frangible screws.

## DESCRIPTION OF FULL-SCALE TEST VEHICLES (UH-1D/H HELICOPTERS)

Three full-scale tests were conducted using two refurbished UH-1D/H helicopters equipped with the crashworthy fuel system.

The UH-1D helicopter used in this test program was equipped with a crashworthy fuel system consisting of five interconnected cells that act as a single tank with a total capacity of 209 gallons.

All of the fuel tanks and tank outlets are of crash-resistant construction and meet the requirements of MIL-T-27422B. For additional protection against localized impact, the system is equipped with self-sealing breakaway valves at its most vulnerable points. Crash-resistant fuel lines and in-line breakaway valves have also been added to reduce the risk of line separation. Frangible connectors are used on the tank-to-structure interfaces to prevent excessive loads on the tank wall during a crash. Figures 2 and 3 show the differences between the standard and modified UH-1D/H fuel systems.

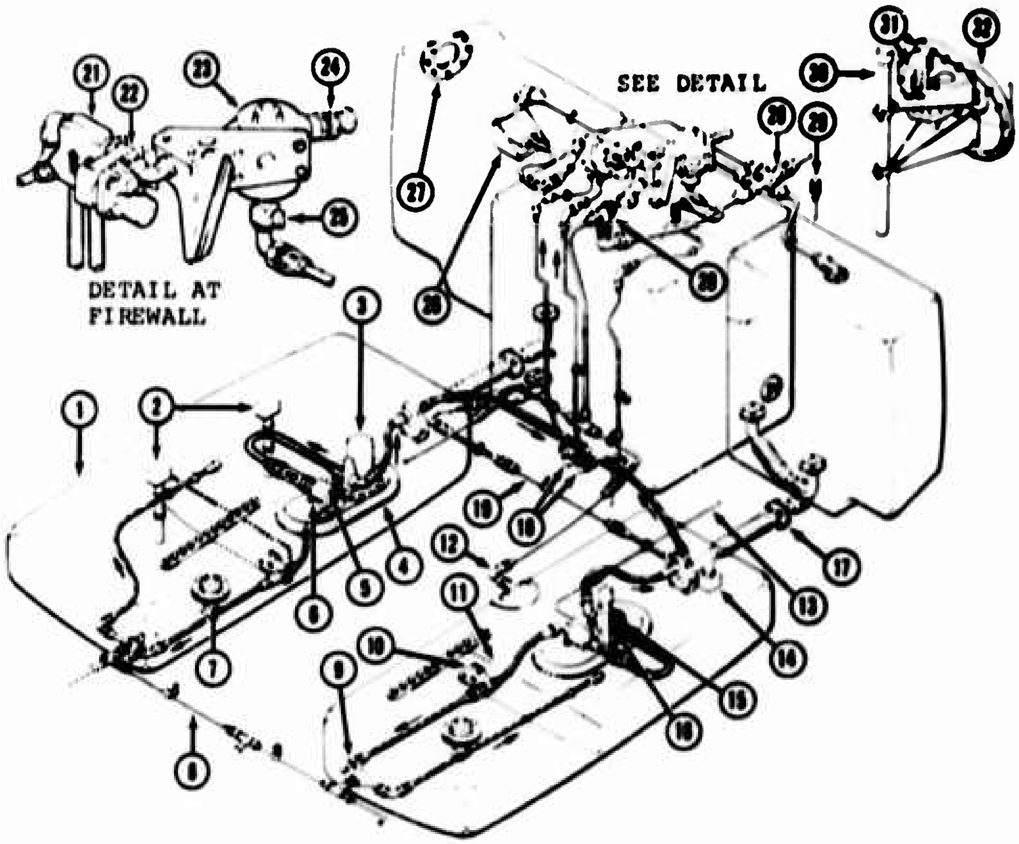


1. Forward Cell
2. Fuel Quantity Transmitters
3. Electric Boost Pump
4. Sump Assembly
5. Flow Switch with Check Valve
6. Sump Drain Valve
7. Drain Valve
8. Crossfeed Line
9. Ejector Pump
10. Flapper Valve
11. Baffle
12. Vent Line
13. Bleed Air Line from Engine
14. Defuel Valve
15. Air Driven Boost Pump
16. Float Switch
17. Crossovers
18. Fuel Lines - Tanks to Valve Manifold
19. Crossfeed Line
20. Siphon Breaker Valve
21. Check Valve Manifold
22. Fuel Shut-off Valve
23. Main Fuel Strainer
24. Coupling for Engine Fuel Hose
25. Strainer Drain Valve
26. Pressure Gage Transmitter
27. Filler Cap
28. Vent Manifold
29. Fuel Control Vent Line
30. Fuel Quantity Transmitter
31. Float Switches - Auxiliary Fuel Transfer Pump Control
32. Center Cell Access Door

**Figure 2. UH-1D/H Standard Fuel System.**

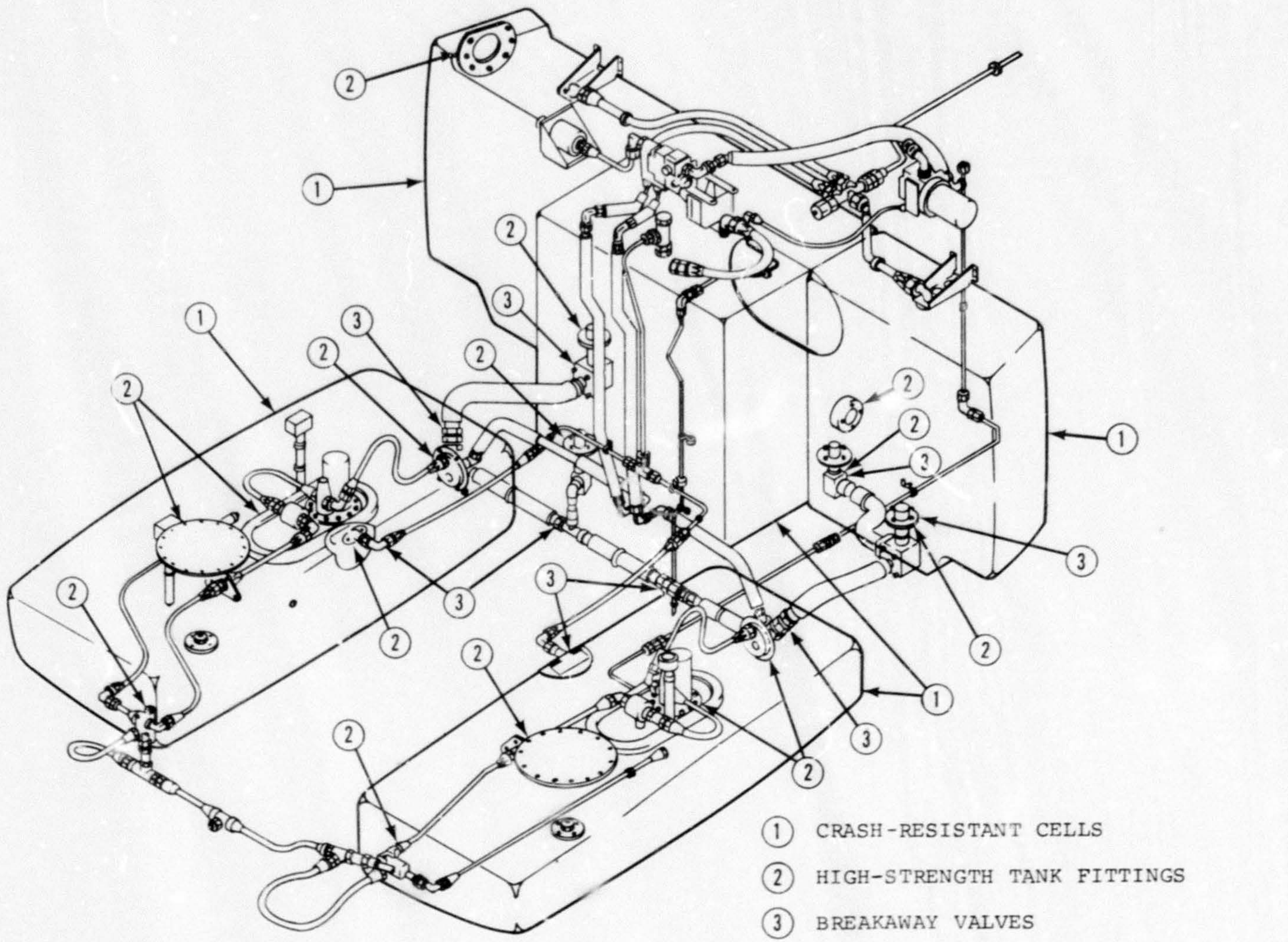


Figure 3. Modified UH-1D/H Fuel System.

## FULL-SCALE TESTS

The full-scale tests are detailed in this section in the order in which they were conducted. For discussion purposes, each test is referred to by number:

Test 1 is the vertical drop test.

Test 2 is the first inclined impact test.

Test 3 is the second inclined impact test.

(These were Tests T-35, T-36, and T-37 respectively in the U. S. Army test series conducted by Dynamic Science.)

### TEST 1 OBJECTIVES/DETERMINATIONS

The specific objectives/determinations of this test were as follows:

1. General integrity of the fuel system.
2. Puncture resistance of the fuel cells from concentrated loads.
3. Integrity of the fuel tank fittings.
4. Acceleration at key points in the system.
5. Ability of the breakaway valves and frangible fittings to function under various types of loading.
6. Ability of the hoses to cope with tank deformation without breaking.
7. Pressure transients in the fuel tank.

### TEST 1 HELICOPTER PREPARATIONS

The UH-1D/H helicopter used as the test vehicle is shown in Figure 4.

#### Fuselage

The helicopter had previously sustained damage to the forward fuselage structure and in the area surrounding the transmission. This damage was repaired to the extent that a simulated transmission could be mounted in the aircraft and actual gross weight could be simulated. Ballast was added to duplicate the

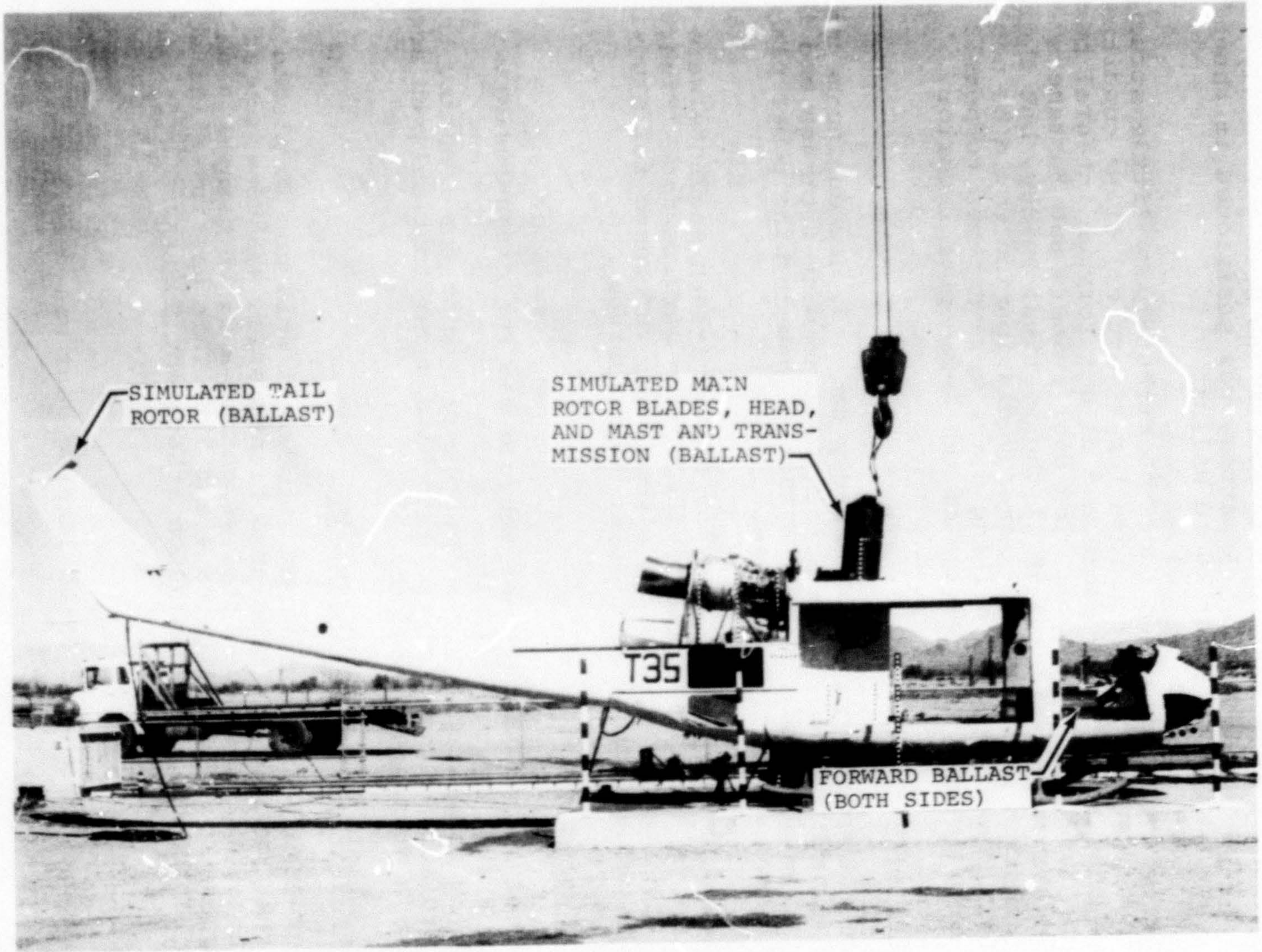


Figure 4. Test 1 Helicopter.

mass of a UH-1D/H tail boom, tail rotor assembly, and forward areas (Figure 4).

All avionics and electronic equipment had been previously removed from the aircraft. A battery was positioned in the aft fuselage compartment for added ballast.

The crew doors and cargo doors contribute very little structural strength to the fuselage for a vertical crash condition, since they are sliding doors and do not form an integral part of the fuselage structure. The door runners and fasteners would absorb a small amount of the vertical energy, but their contribution to the overall energy dissipation would be negligible. Therefore, the sliding doors were omitted to permit better photographic coverage of the helicopter interior.

Power Plant

Since the engine mounts were badly damaged, new engine mounts were fabricated using the original attachment fittings and the same type of steel tubing. A T53-L-1 gas-turbine power plant was installed on these mounts.

Three small stadia poles marked off in 1-inch segments were installed on the right side of the engine service deck (Figure 5). These poles provided a dimensional reference for studying engine deflection in high-speed film footage.

Fuel System

The fuel system in the test vehicle was the crash-resistant UH-1D/H fuel system described in the previous section. No repairs or modifications were necessary except for adapting the forward access cover of the left-hand underfloor cell to accommodate a pressure transducer.

Transmission and Rotor Assembly

The UH-1D/H transmission and rotor mast were not furnished with the test vehicle. A simulated transmission was constructed and ballasted to match the total weight of a UH-1D transmission and rotor assembly (see Figures 4 and 5). This was installed at the four standard transmission attachment points.

Landing Gear

A standard, undamaged UH-1D landing gear was used.

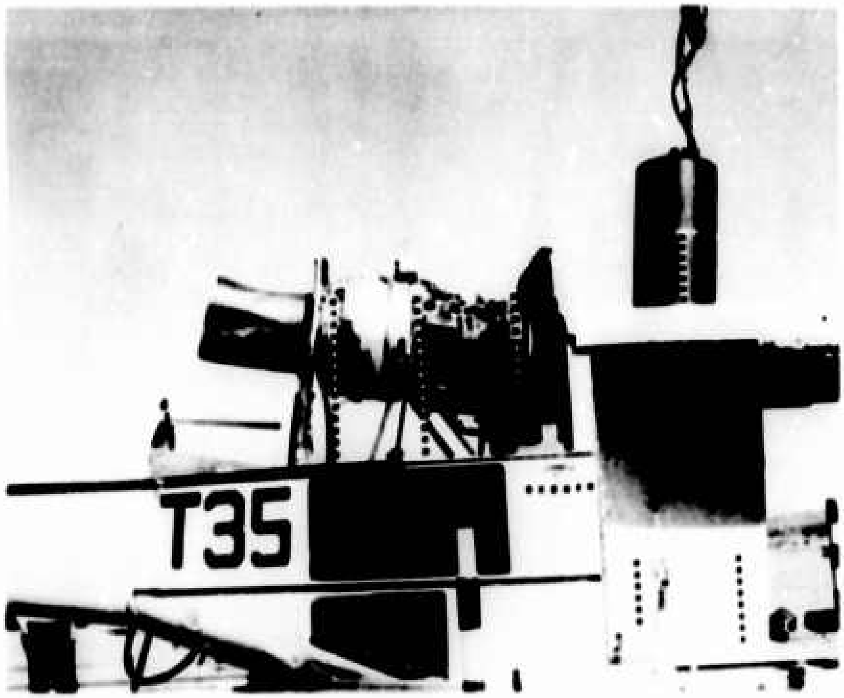


Figure 5. Stadia Pole Installation on Engine Service Deck (Test 1).

## Ground Protuberances

Simulated ground protuberances were attached to the bottom of the aircraft by means of straps and cables. These were located beneath vulnerable points of the fuel system as shown in Figure 6. The left forward stump was intended to impact the underfloor cell so that it would be displaced upward and load all the attachment points. The left rear stump was placed to strike the left inlet/outlet fitting, valve, and boost line outlet. The right-rear stump was intended to load the right-hand cell-to-cell interconnect fitting and the right-hand drain valve. A boulder was placed under the right-hand boost pump and another under the forward cross-feed line for direct loading of these components.

## Left-Hand Drain Valve Illumination

The compartment which housed the left-hand drain valve was equipped with a 1-3/4-second long-duration flash bulb to illuminate the separation sequence that was expected to occur when the stump impacted the forward end of the line connected

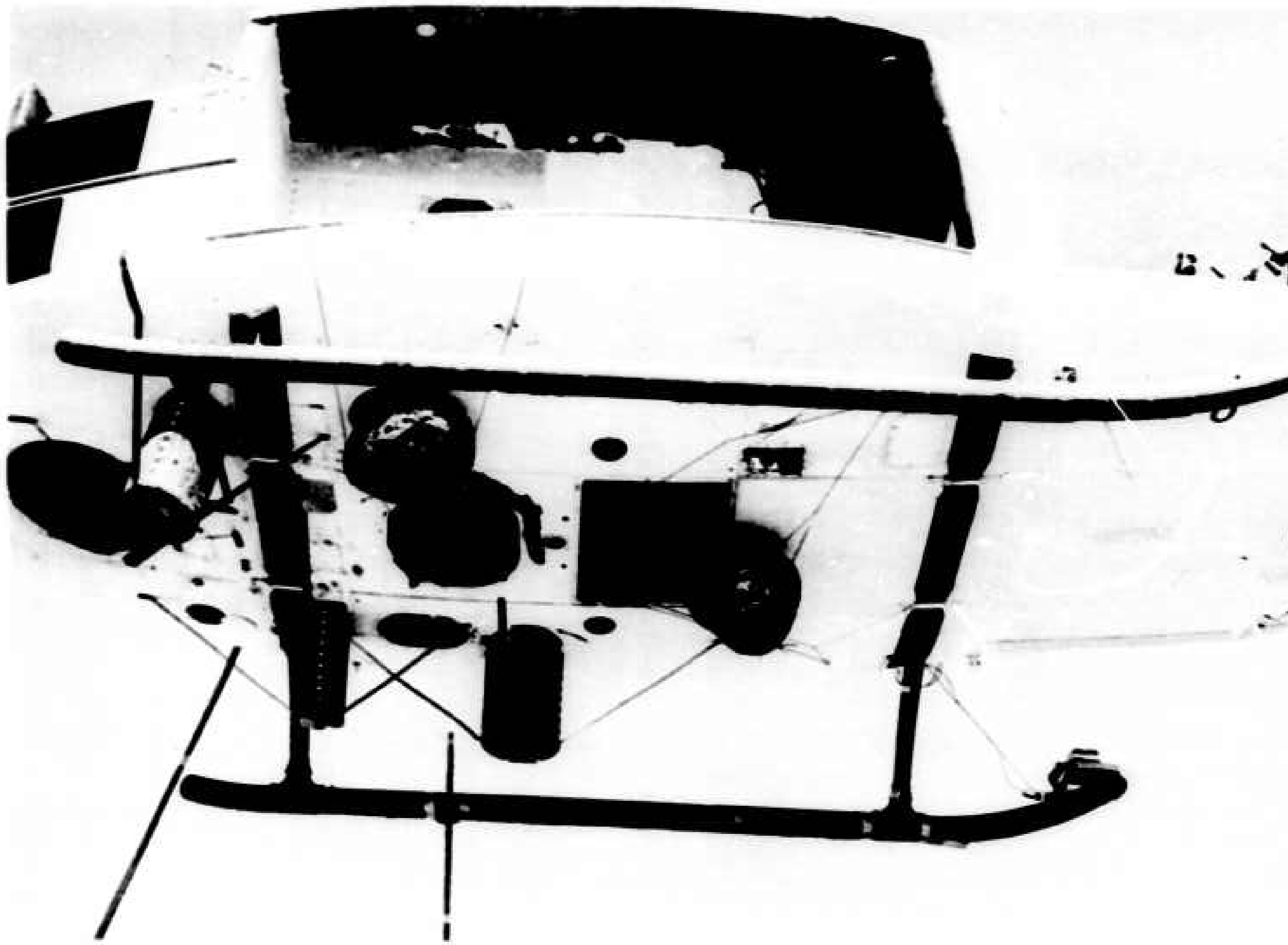

Figure 6. On-Vehicle Ground Protuberances Installation (Test 1).

to this valve. A ground impact switch was constructed to make contact 4 feet above the skid impact point. This would permit the bulb to fire early and reach maximum illumination prior to the separation sequence.

### Painting and Identification

The entire exterior and certain portions of the cabin of the test vehicle were painted a flat light yellow. The left-hand vertical cell drain valve compartment and the compartment which housed the left-hand inlet/outlet breakaway fitting were painted white to give better reflectance and contrast to the valves and the stump.

### Weight and Balance

The test vehicle was weighed after all components, equipment, simulated fuel, and instrumentation had been added. It weighed 7,200 pounds at the time of the test. This included the ballast added to bring the gross weight up to the desired amount and to balance the aircraft at the correct impact attitude.

## TEST 1 FACILITY PREPARATION

### Impact Pad

The 15-foot x 25-foot x 1-foot reinforced concrete pad shown in Figure 4 was used as the impact surface for the test vehicle. This impact surface was chosen because it closely represents the infinitely rigid impact surface used in the computer simulation described in USAAVLABS Technical Report 70-71, "Analysis of Helicopter Structural Crashworthiness", dated January 1971.

### Stadia Poles

Six stadia poles marked off in 6-inch segments were located on the concrete pad as shown in Figure 7. These poles provided a dimensional reference for the ground-mounted high-speed cameras at time of impact.

### Camera Stands

Camera stands were installed at nine locations around the impact area to provide mounts for the high-speed cameras (see Figure 7). Two of these were placed close to the helicopter at angles calculated to show the separation sequence of the left-hand inlet/outlet breakaway valve and the left-hand vertical drain valve (Figure 8).

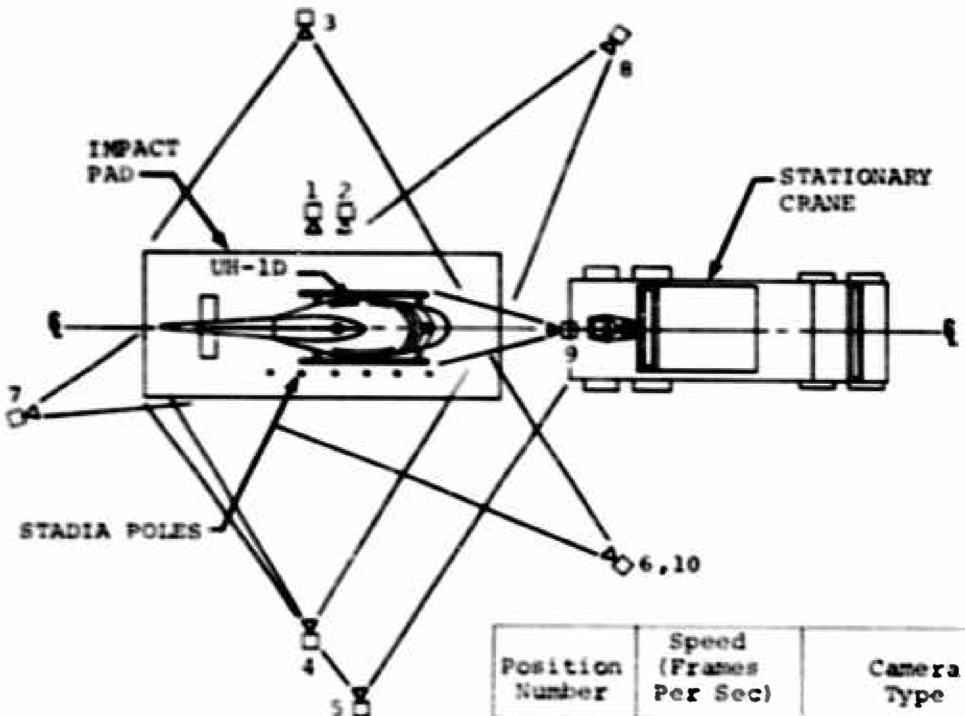


| Position Number | Speed (Frames Per Sec) | Camera Type | Coverage |
|---|---|---|---|
| 1 | 1000 | Photosonic | Closeup - Port Side |
| 2 | 1000 | 1B | Closeup - Port Side |
| 3 | 1000 | 1B | Overall - Stbd. Side |
| 4 | 1000 | 1B | Overall - Stbd. Side |
| 5 | 1000 | 1B | Overall - Front |
| 6 | 1000 | 1B | Quarter - Front, Stbd. |
| 7 | 1000 | 1B | Quarter - Rear, Stbd. |
| 8 | 1000 | 1B | Quarter - Front, Port |
| 9 | 1000 | 1B | Closeup - Straight On |
| 10 | 24 | Bolex | Tracking |

Figure 7. Camera Layout (Test 1).

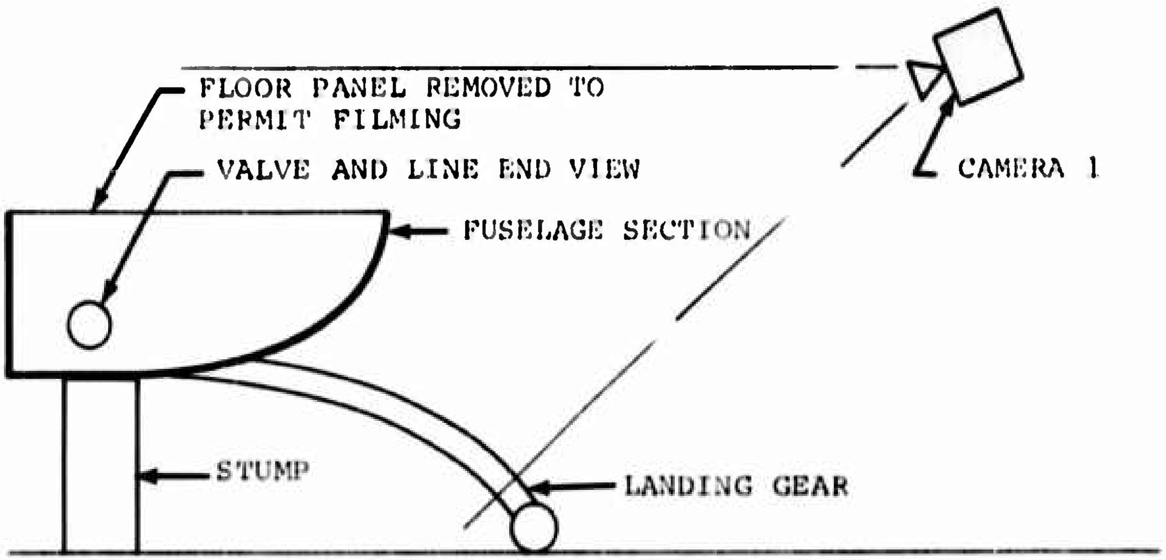


Camera Viewpoint for Inlet/Outlet Breakaway Valve

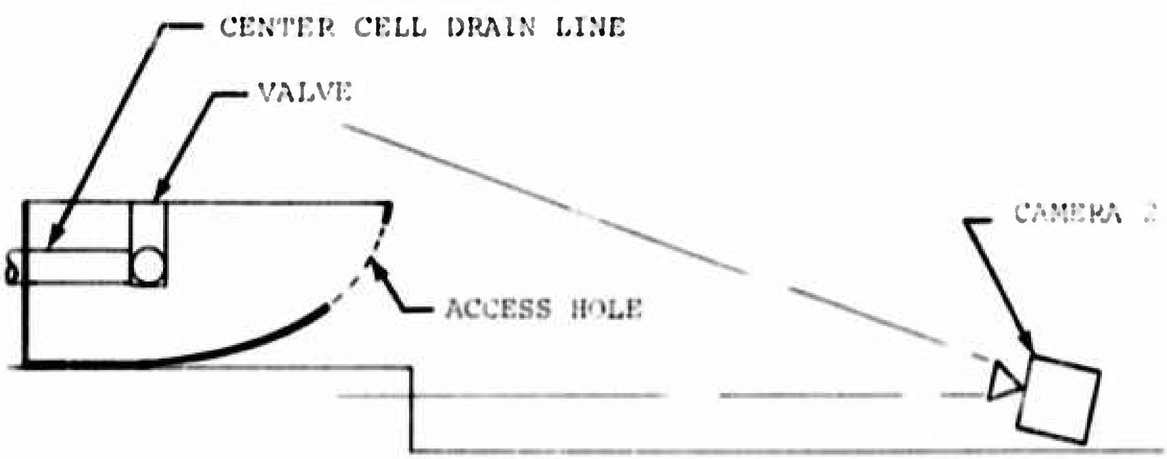


Camera Viewpoint for Left Vertical Cell Drain Valve

Figure 8. Camera Layout for Breakaway Valve Coverage (Test 1).

## Ground Lines and Batteries

A wiring network of ground lines and batteries was put into position to insure the proper sequencing and operation of all high-speed cameras.

### Stabilizing Ropes

Two 1/4-inch nylon ropes were attached to the tail boom skid of the test vehicle. These ropes prevented lateral rotation of the test vehicle prior to and during hook release.

### Release Mechanism

A pneumatic release mechanism was used on this drop test that had been used successfully on numerous full-scale and component tests.

## TEST 1 INSTRUMENTATION

### On-Board Data Acquisition System

Accelerometers were placed at various locations on board the helicopter to record accelerations during the impact sequence. The relative locations of the metal-encased instruments are shown in Figure 9. A typical installation is shown in Figure 10. The accelerometer outputs were fed individually to a central junction box mounted at the rear of the test vehicle cargo area. In addition to the accelerometers, one pressure transducer was placed in the forward access opening of the left-hand underfloor cell.

### Impact-Sensitive Switch and Correlation Lights

An impact-sensitive switch was mounted near the forward end of the left landing skid. This switch completed an electrical circuit on impact that fired a flash bulb mounted on top of the engine accelerometer for camera correlation and provided an electrical signal to correlate the data that were recorded on the FM/FM multiplex tape recorder.

### Umbilical Cable

A 50-foot-long umbilical cable fed the output of all instrumentation to the signal conditioning equipment in an instrumentation trailer located near the test site.

### Signal Conditioning and Recording Equipment

The outputs from the accelerometers were fed into signal conditioning equipment that provided for balancing and controlling of the outputs. The conditioned signal was then fed into individual voltage-controlled oscillators. This voltage varied the frequency of the oscillators in proportion to the G-forces acting on the accelerometers. The output of the

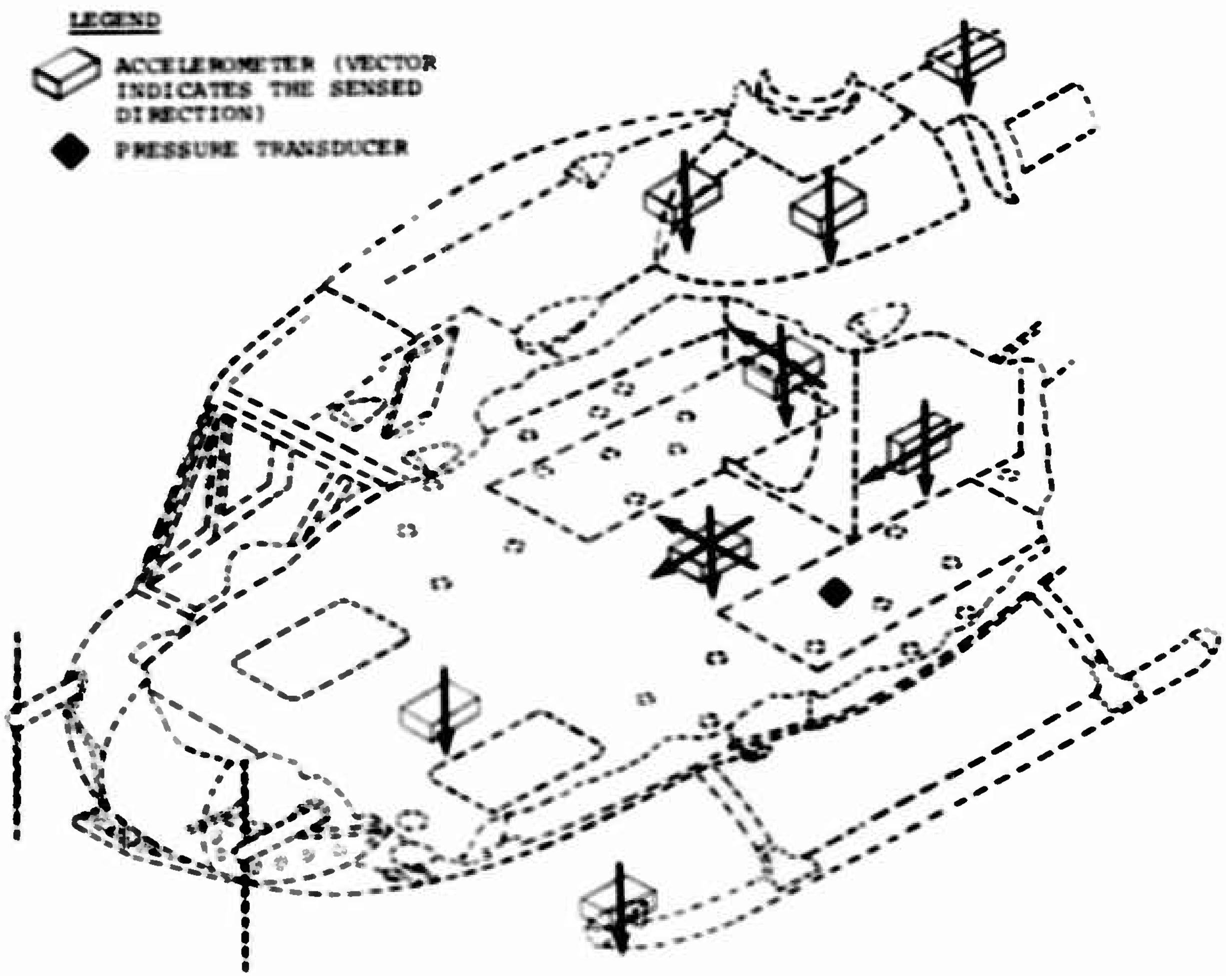


Figure 9. Instrumentation Installation.

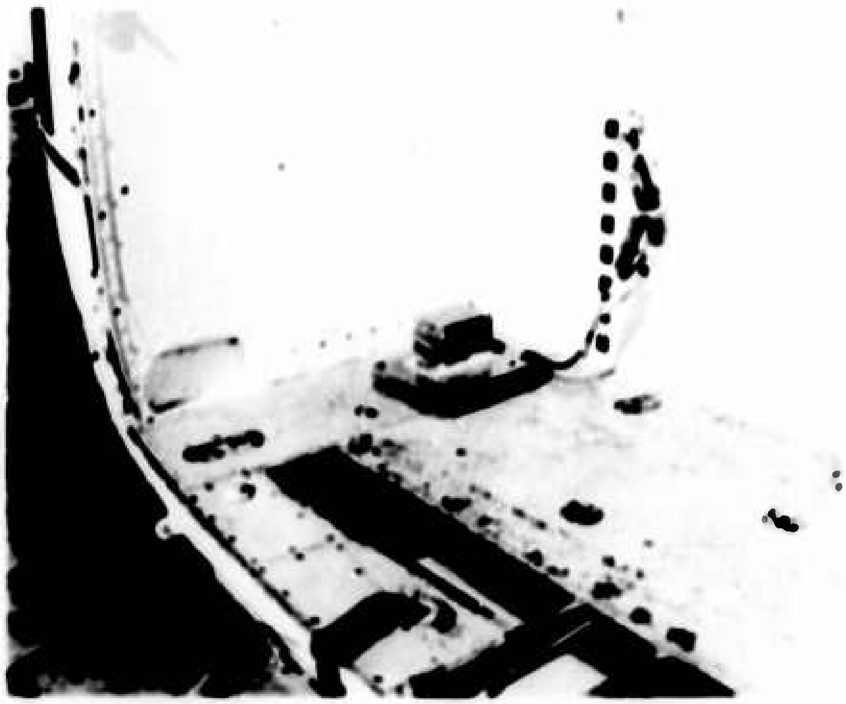

Figure 10. Typical Accelerometer Installation.

voltage-controlled oscillators was amplified and recorded on magnetic tape.

An FM tape recorder operating at a tape speed of 60 in./sec and capable of handling up to 25 channels of data was used to record the signals from the instrumentation.

## FM Tape Playback

A data tape equipped with filters and discriminators was used to reproduce the analog data from the test tape.

## TEST 1 PHOTOGRAPHY

### Motion Photographic Coverage

High-speed (1000 frames per second) color film coverage of the helicopter drop sequence was provided from the nine locations shown in Figure 7 to record the kinematics of the test items in the time interval between hook release and for several seconds following the completion of action after impact.

Color documentary coverage (24 frames per second) of the drop sequence was also provided.

### Still Photographic Coverage

Black and white 4- x 5-inch photographs and 35mm slides were taken of the test vehicle and experiments before and after the test. These included general overall views of the helicopter and test site as well as detailed close-ups of the test articles during installation and during posttest investigation and disassembly.

## TEST 1 TARGET CRASH CONDITIONS AND FINAL PREPARATION

### Target Crash Conditions

The target crash conditions at impact were as follows:

- Drop Height - 30 Feet (measured from skid)
- Vertical Velocity - 44 Feet Per Second
- Longitudinal Velocity - 0 Feet Per Second
- Lateral Velocity - 0 Feet Per Second
- Flight Path Angle - 90 Degrees
- Resultant Flight Path Velocity - 44 Feet Per Second
- Pitch Angle - ±3 Degrees
- Roll Angle - ±3 Degrees
- Test Weight - 7,200 Pounds

### Final Preparations

The test vehicle was positioned on the impact pad. The fuel tanks were filled with 165 gallons of dyed water to simulate the weight of a UH-1D/H's normal servicing of 209 gallons of JP-4 fuel.

The high-speed cameras and associated wiring were placed in position. The umbilical cable was attached to the test vehicle and the instrumentation was made ready.

A mobile crane equipped with a 70-foot boom was used to lift the helicopter. Prior to lifting, a 0- to 10,000-pound load

cell was installed between the crane hook and the attachment point on the test vehicle. Final ballast adjustments were made to obtain the gross drop weight of 7,200 pounds.

The roll and static pitch angles were then checked and found to be 0 and 3 degrees, respectively.

The ground stadia poles were placed in position, and final instrumentation and camera adjustments were made. After a final check-out of all systems, the test vehicle was raised to a height of 30 feet and released.

## RESULTS OF TEST 1

### Impact Attitude

The impact attitude of the test vehicle was approximately the same as the release attitude: 2 degrees nose-down pitch and 0 degrees roll. No appreciable energy appeared to be absorbed during the descending aircraft's envelopment of the rocks and stumps. The floor panels above both underfloor cells were torn free of the structure, and the entire nose section was ruptured and settled on the pad as shown in Figure 11. The tail section also yielded and partially separated from the main fuselage section as shown in Figure 12.

### Transmission

The transmission deflected downward 3 inches at the base and approximately 4 inches forward at the point of exit from the top of the fuselage. The downward force of the transmission induced failure of the right side panel of the transmission housing, causing the entire housing to shift downward about 4-1/2 inches relative to the floor as shown in Figures 13 and 14.

### Engine

The engine broke free of the right engine mount when the trunnion bolt sheared. This allowed the engine to roll onto its right side on the service deck (Figure 15). Both left and right engine mounts buckled, the left side more than the right. Both fuel hoses, firewall-to-filter and filter-to-engine, remained intact, although the left forward link put a slight crimp in the filter-to-engine hose.

### Floor Deformation

Both floor panels above the underfloor cells were broken free of the structure and deflected upward by the localized impact

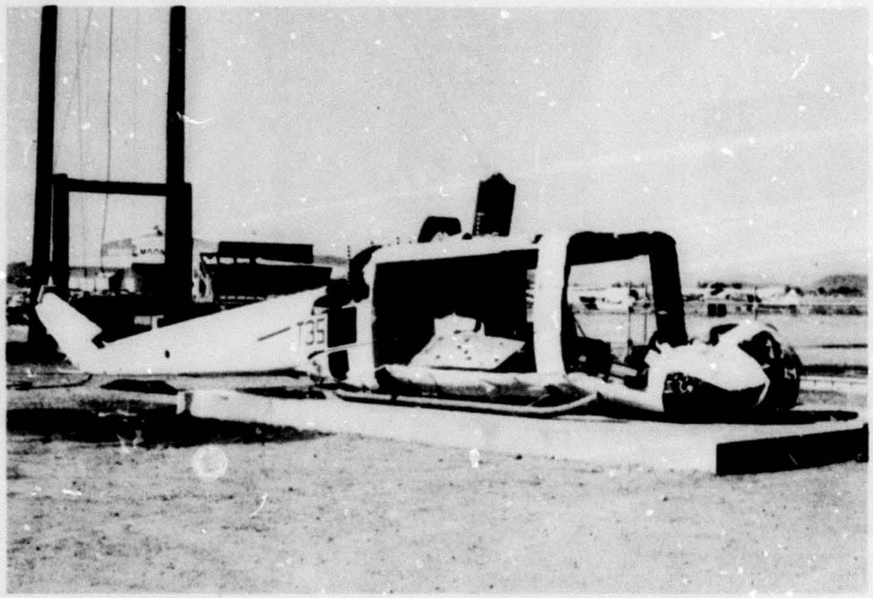

Figure 11. Fuselage Deflection - Front and Right Side (Test 1).

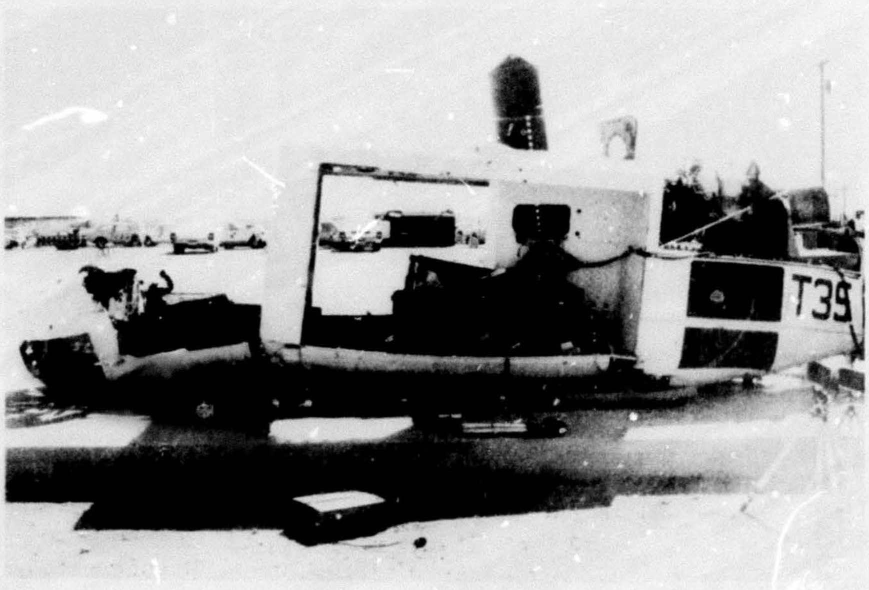


Figure 12. Fuselage Deflection - Left Side (Test 1).

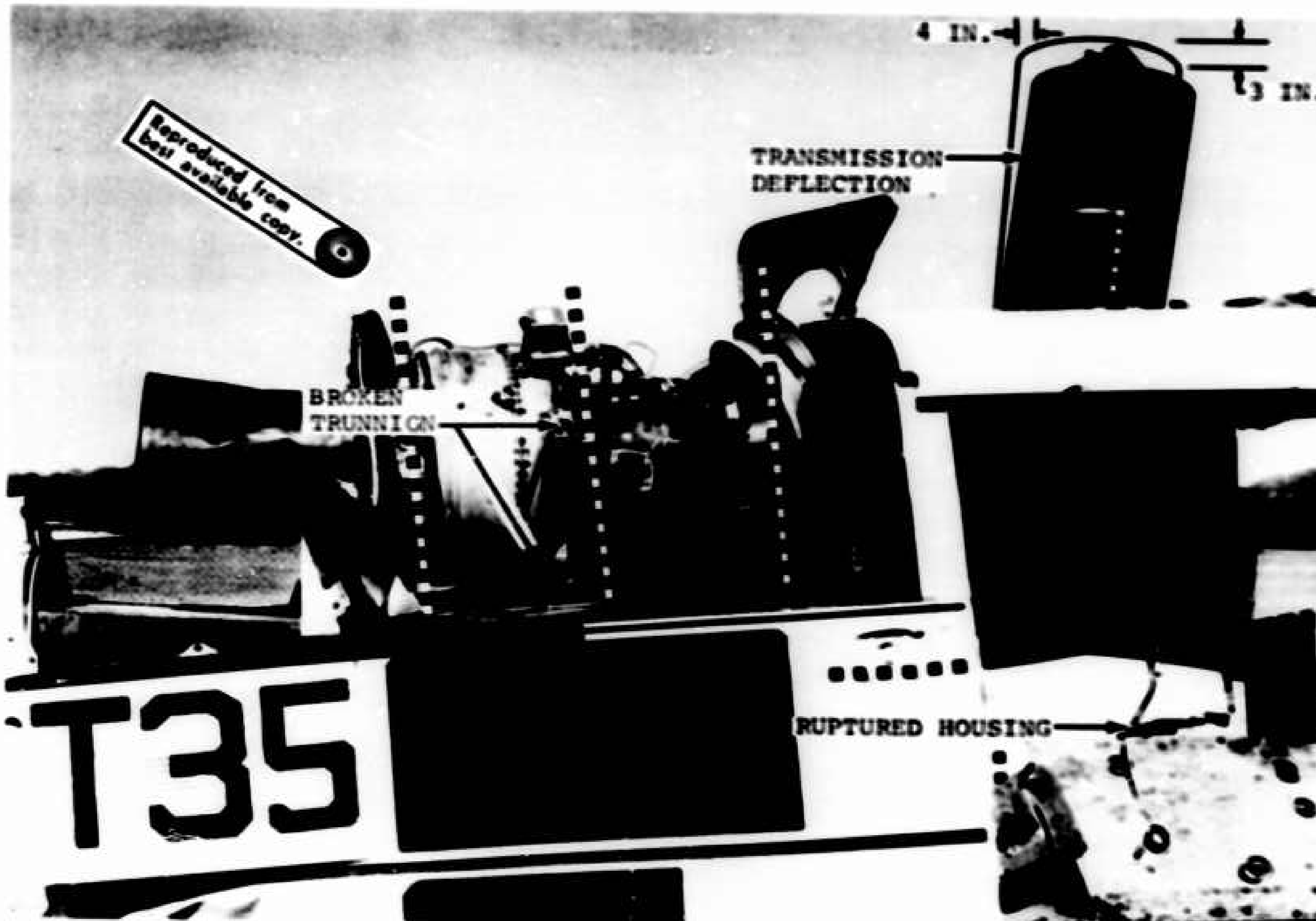


Figure 13. Engine and Transmission Deflection (Test 1).

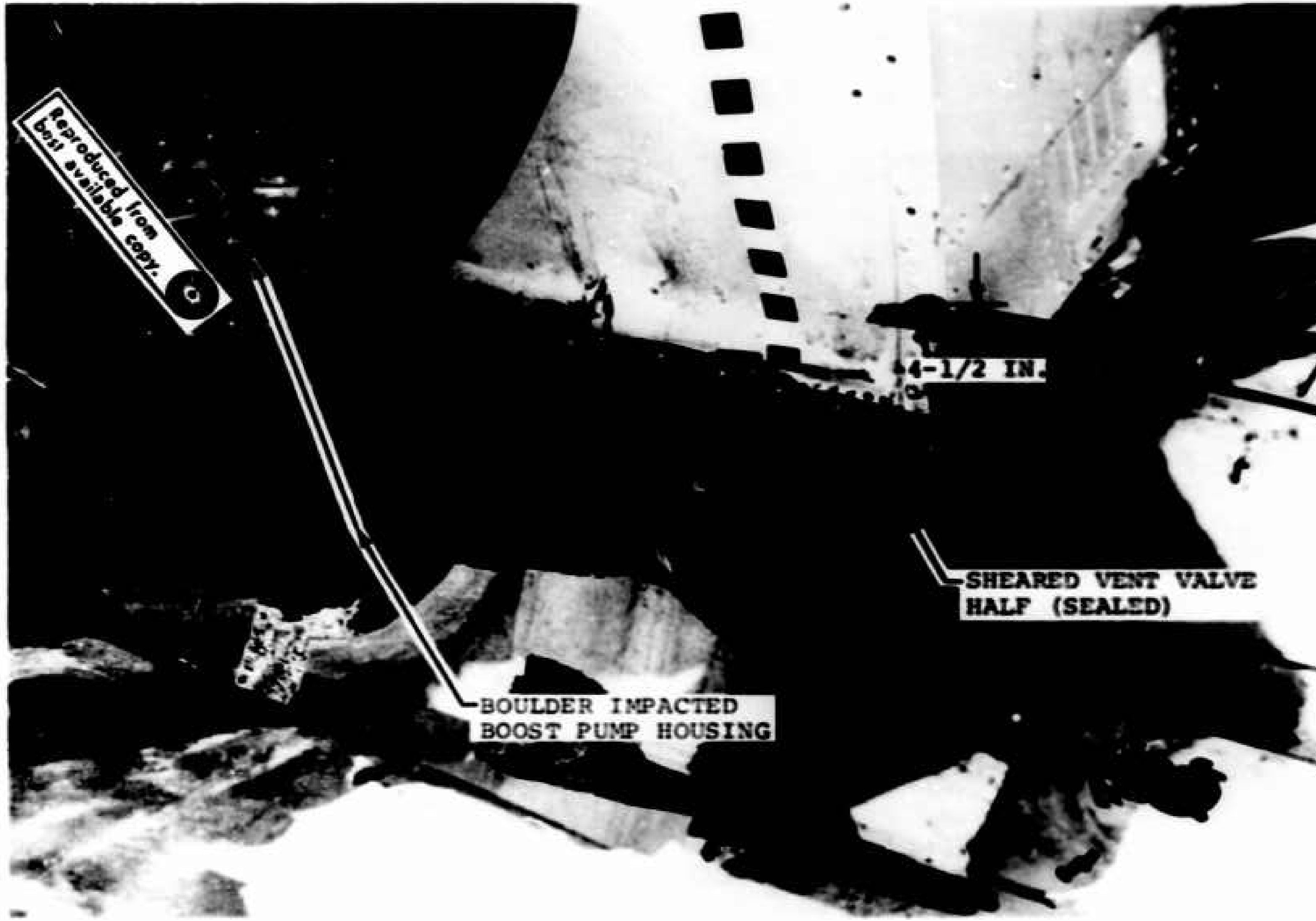




Figure 14. Transmission Housing Deflection (Test 1).

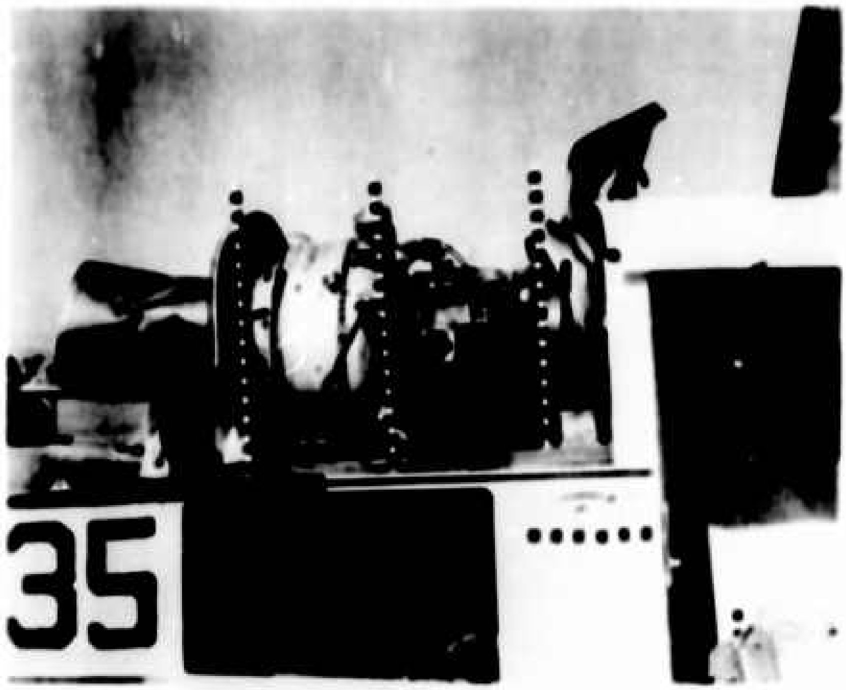

Figure 15. Posttest Position of Engine (Test 1).

on the rock and stump. The right panel was still held in place along its right side, and the left panel also held by its right side as shown in Figure 16.

## TEST 1 FUEL SYSTEM DAMAGE ASSESSMENT

### Left-Hand Underfloor Fuel Cell

The stump under the center of the left-hand underfloor fuel cell pushed the cell upward, in turn lifting the deck panel as just discussed. The tank wrapped itself partially around the stump, and the stump pushed outward slightly so that the full shear load of the stump acting on the tank and fittings was somewhat dissipated (Figure 16). This allowed the tie-bolt linking the forward end of the tank to the structure to remain in place. The vent valve, also located on the inboard side of the cell, was sheared and both halves sealed (Figure 14). The forward cross-feed exiting the tank through the bulkhead was extended almost to its limit but was not broken at the point of exit from the tank (Figure 17). The extra length of hose in this location appears to have been sufficient to cope with


Figure 16. Left-Hand Underfloor Fuel Cell Deflection (Test 1).

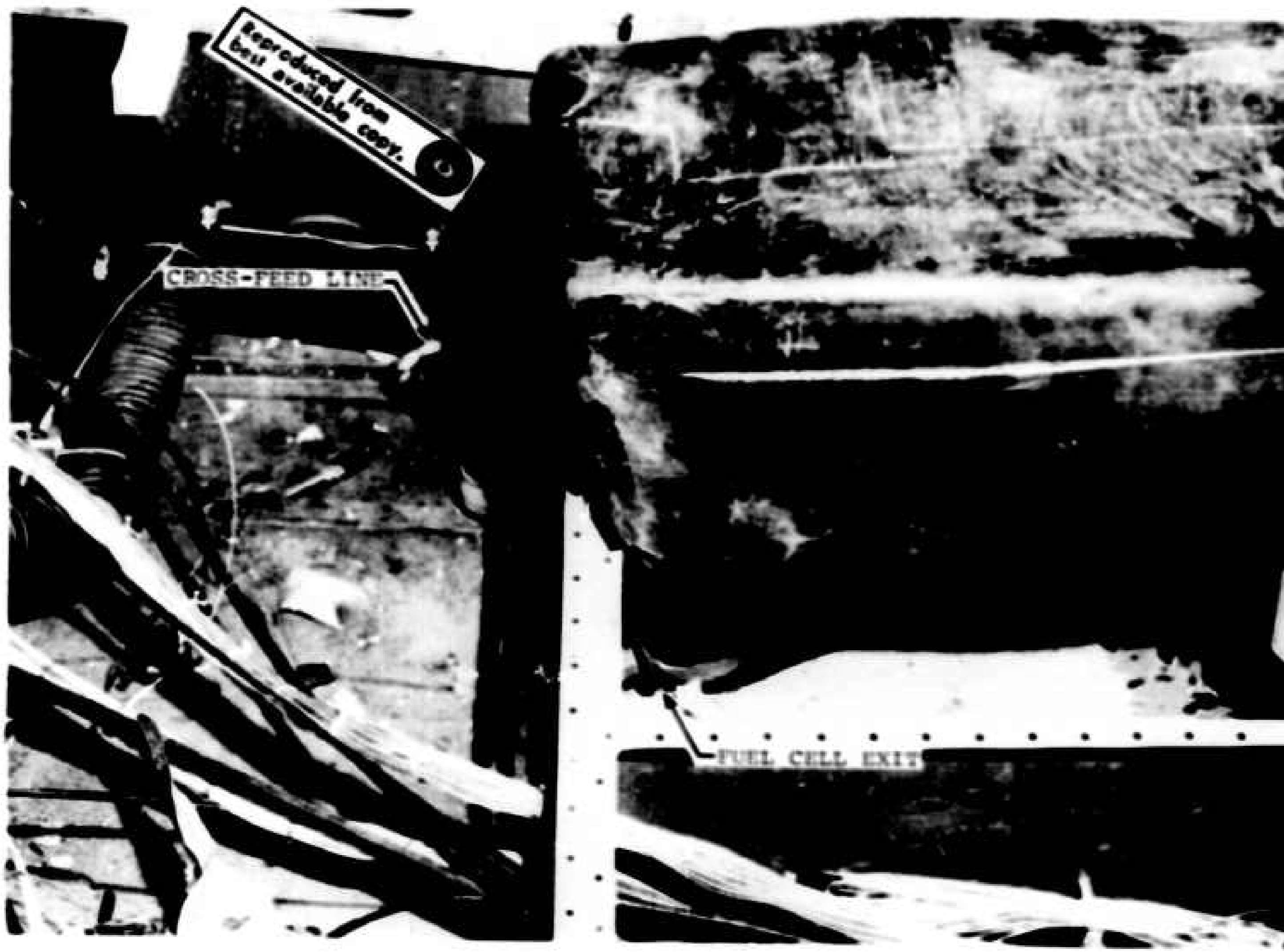



Figure 17. Left-Hand Forward Cross-Feed Line (Test 1).

tank deformation of the type experienced. The inlet/outlet fitting remained intact despite the fact that it received a direct impact from a stump (Figure 18). The inlet/outlet breakaway valve functioned, but the half which was mounted in the tank fitting lost part of the seal boot and was leaking approximately 1/2 gallon per minute immediately after the crash. The aft cross-feed line exiting the left-hand underfloor cell remained intact, but only because the stump impact on the inlet/outlet fitting applied a hard enough load on the cross-feed line to separate it at the breakaway valve and pull it through the hole in the buttline 14 keel before that member collapsed. Postcrash observation showed this hole to be completely closed. This would have made the probability of retaining the line at its outlet very low.

The boost line outlet from this same point failed as indicated in Figure 19. This could be expected when considering the amount of cell deflection and the fact that the boost line had no slack (as does the forward crossover) or breakaway valve. The boost pump plate was intact, but some leakage resulted from the drain valve which was opened on impact by the left forward stump. The force of the impact apparently depressed the valve and rotated it to a full ON position. The leakage from this point amounted to less than a gallon per minute (Figure 16).

Figure 20 is a general illustration summarizing the spillage and potential spillage from the system.

Right Underfloor Tank

Like the left-hand tank, the right-hand tank sustained the impact without any noticeable damage to the tank itself. The rock directly under the boost pump broke the boost pump fitting in four places and cracked the base of the boost pump in three places (Figure 21). Fluid loss as a result of the damage was estimated at 2 to 4 quarts per minute. The vent valve in this cell also sheared off during the impact and both halves closed completely. The forward tie-down bolt was pulled out of the structure and remained in the tank wall. The forward cross-feed tube outlet remained in place and showed no extensive deformation in the tank area.

The aft inlet/outlet fitting was broken around the perimeter of the case housing (Figure 22). This liberated large quantities of fluid, estimated at 15 to 25 gallons per minute. The breakaway valve in the inlet/outlet fitting functioned. Both the boost line and the cross-feed line were pulled out of their fittings in the inlet/outlet fitting.

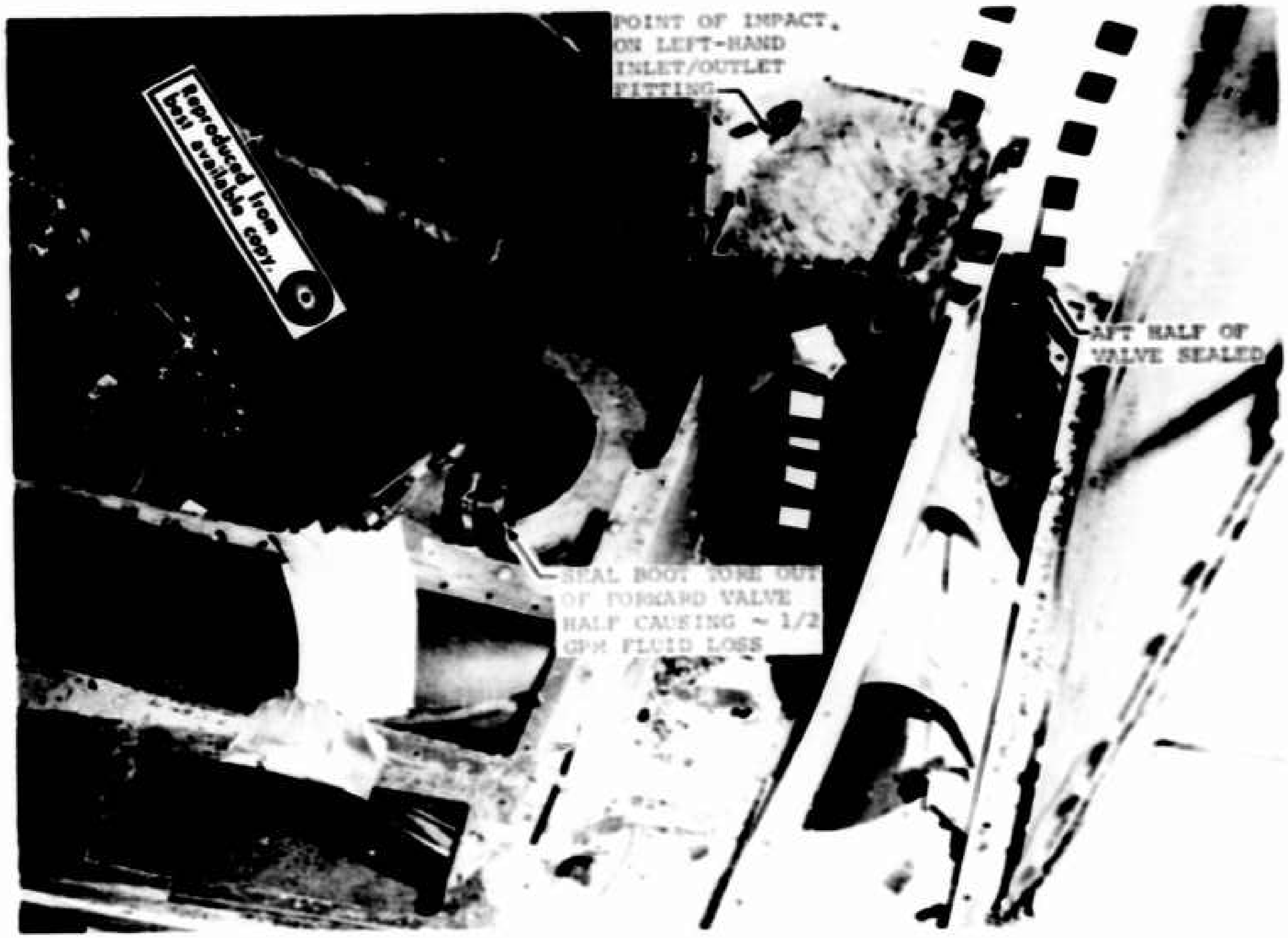


Figure 16. Stump Impact On Left-Hand Inlet/Outlet Fitting (Test 1).

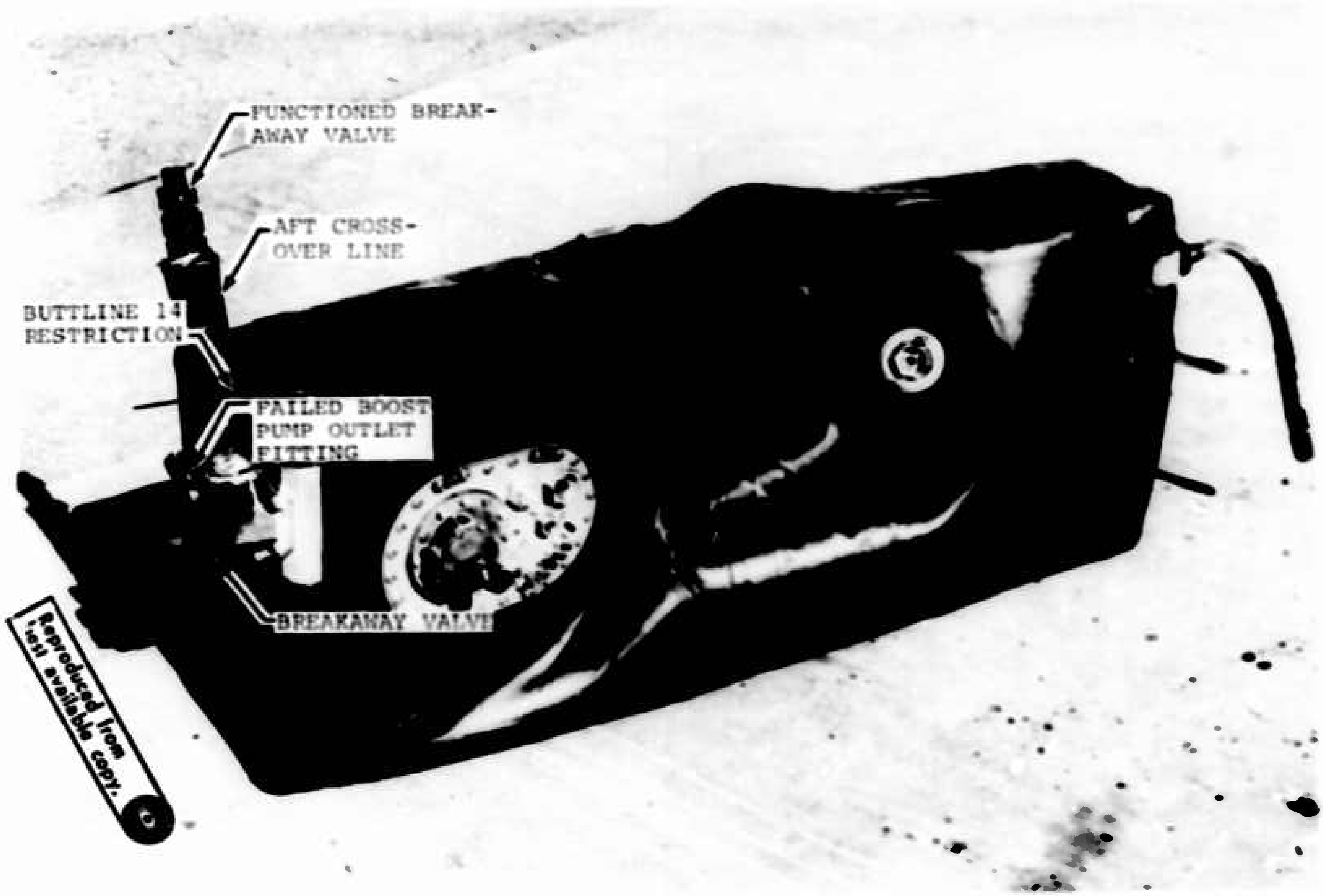


Figure 19. Aft View of Left-Hand Underfloor Cell (Test 1).

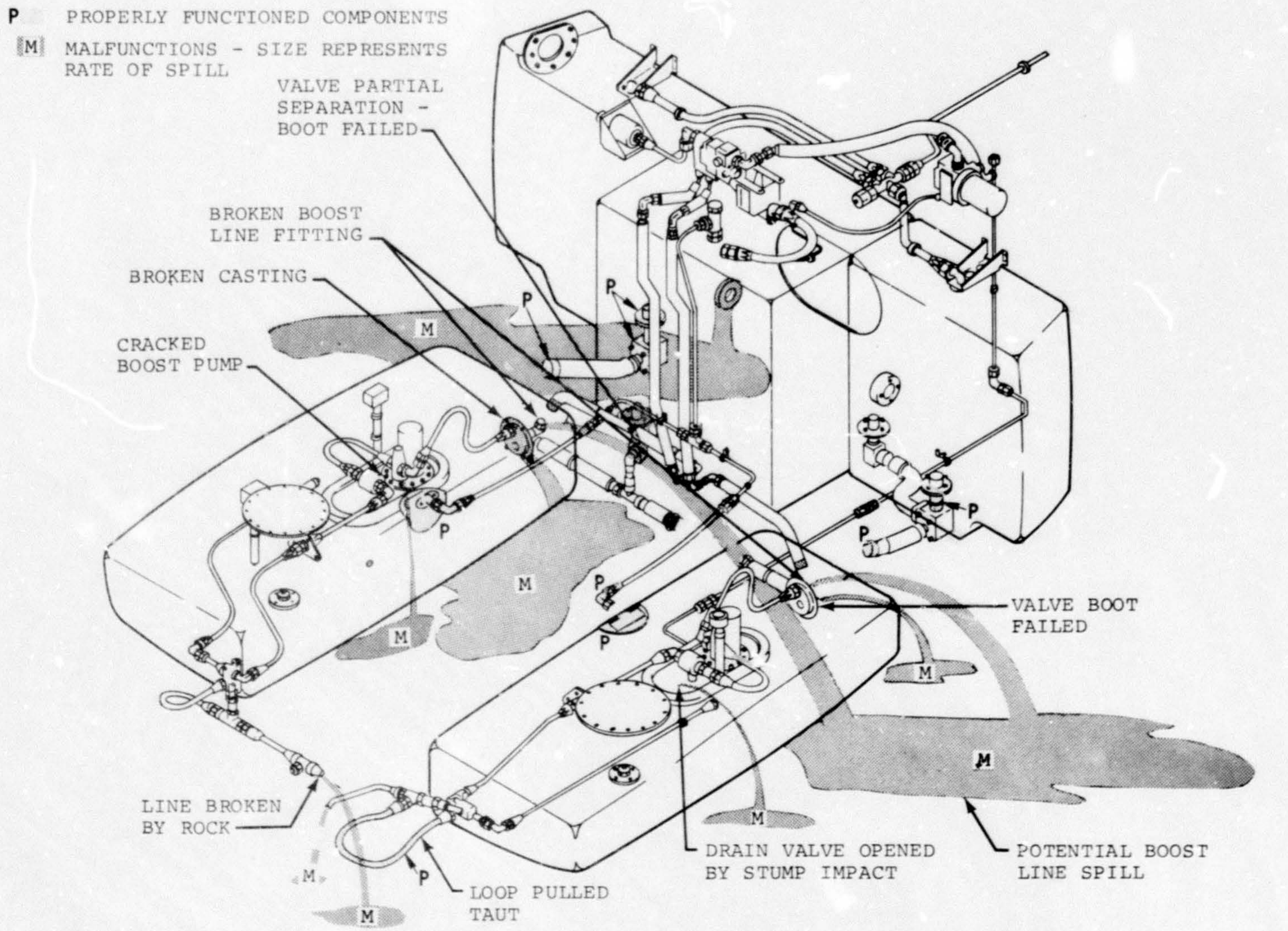


Figure 20. Summary of Actual and Potential Fuel System Spillage (Test 1).

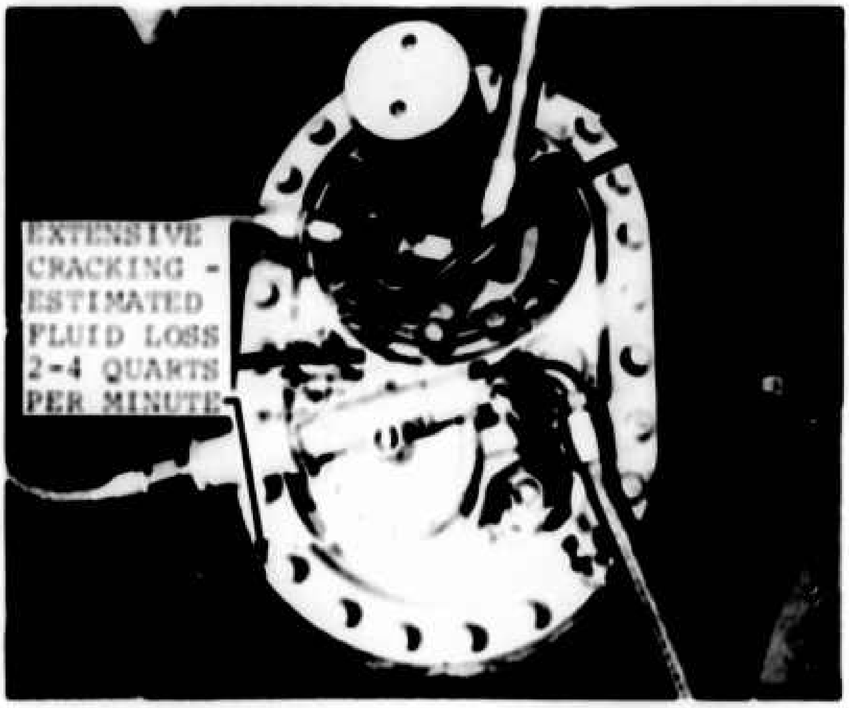


Figure 21. Damage to Right-Hand Boost Pump Plate (Test 1).

Left Vertical Cell

The left vertical cell apparently was untouched by the impact. The only portion of this cell that received any deformation was the drain valve. The frangible section of this valve had several corrugations, indicating that it sustained a vertical impact sufficient to deform it. If any forward load was imposed on this valve by the stump action on the forward end of the line, it was not sufficient to separate the valve at the frangible section. No appreciable load was exerted on the connection between the drain valve of the center tank and the drain valve of the left vertical cell.

Right Vertical Cell

The stump located under the inboard side of the right vertical cell drove up slightly beyond the axis of the cell-to-cell interconnect (Figure 23). This resulted in failure of the cell-fitting interface and, consequently, a massive loss of fluid (Figure 24). A secondary effect of this impact was that the drain valve in this tank functioned and sealed both halves.

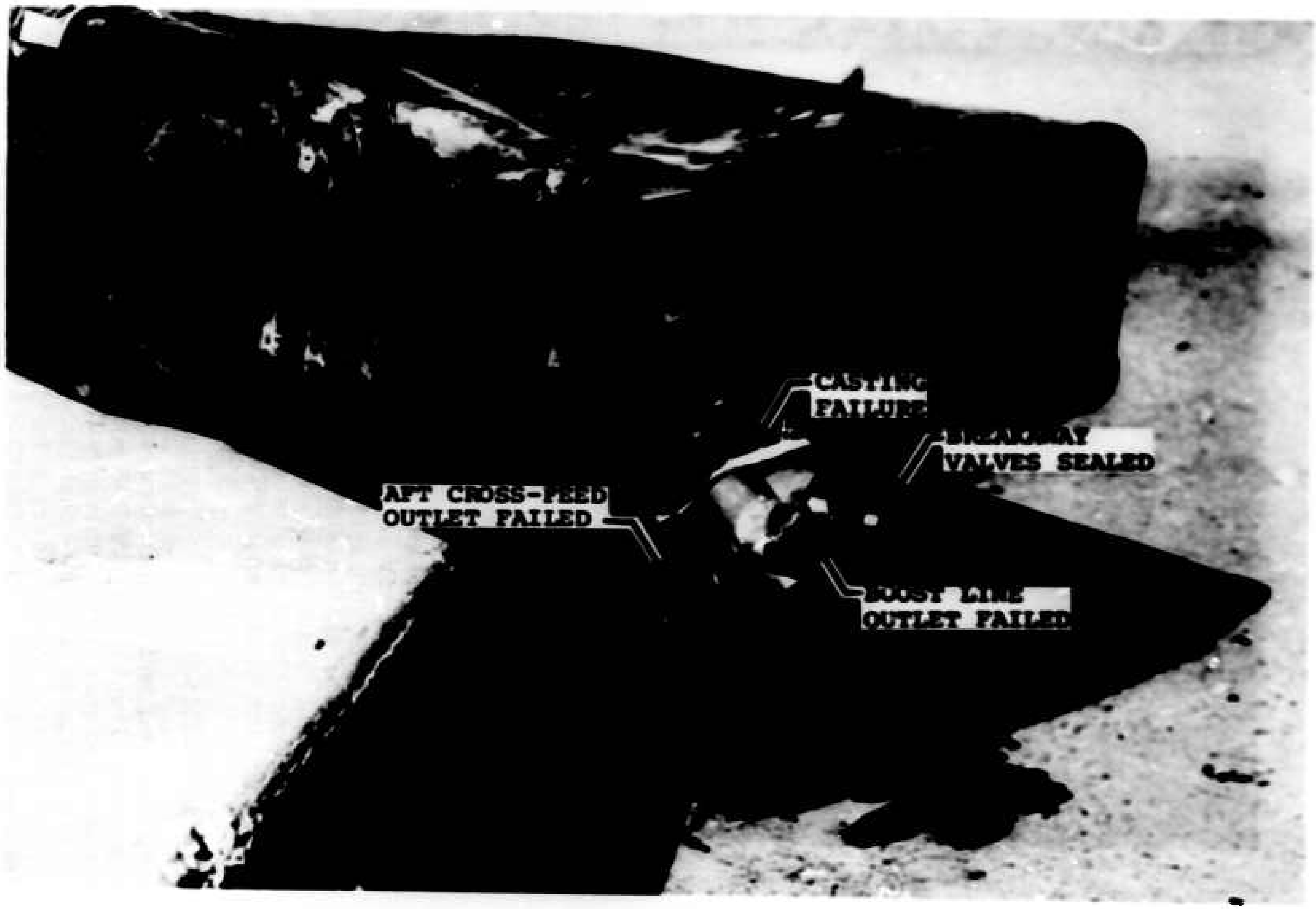


Figure 22. Failure of Right-Hand Inlet/Outlet Hardware (Test 1).

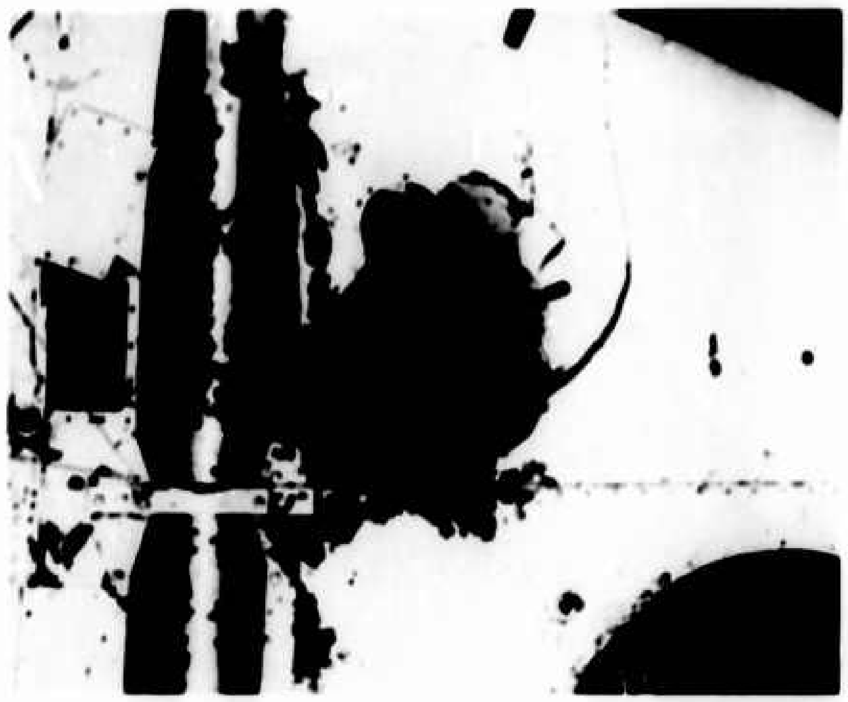

Figure 23. Stump Still in Place at Base of Right-Hand Vertical Cell (Test 1).

The filler fitting was broken free of the structure at its frangible section.

## Center Vertical Cell

The center vertical cell was untouched by the impact except for the partial separation of the forward drain valve. This appeared to have been induced either by the movement of the aft cross-over tube or from the upward movement of the landing gear cross-tube. The seat boot in this valve was cut in two places, but the displacement between the two halves was only about 1/4 inch. This left some doubt as to whether the valve actually closed at the time of impact. Unfortunately, the valve could not be removed from the wreckage without completing the poppet closure, and whether or not leakage occurred at this point could not be resolved.

## Forward Cross-Feed Line

The forward cross-feed line was struck in its midsection by a boulder which caused it to separate at the fitting (Figure 25).


Figure 24. Stump Removed, Exposing Tank-Fitting Separation (Test 1).

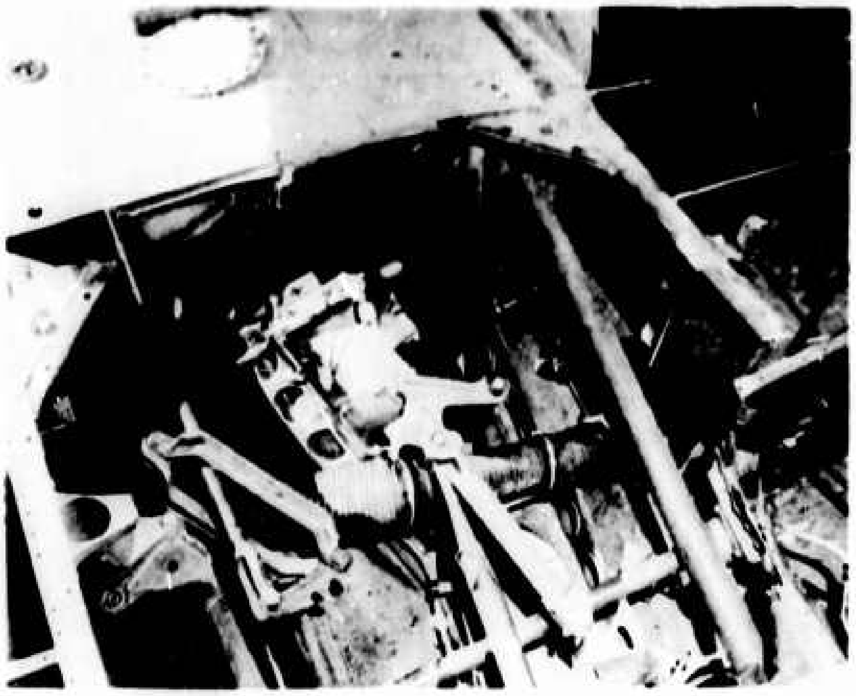

Figure 25. Forward Cross-Feed Line Failure (Test 1).

Only a small amount of fuel escaped, primarily because the left half of the line was pinched off by the stretch imposed by the left-hand underfloor cell deflection. The hard fittings in this line just outboard of the buttline 14 keels made it impossible for the line to pull slack into the center; thus, failure had to result.

## TEST 1 HAZARD ASSESSMENT

### Fuel Spillage

Several points in the system were responsible for a high fluid loss rate. A discussion is presented on each of these as well as those points which would have leaked had the entire aircraft been functioning.

### Right-Hand Cell-to-Cell Interconnect

The greatest spillage was the result of the right-hand cell-to-cell interconnect peeling out of the right-hand vertical fuel cell. This left a half-moon shaped hole in the cell and completely exposed the throat of the fitting, allowing maximum

flow from both the center and right-hand cells. The flow rate from this area was estimated at 30 - 50 gallons per minute. The test fluid did not mist, and the closest ignition source was the engine compartment; thus, whether ignition would have occurred is questionable. If ignition had occurred, the fire would have been uncontrollable.

Right-Hand Underfloor Cell Inlet/Outlet Fitting

The broken inlet/outlet casting in the right-hand underfloor cell was also responsible for the loss of liberal quantities of fluid. The estimated rate of this spill was 15 to 25 gallons per minute. This break also caused a short spurt of fuel to escape during the crash pulse. Whether this would have reached ignition sources is also questionable, but this too represents a very serious potential hazard in that the fire from this spill alone would have been uncontrollable if only the on-board fire-fighting equipment had been used.

Boost Pump Lines

Both boost pump outlet lines were pulled out of their fittings. If the pumps had been operating, the spillage from these two sources would have been considerable. In addition, the pressure in these lines would have caused a spray hazard, thereby greatly increasing the ignition potential.

Aft Cross-Feed Line

The severance of the right-hand outlet of the aft cross-feed line was not responsible for any spillage in this crash except for a possible increase in flow through the broken inlet/outlet fitting. Its hazard potential is appreciable, however, because of its proximity to electrical spark sources in the lower part of the aircraft.

Left-Hand Inlet/Outlet Breakaway Valve

The spillage from the inlet/outlet breakaway valve was relatively small, not exceeding 2 quarts per minute. Its primary hazard was its proximity to electrical ignition sources. Ignition of this spill would greatly increase the hazard of ignition of the more massive spill areas.

Left-Hand Boost Pump Sump Drain Valve

The spill from actuation of this valve represented a very minor hazard in that the probability of a recurrence of this incident is very low, irrespective of crash conditions.

**Right-Hand Boost Pump Plate and Fitting**

The damage caused by the boulder's striking the right-hand boost pump plate was responsible for the plate's cracking in several locations and causing a spill rate estimated at 1/2 gallon per minute. In the same impact the lead wires were crushed and cut, making the ignition potential fairly high. The actual fire hazard from this spill is negligible except for its potential to spread fire to other spills, such as that from the broken inlet/outlet fitting. This would be the probable cause of catastrophic fire from both of the major spills mentioned earlier.

Forward Cross-Feed Line

The break in the forward cross-feed line represents a relatively low hazard in that its leak rate was very low, less than a quart per minute, and no ignition sources were immediately available.

Total Spillage Rate

The entire fuel system except for the left-hand underfloor cell and the forward end of the right-hand underfloor cell drained in approximately 5 minutes. The high initial rate diminished sharply when the level of fluid dropped below the hole in the right-hand vertical cell. The spillage from all openings during the first minute was estimated at roughly half the total, or about 80 gallons.

Deformation Hazards

Neither the engine nor the transmission constituted a hazard in this test. The floor panels above the underfloor cells were the greatest deformation hazard and probably would have caused fatal injury to anyone seated above them.

TEST 1 HAZARD ANALYSIS

Table I lists the components under study in Test 1 and gives the impact reaction of each. The last column in Table I provides a hazard rating for each component based only on individual performance in Test 1.

TEST 1 DATA ANALYSIS

Acceleration data recorded during Test 1 peaked at 15 to 100G as shown in Figure 26. The maximum magnitude is not representative, however, since data from the vertical accelerometer mounted on top of the skid were lost. From previous vertical

| TABLE I. TEST 1 COMPONENT REACTIONS AND HAZARD RATINGS | | |
|---|---|---|
| Component | Reaction | Rating* |
| Forward cross-feed | Failed center | Low Hazard |
| Forward cross-feed loops | Stretched taut | Low Hazard |
| Left-hand sump drain | Valve depressed and locked open | Low Hazard |
| Left-hand inlet vavle | Closed but boot failed at seat | Low Hazard |
| Left-hand cross-feed line | Stretched but intact | Low Hazard |
| Right-hand aft cross-feed | Pulled out of fitting | Moderate Hazard |
| Right-hand and left-hand boost outlet | Fitting failed | High Hazard |
| Aft cross-feed valve | Functioned satisfactorily | Safe |
| Left-hand and right-hand underfloor vent valves | Functioned satisfactorily | Safe |
| Right-hand inlet valve | Functioned satisfactorily | Safe |
| Right-hand inlet casting | Broke out | Very High Hazard |
| Right-hand boost pump and fitting | Cracked several places | Moderate Hazard |
| Left-hand vertical drain valve | Corrugated neck | Safe |
| Center forward vertical drain valve | Partial separation, boot cut | Moderate Hazard |

| TABLE I - Continued | | |
|---|---|---|
| **Component** | **Reaction** | **Rating*** |
| Right-hand vertical drain valve | Functioned satisfactorily | Safe |
| Right-hand cell-cell interconnect | Separated from cell | Very High Hazard |
| *Values in Rating column are based on experience in one test and do not necessarily represent a statistically supported hazard rating. | | |

drop tests, the readings from a vertical accelerometer mounted on top of the skid were approximately 200G.

The high-response pressure gage indicated a nearly vertical change at impact to an off-scale condition (which would have been equal to >10,000 psi). However, posttest examination revealed that the cable leading to this transducer had been stretched and broken. It was therefore concluded that the recorded trace was probably not representative of the pressure within the tank.

TEST 2 OBJECTIVES/DETERMINATIONS

The specific objectives/determinations of this test were as follows:

1. Accelerations at key points in the system.

2. General resistance of fuel system to failure from forward impact on ground irregularities.

3. Resistance of tanks to failure from snagging on ground irregularities.

4. Integrity of fuel tank fittings.

5. Ability of breakaway valves to function under various types of loading.

6. Ability of hoses to cope with tank and structural deformation without breaking.

7. Pressure transients in fuel tank.

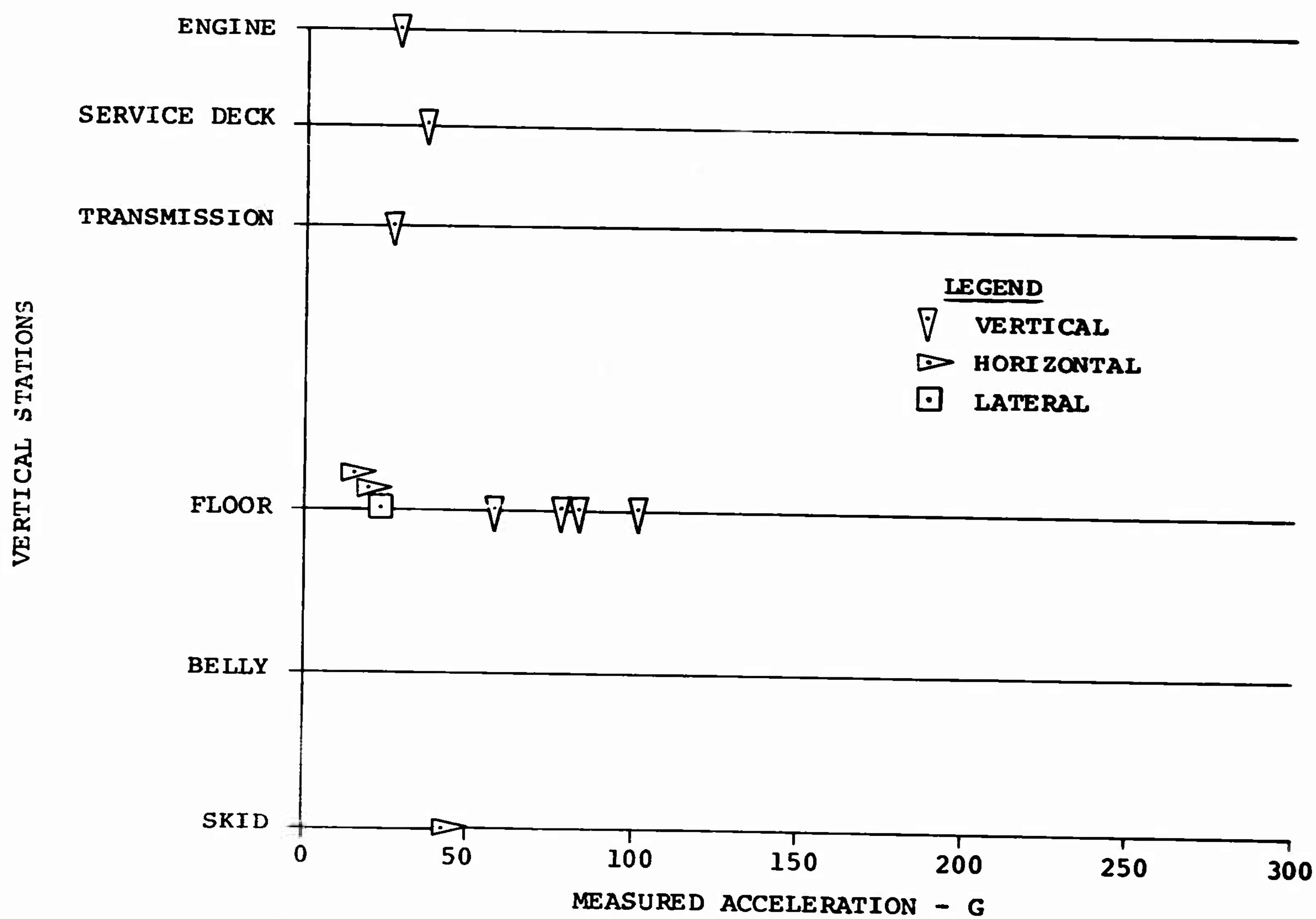


Figure 26. Peak Acceleration Data for Test 1.

## TEST 2 HELICOPTER PREPARATIONS

### Fuselage

The helicopter used in this test had received only minor structural damage prior to the test and did not require extensive rework. Some delamination of the engine service deck was noted in the area of the center engine mount points, but it was not extensive enough to warrant repairs. The structure surrounding the occupiable area was sound, and repairs were minimal. The windshields and the floor panel over the inlet/outlet fitting of the right-hand underfloor cell were removed for photographic coverage. As in Test 1, the crew doors and cargo doors were removed for better photographic coverage of the interior. All avionics and electronic equipment had been previously removed from the aircraft. The battery was positioned in the aft fuselage compartment.

### Power Plant

Since the only available set of engine mounts was badly damaged in Test 1, new engine mounts were fabricated using the original attachment fittings and the same type of steel tubing. The T53-L-1 gas-turbine power plant used in Test 1 was installed on these mounts. Flammable fluid lines were attached between the engine and fuel filter and firewall. Three small stadia poles marked off in 1-inch segments were installed on the service deck to the right of the engine.

### Fuel System

The fuel system in the test vehicle was the standard crash-resistant UH-1D fuel system described previously. The fuel cells needed no rework except for a modification of the forward access cover in the left-hand underfloor tank to accommodate the mounting of instrumentation for monitoring tank pressure.

### Transmission and Rotor Assembly

A UH-1D transmission and rotor mast was not available for installation in the test vehicle. It was therefore necessary to substitute the UH-1A transmission and rotor mast that had been used in previous Army tests. This assembly had been modified by adding lead ballast to bring the transmission and rotor assembly up to the proper weight for the UH-1D.

The main rotor blades from a previously crashed helicopter were used. The damaged outer portions of these blades had been removed and equivalent ballast weights securely attached to the remaining 3-foot blade sections.

### Landing Gear

A standard undamaged UH-1D landing gear was installed on the repaired fuselage.

### On-Board Cameras

Three high-speed cameras were mounted on board the aircraft as shown in Figure 27.

### Right-Hand Vertical Cell Drain Valve Flash Bulb

A 1-3/4-second delay flash bulb was mounted in the right-hand vertical cell drain valve compartment to illuminate the valve separation. The mounting and switching technique was the same as in Test 1.

## TEST 2 CONVEYANCE SYSTEM

A conveyance system consisting of a guide cable, trolley, trolley brake, and release mechanism was constructed to assure proper vehicle impact attitude.

### Guide Cable

A 1-1/2-inch-diameter cable with a rated minimum breaking strength of 216,000 pounds and an elongation at failure of approximately 2 percent was used. The cable consisted of a single slack loop strung between two buried "deadmen". The slack was sufficient that, when the cable was raised to maximum height at its center point, it would intersect ground level at a 45-degree angle. A crane equipped with a hydraulically-actuated boom raised the cable to its correct height and angle (Figure 28).

### Trolley

The trolley consisted of a kite-shaped tubular structure with bearing points at all four corners (Figure 28). Eight-inch-diameter sheaves designed to ride the guide cable were mounted to the two top corners. A socket mounted on the lower forward corner controlled the attitude of the test vehicle. An explosive release mechanism at the lower aft corner separated the vehicle from the trolley just prior to ground impact.

### Trolley Brake

A braking system stopped the trolley before the aircraft struck the ground. This was necessary to prevent damage to the top side of the helicopter and possibly compromising the data. To

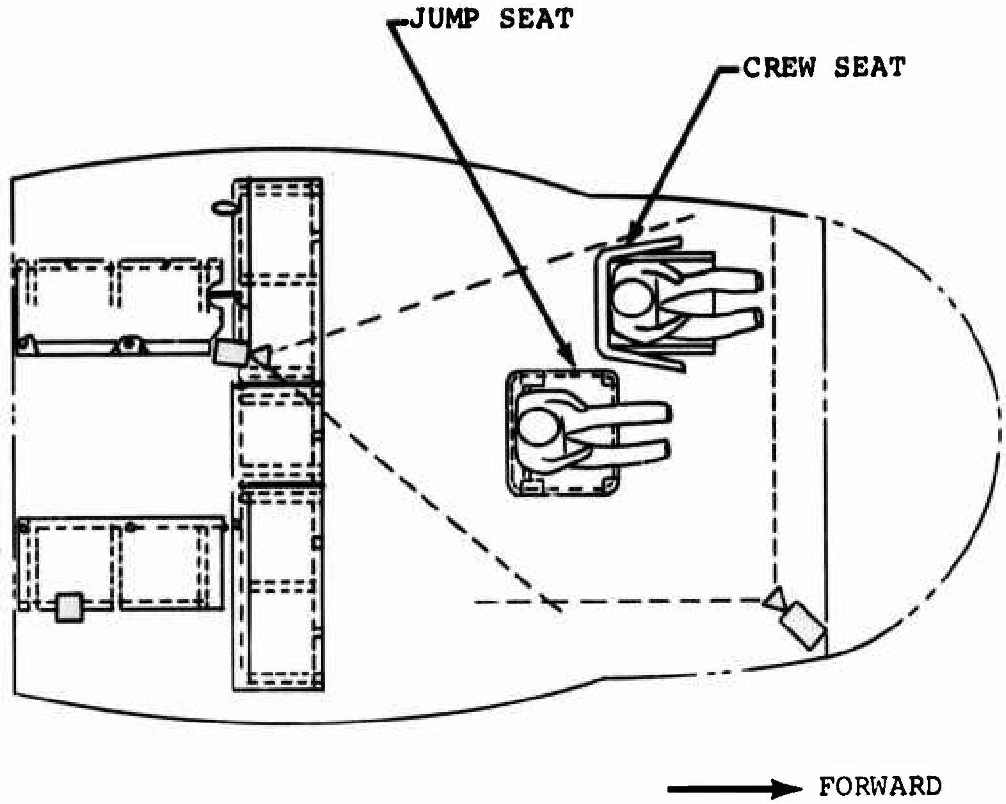


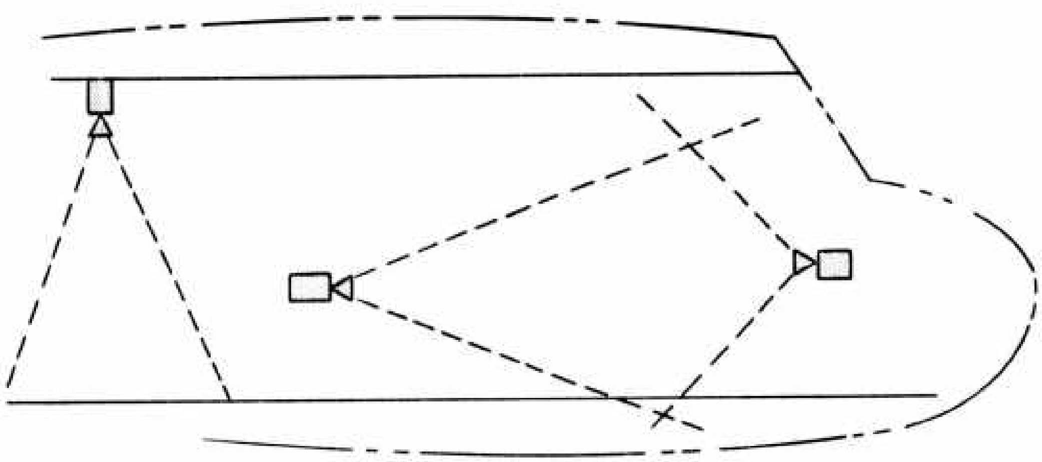

Figure 27. Photographic Coverage (Test 2).

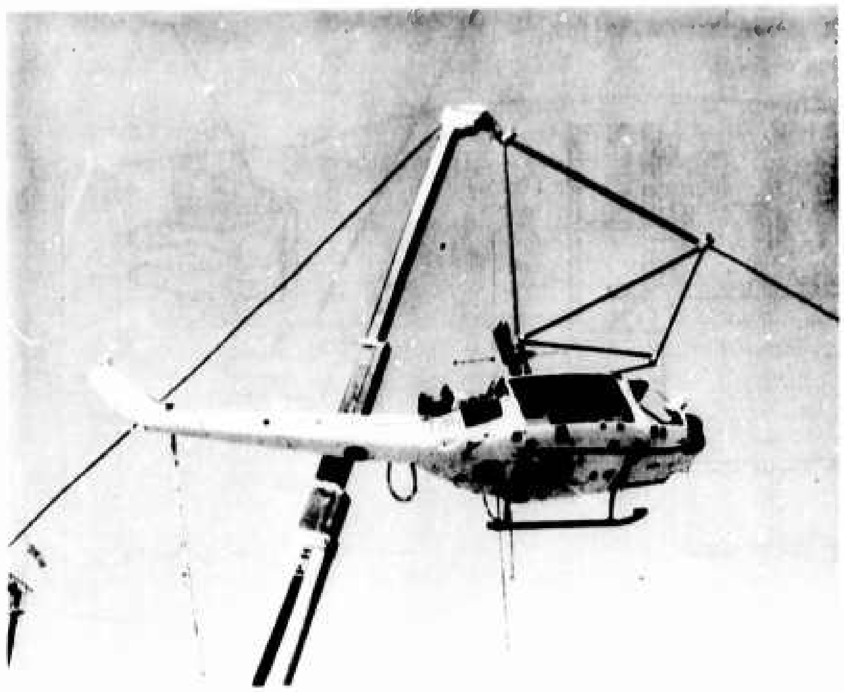

Figure 28. Helicopter Suspension System (Test 2).

do this it was also necessary to devise a release mechanism (described in the following paragraph) which would allow the aircraft to fall free immediately before braking the trolley. The trolley brake consisted of a rectangular tube filled with a high-density aluminum honeycomb. A ram rod was used to compress the honeycomb during impact and bring the trolley to a gradual halt without overloading either the cable or the aircraft. An impact switch was mounted on the forward end of the brake to trigger the detonator in the release mechanism.

## Explosive Release

The explosive release mechanism consisted of a steel block in which two electrical detonator caps drove the main lift bolt forward. This, in turn, caused the two retainer bolts to fail, allowing the main lift bolt to clear the retainer.

## Helicopter Suspension Frame

The main attachment point consisted of a tripod attached to the aft and left forward transmission mount bolts. The apex of this tripod was at a point near the longitudinal center of

gravity of the aircraft and 10 degrees to the right side of the rotor mast. A swivel link was mounted to the top of the tripod to allow free rotation of the main support shackle (Figure 29). This, in turn, was connected to the release mechanism described earlier. In addition to the main attachment point, a diagonally oriented yaw and pitch stabilizer arm was mounted on top of the cabin area, extending to a point near the upper right corner of the windshield (Figure 29). A stud on the end of this arm was fitted in a receptacle at the forward end of the trolley mechanism. This was designed to release automatically when the main support point was released. A general illustration of the overall test setup is shown in Figure 30.

## TEST 2 FACILITY PREPARATION

### Impact Zone

The impact zone consisted of hardened desert soil. A stump was buried 4 feet deep at a point which would coincide with the right aft landing gear cross tube just outboard of the buttline 14 longitudinal member. Three boulders (approximately 14 inches in cross section) were also placed in the ground at points that would strike the center of the right-hand underfloor cell, the left-hand underfloor cell boost pump, and the left-hand vertical cell drain valve. After these obstructions were implanted, the soil was packed, wetted, and allowed to dry. Figure 31 shows the obstructions in relation to their intended impact points.

### Camera Stands

Camera stands were erected at seven locations around the impact area as shown in Figure 32 to provide mounts for the high-speed cameras during the drop sequence. The location of the 24-frame-per-second documentary camera is also indicated.

### Ground Lines and Batteries

A wiring network of ground lines and batteries was put into position to insure the proper sequencing and operation of all high-speed cameras.

### Stabilizing Rope

A 1/4-inch nylon rope was looped over the right landing gear skid of the test vehicle to prevent it from swaying prior to hook release.

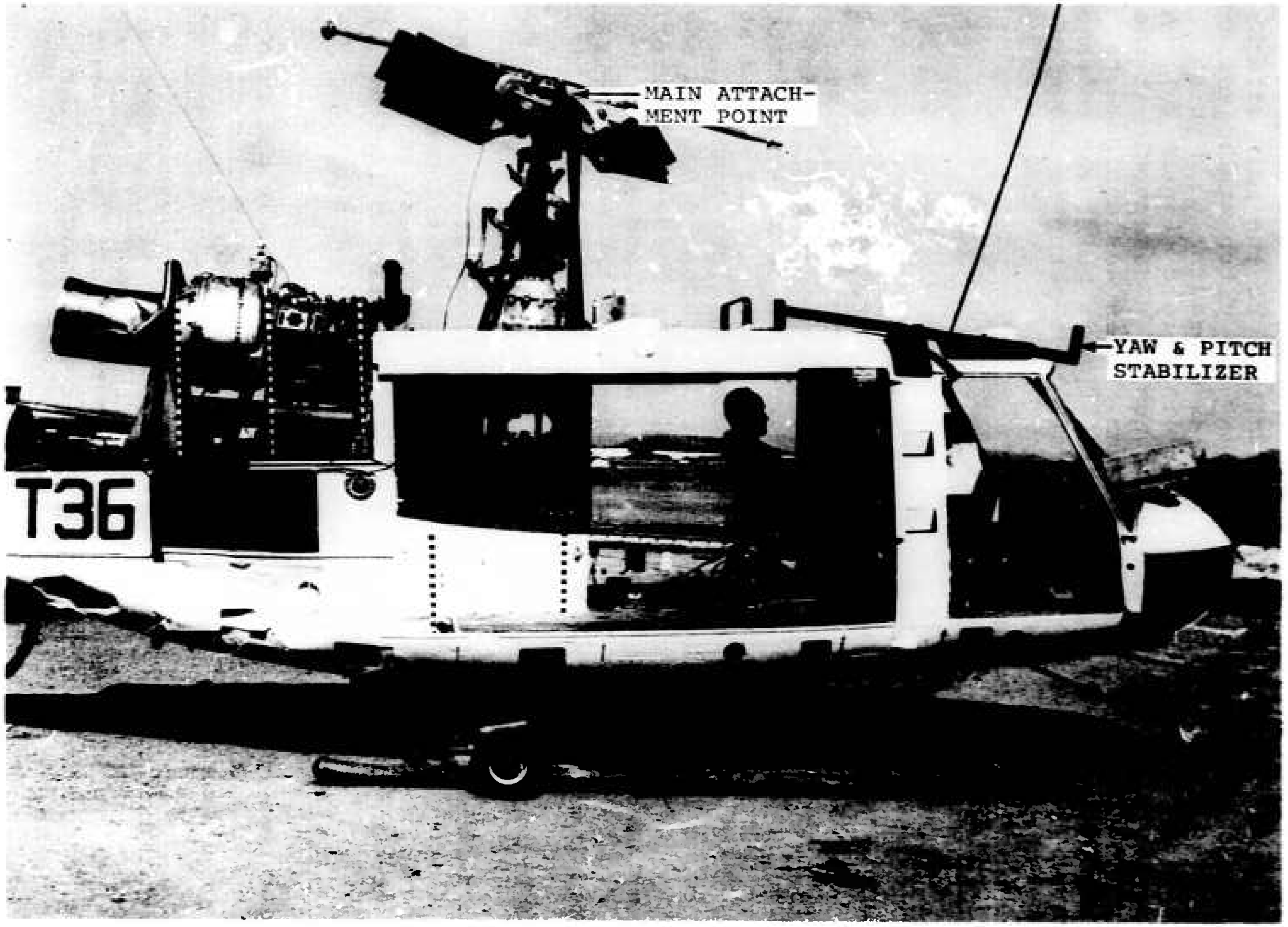


Figure 29. Suspension/Stabilization Systems (Test 2).

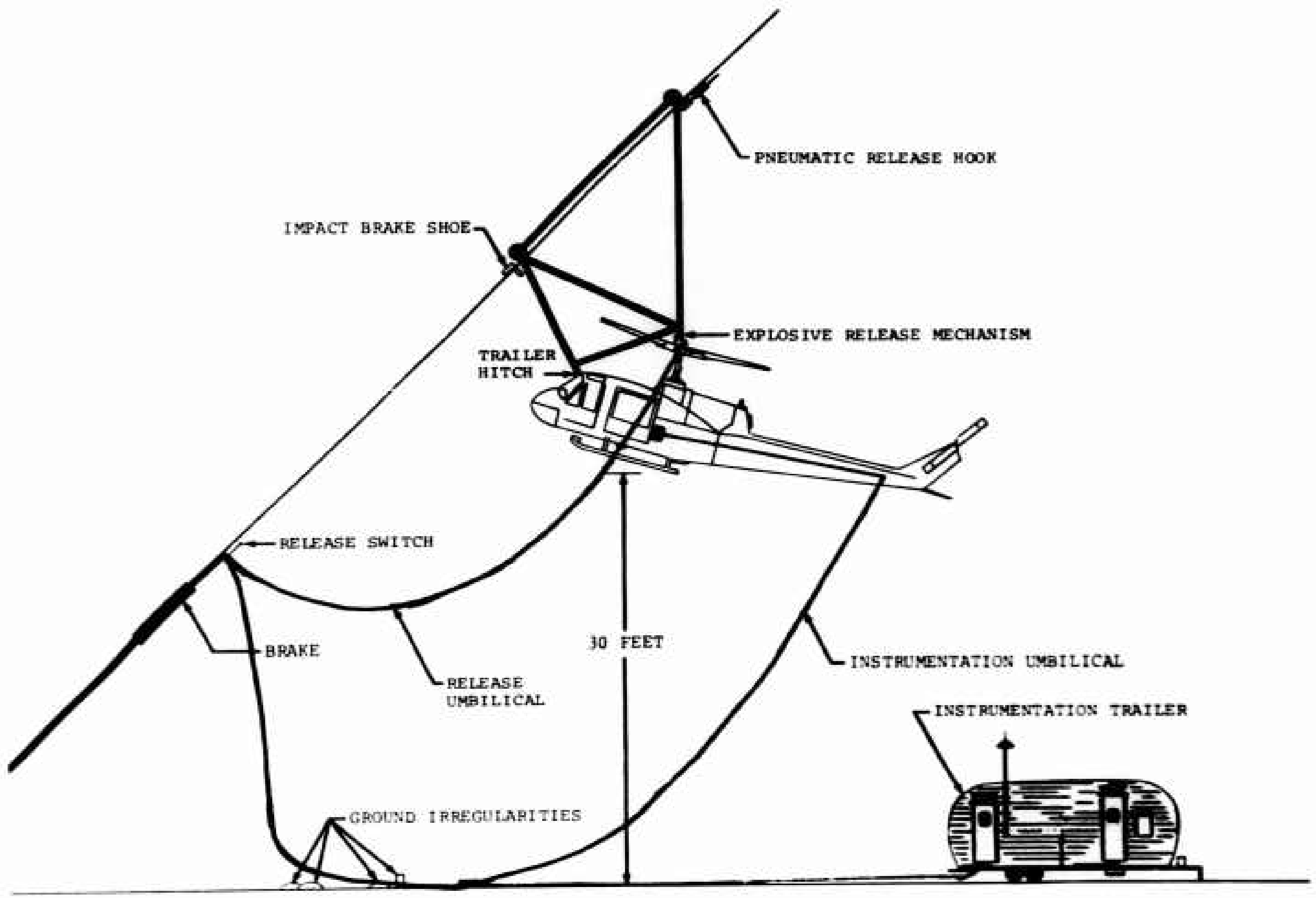


Figure 30. Schematic of Test 2 Setup.

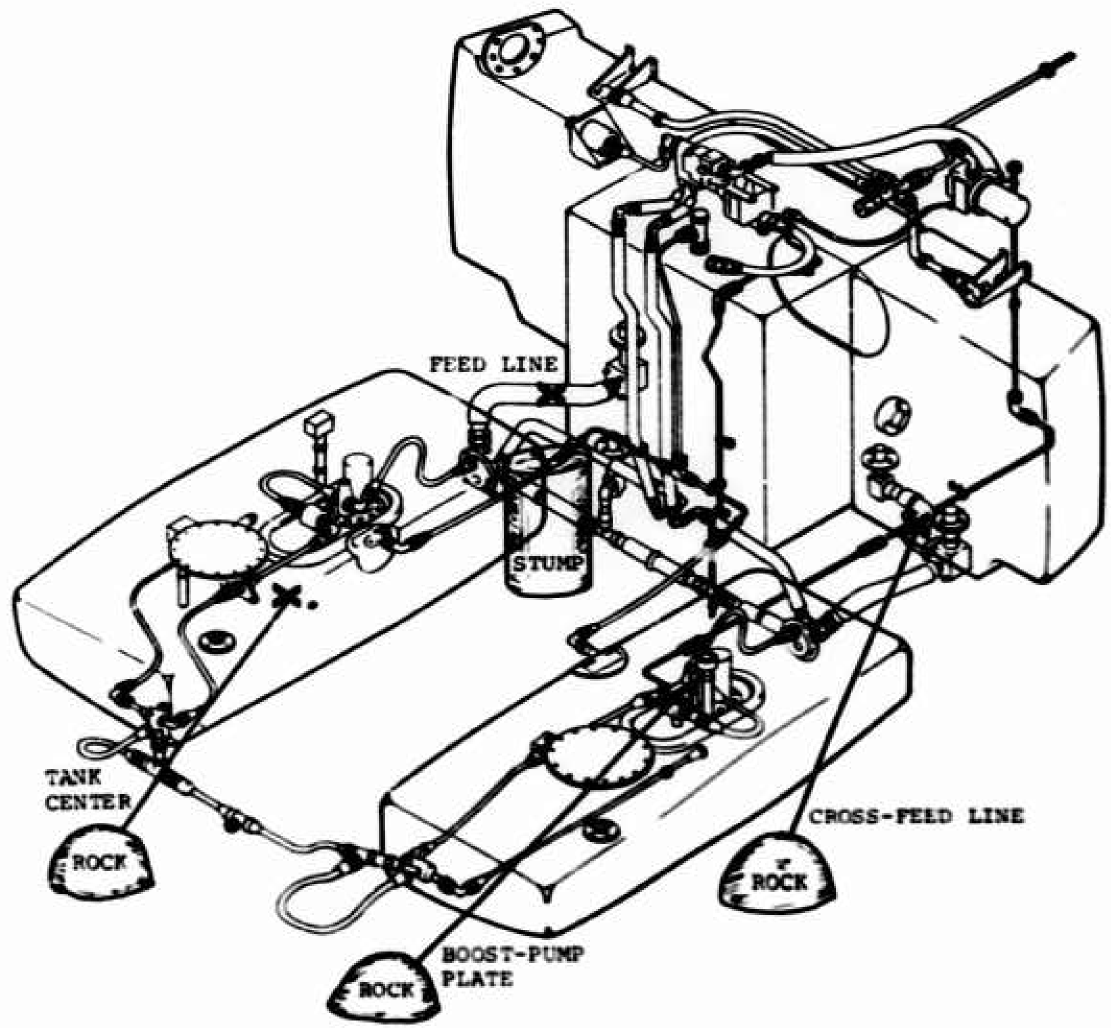


Figure 31.  Intended Impact Points (Test 2).

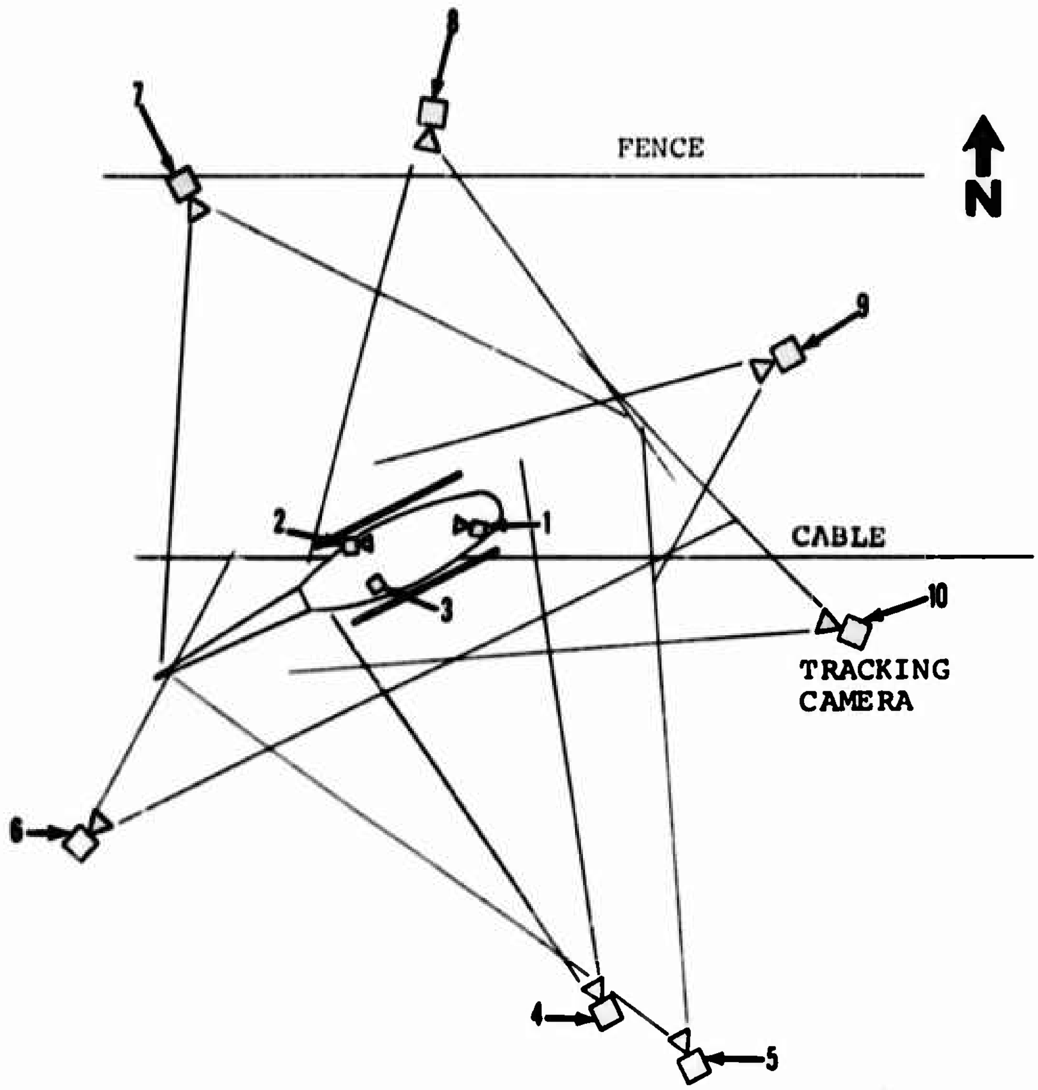


Figure 32. Camera Locations (Test 2).

## Master Release Mechanism

A pneumatic trolley release mechanism was attached to a lift point located at the tail end of the trolley (Figure 30) and hoisted by a tow cable guided through the top sheave of the crane boom.

## TEST 2 INSTRUMENTATION

### On-Board Data Acquisition System

Accelerations at eight locations and fluid pressure at one location were to be recorded during the impact sequence. The relative locations of the sensing instruments are shown in Figure 33. As in Test 1, all accelerometers other than those installed in the anthropomorphic dummies were housed in metal cases.

The outputs of the instruments were fed individually to a central junction box mounted on the left side of the engine service deck.

### Impact-Sensitive Switch and Correlation Lights

An impact-sensitive switch was mounted near the aft end of the left landing skid. This switch completed an electrical circuit on impact that fired a flash bulb mounted on top of the engine accelerometer for camera correlation and provided an electrical signal to correlate the data that were recorded on the FM tape recorder.

### Umbilical Cable

A 1,000-foot-long umbilical cable fed the output of all instrumentation to the signal conditioning equipment in an instrumentation trailer located near the test site.

### Signal Conditioning and Recording Equipment

The outputs from the accelerometers were fed into signal conditioning equipment that provided for the balancing and the controlling of the outputs. This conditioned signal was fed into individual voltage-controlled oscillators. This voltage varied the frequency of the oscillators in proportion to the G-forces acting on the accelerometers. The output of the voltage-controlled oscillators was amplified and recorded on the magnetic tape.

An FM tape recorder operating at a tape speed of 60 in./sec and capable of handling up to 25 channels of data was used to record the signals from the instrumentation.

### FM Tape Playback

A data tape equipped with filters and discriminators was used to reproduce the analog data from the test tape.

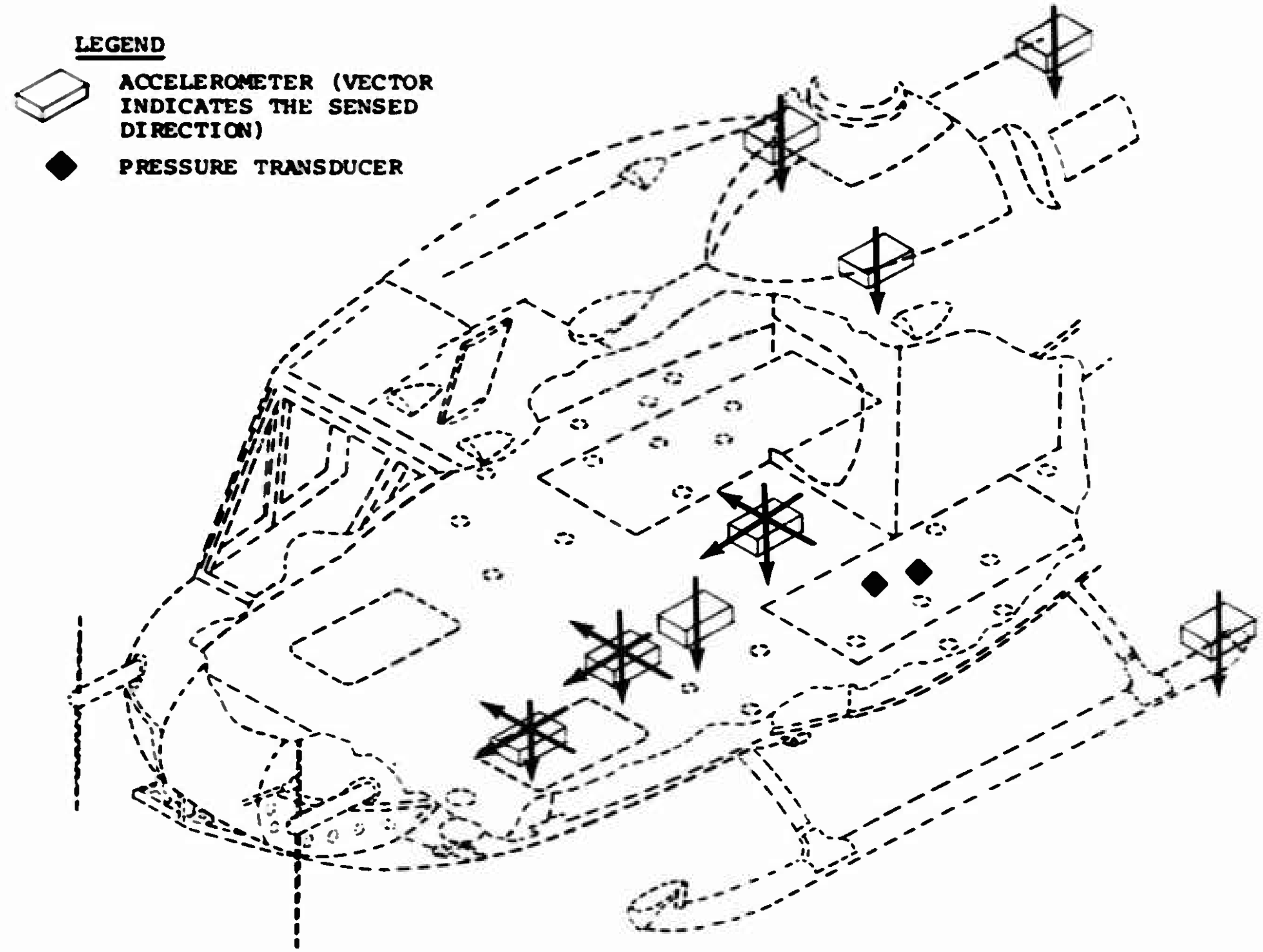


Figure 33. Instrumentation Location (Test 2).

## TEST 2 PHOTOGRAPHY

### Motion Photographic Coverage

High-speed (500 - 1000 frames per second) color film coverage was provided to record the kinematics of the test items in the time interval between hook release and for several seconds following the completion of action after impact.

In addition to the three high-speed on-board cameras, seven high-speed cameras were located at the ground positions shown in Figure 32. Color documentary coverage (24 frames per second) of the drop sequence was also provided.

### Still Photographic Coverage

Black and white 4- x 5-inch photographs were taken of the test vehicle and experiments before and after the test. These included general overall views of the helicopter and test site as well as detailed close-ups of the test articles during installation and posttest investigation.

## TEST 2 TARGET CRASH CONDITIONS AND FINAL PREPARATIONS

### Target Crash Conditions

The target crash conditions at impact were as follows:

Drop Height - 44 Feet

Vertical Velocity - 42.8 Feet Per Second

Longitudinal Velocity - 24.5 Feet Per Second

Lateral Velocity - 8.7 Feet Per Second

Flight Path Angle - 45 Degrees

Resultant Flight Path Velocity - 50.1 Feet Per Second

Pitch Angle - 11 ±5 Degrees

Roll Angle - 10 ±5 Degrees

Yaw Angle - 26 ±5 Degrees

Test Weight - 6,100 Pounds

The test weight for Tests 2 and 3 was less than for Test 1 due to a cable/hoist limitation. As the system was originally designed, the suspension system was capable of handling over 8,000 pounds. However, angular adjustments made during the actual test setup required that the drop weight be restricted to approximately 6,000 pounds. This is typical of a UH-1D/H with an operating load of approximately 25 percent of capacity.

### Final Preparations

The test vehicle was moved to the impact area, and the fuel tanks were filled with 165 gallons of colored water to simulate the weight of a UH-1D/H's normal servicing of 209 gallons of JP-4 fuel.

The high-speed cameras and associated wiring were placed in position. The umbilical cable was attached to the test vehicle, and the instrumentation was checked out.

Prior to attachment of the trolley mechanism, a 0- to 10,000-pound load cell was installed between the crane hook and the attachment point on the test vehicle and the test vehicle was weighed. Final ballast adjustments were then made, and a gross drop weight of 6,100 pounds was recorded. The center of gravity was slightly behind the main lift point, which put a rearward force on the yaw stabilizer socket of approximately 300 pounds.

The static pitch, roll, and yaw angles were then checked and found to be 11, 10, and 26 degrees, respectively.

Pretest photographs were taken and final checks were made on all systems.

## RESULTS OF TEST 2

### Guidance Mechanism Malfunction

Upon actuation of the main release hook, the top of the trolley jerked forward on the cable in reaction to the release of tension. This forward movement also rotated the forward yaw stabilizer contact point downward, putting an excessive load on the yaw stabilizer boom and dislocating it from its socket. This, in conjunction with the inertia of the helicopter, started the helicopter rotating about its pivot point (at the explosive release hook) into a nose-down attitude.

The pitch angle was measured at 25 degrees on impact. This, coupled with a lateral rotation to a 45-degree yaw angle, caused the helicopter to strike the ground short of its target

impact zone. The roll attitude was also affected and changed from a 10-degree left to a 10-degree right roll attitude. After impacting the ground, the helicopter rolled over on its right side.

Figure 34 shows the attitude changes which occurred during the drop sequence.

The test failed to meet its first objective, i.e., for the helicopter to strike in the prescribed attitude and on the specified ground protrusions. The two boulders which were intended to strike the left rear portion of the fuel cell system were struck by the right landing skid and were ejected from their holes. The stump which should have struck the right side of the aft landing gear cross tube barely made contact with the right landing skid at impact, and, as the aircraft rolled over, it became wedged between the fuselage and the skid.

## TEST 2 DAMAGE ASSESSMENT

### Fuel System

A survey of the fuel system showed that it was undamaged except for a ruptured panel under the forward half of the right-hand underfloor cell. None of the breakaway valves had functioned, and all frangible fittings appeared to be intact except for the forward drain fitting of the right-hand underfloor cell. The vent line was leaking at a rate of slightly more than 1 gallon per minute.

### Structure

The top half of the transmission failed, and its tie-bolts broke away from its base. The engine buckled its mounts and was displaced downward and to the right, but the fuel lines remained in place. The landing skid was severely damaged, and the tail boom was also badly buckled. The remainder of the aircraft suffered considerable deformation of the right forward area. The major portion of this damage did not extend to the left side of the aircraft, as Figure 35 indicates. The high-speed films revealed two reasons for the minimal damage to the fuselage. As the vehicle rotated into a nose-down attitude, its effective drop height was diminished by approximately 6 feet, as Figure 34 illustrates. Second, the whipping of the cable induced by the initial jerk of the trolley put a considerable bind on the guides throughout the entire sequence, thereby greatly increasing the friction in the system and causing a further reduction of the velocity. The actual striking velocity was determined by scaling the high-speed

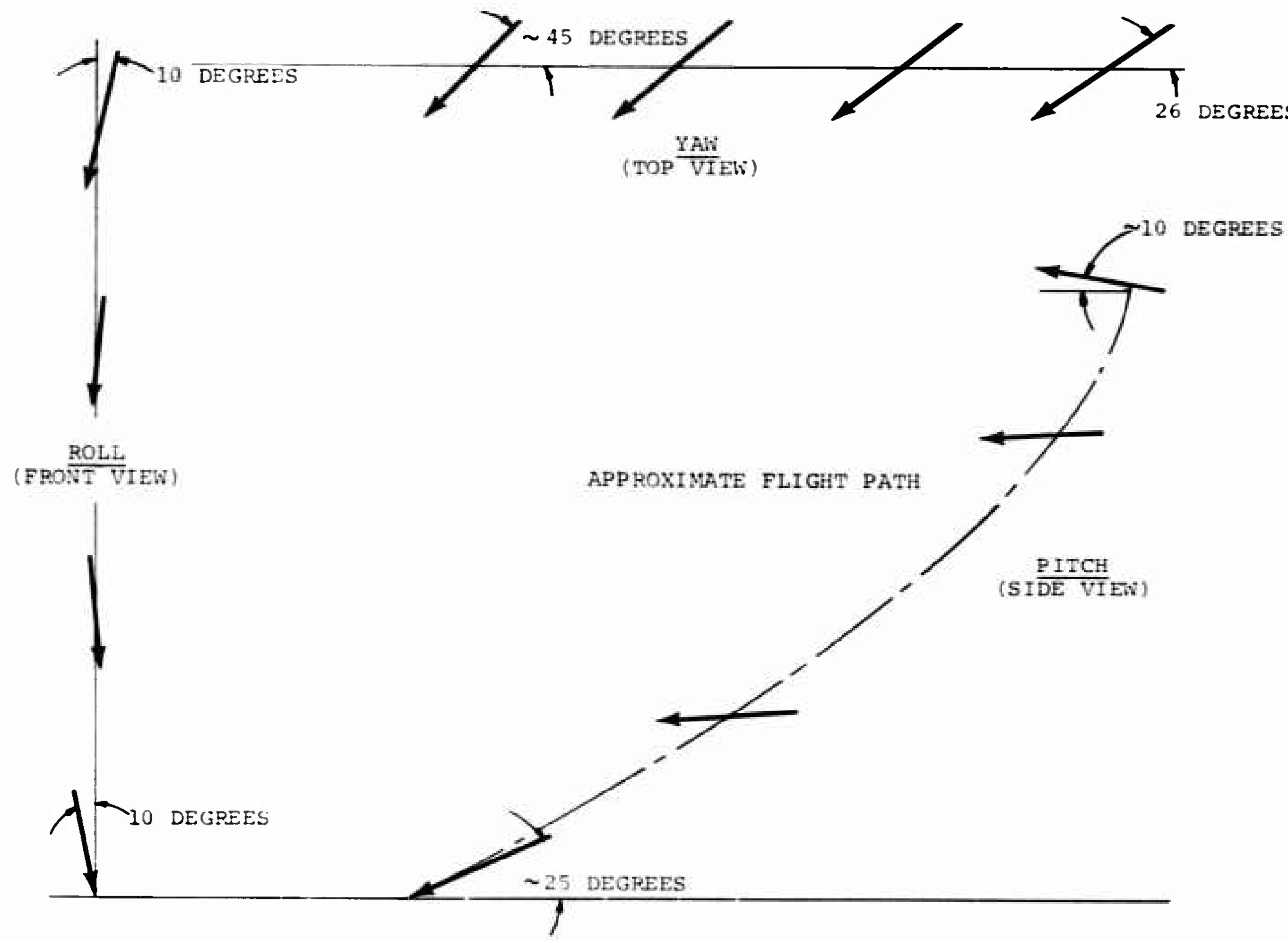


Figure 34. Vehicle Attitude Change (Test 2).

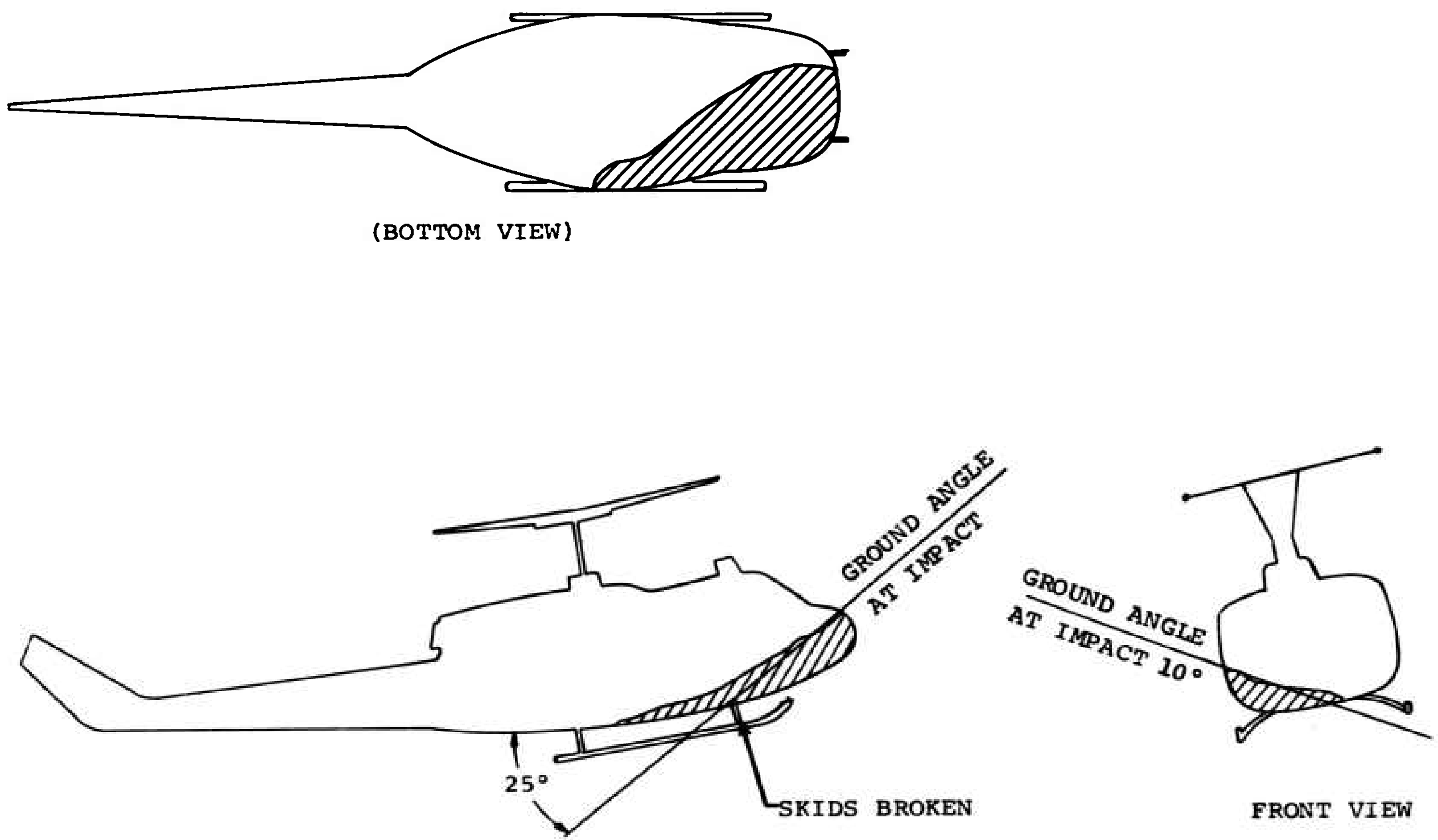


Figure 35. Impact Damage (Test 2).

films in relation to the time references on the film. The resultant velocity was 42.5 feet per second.

Instrumentation

All data were lost because of the inadvertent counterclockwise rotation of the tail boom of the helicopter. This caused the pressure transducer lead wire to snag on the crane, triggering a sequence of events which eventually caused a power failure in the recorder.

Cameras

All on-board cameras functioned throughout the entire sequence. Two of the ground cameras on the right side of the aircraft malfunctioned. All others performed as planned.

## TEST 2 REPAIR REQUIREMENTS

Structure

An examination of the structural damage to the helicopter showed that the test could be conducted again by making minor repairs. These included:

1. Replacement of the landing skid.

2. Replacement of the tail boom. (A UH-1B tail boom was available and adaptable to the UH-1D/H fuselage.)

3. Replacement of transmission. (This required only the removal and replacement of the broken bolts.)

4. Repair of right forward structural column at Station 72. (This was necessary to support the roof against collapse in Test 3).

5. Repair of the belly panel under the right-hand underfloor fuel cell to the extent that the cell would be firmly retained in its correct position.

Instrumentation

All accelerometer and pressure transducer installations were still intact and required no rework. One change appeared desirable - to relocate the umbilical cable departure point from the fuselage to the left rear corner of the engine service deck to avoid its being affected by any tail boom shift. The pressure transducer line would also have to be extended an

additional 30 feet and securely taped to the main umbilical to avoid a recurrence of the snagging problem.

### On-Board Cameras

Because of the damage to the nose of the helicopter, the forward-mounted camera had to be removed. It was changed to a ground mount and placed at a point directly beside the crew seat impact area for Test 3.

## TEST 3 OBJECTIVES/DETERMINATIONS

The specific objectives/determinations of Test 3 were the same as for Test 2.

## TEST 3 HELICOPTER PREPARATIONS

### General

The helicopter preparations consisted primarily of repairing the damage sustained in Test 2. It was also necessary to rebuild the fore and aft helicopter support points.

### Fuselage

The belly panel under the right-hand underfloor fuel cell was brought back into place from its deformed condition and held by a series of steel bands as shown in Figure 36. The right-hand vertical column at Station 72 was reinforced with steel angle to restore at least a degree of the structural continuity of this section. No effort was made to return the right side of the floor to its original condition.

### Tail Boom

The original boom was replaced with an undamaged boom from a UH-1B helicopter. Although this boom did not precisely match the fuselage (see Figure 37), it maintained proper distribution of mass in the vehicle.

### Landing Gear

The damaged gear was replaced with the gear from another UH-1 helicopter. Some additional guying was necessary to keep the right side of the forward cross tube in place because of the structural deformation sustained in Test 2 (see Figure 36).

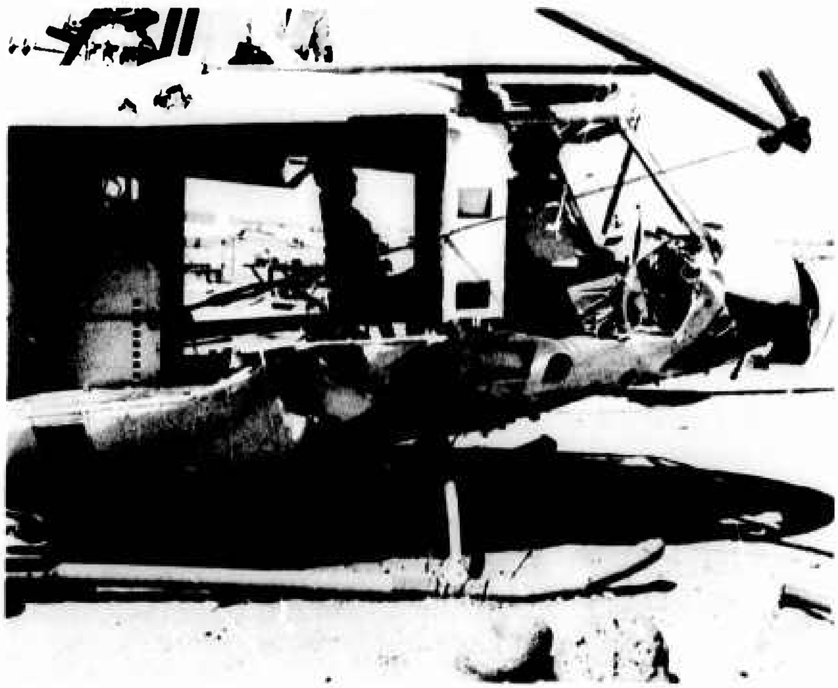

Figure 36. Preparations for Test 3.


Figure 37. Test 3 Helicopter Poised Over Impact Area.

## Engine

The deformed engine mounts were replaced with new tube sections. The engine was relocated in its proper position, and the fuel line was reconnected.

## Transmission

The broken transmission bolts were replaced, and the transmission housing was restored to its correct position. All the main mounting points were still intact and needed no modification or repair.

## Helicopter Suspension Frame

The suspension frame was similar to that used in Test 2 except that the construction was much sturdier. Two changes were made to the system:

1. The main attachment point was shifted 12 inches forward from its previous location. The 10-degree roll angle was maintained by keeping the lift point 12 inches to the right of the rotor mast.

2. The forward attachment point was changed to a bayonet type probe which could not be removed from its receptacle until the explosive release mechanism fired.

## Instrumentation

The umbilical cable departure point was changed from its point on the tail boom to a point at the aft end of the engine service deck as shown in Figure 37. The central junction box, located on the engine service deck, was covered with a pad to absorb any impact from the release point during the drop. The pressure transducer line was also extended 30 feet and taped securely to the umbilical cable.

## TEST 3 FACILITY PREPARATION

## Impact Zone

Because of the relocation of the lift points on the helicopter, its position relative to the ground protuberances was changed. This made it necessary to shift the protuberances to match the impact points on the helicopter. The boulders presented no problem, but the stump was firmly implanted in the ground and could not be easily moved. Since the stump, originally intended to strike the aft cross-feed outlet of the right-hand underfloor cell, was now in a position to strike the forward

end of the right-hand boost pump plate, the stump was left as it was. A large boulder was implanted in its place at the point of impact for the right-hand aft cross-feed outlet. The boulder locations at the left side of the aircraft were also shifted, and two additional boulders were placed in the impact zone. An 18-inch-high x 10-inch-diameter stump was also added to the left side impact zone to increase the protuberance height in the aft vertical cell zone. This was done to test the left-hand cell-to-cell interconnect fitting.

### Helicopter Hoist Mechanism

The hoist point was shifted from the top of the trolley mechanism to the center of gravity of the helicopter. The hoist cable was run through a snatch block located 20 feet below the top of the boom to permit hoisting of the test vehicle with the load applied parallel to the main guy cable. A pad was suspended behind the snatch block to prevent recoil damage to the hook and boom upon release.

### Camera Stands

Camera locations were essentially the same as in Test 2 except that the nose-mounted on-board camera was placed in a position immediately adjacent to and aimed at the impact zone for the crew seat.

## TEST 3 FINAL PREPARATIONS AND CRASH CONDITIONS

The test vehicle underwent the same final preparations as did the Test 2 vehicle. The fuel cells were refilled to the 165-gallon level to replace the fluid lost through the vent line. When all systems were ready, a final check was made on the ground protuberances. The starboard stump was still too far forward to strike the boost pump. Since this was considered to be a very important part of the test, the angle of the cable was changed from 45 to 48 degrees. This brought the helicopter farther forward into the impact zone but also increased the glide angle to 50 degrees. Final adjustment was then made on the rock locations, and the helicopter was hoisted to its release point. Because of the changes made in the hoist mechanism, the drop height (measured from the bottom of the helicopter) was reduced slightly from that of Test 2.

The planned test conditions and the actual test conditions were as follows:

| | Planned | Actual |
|---|---|---|
| Drop Height | 44 Feet | 40 Feet |
| Vertical Velocity | 42.8 Feet Per Second | 38.9 Feet Per Second |
| Longitudinal Velocity | 24.5 Feet Per Second | 24.5 Feet Per Second |
| Lateral Velocity | 8.7 Feet Per Second | 9.8 Feet Per Second |
| Flight Path Angle | 45 Degrees | 50 Degrees |
| Resultant Flight Path Velocity | 50.1 Feet Per Second | 47 Feet Per Second |
| Pitch Angle | 11 Degrees Nose Up | 7 Degrees Nose Up |
| Roll Angle | 10 Degrees Nose Up | 8 Degrees Nose Up |
| Yaw Angle | 26 Degrees Left | 28 Degrees Left |
| Test Weight | 6,100 Pounds | 6,100 Pounds |

## RESULTS OF TEST 3

### Impact

A study of the high-speed films indicated the following: The test vehicle made a smooth flight from release to impact point. The actual impact attitude was close to the planned attitude as stated in the preceding paragraph. There was a slight reduction of forward velocity just before the belly touched the ground as a result of the braking effect from the stump and rock impacts. Considerable structural deformation was noted as the starboard stump drove up into the underfloor fuel cell cavity. The aircraft "bottomed" and began its rebound, but did not skid out of its impact track. The rebound was characterized by a rise at the intersection of the tail boom and fuselage while, at the same time, rolling toward the right side. This roll continued until the fuselage had rotated almost 55 degrees beyond its vertical axis, whereupon it recovered its normal orientation (Figure 38).

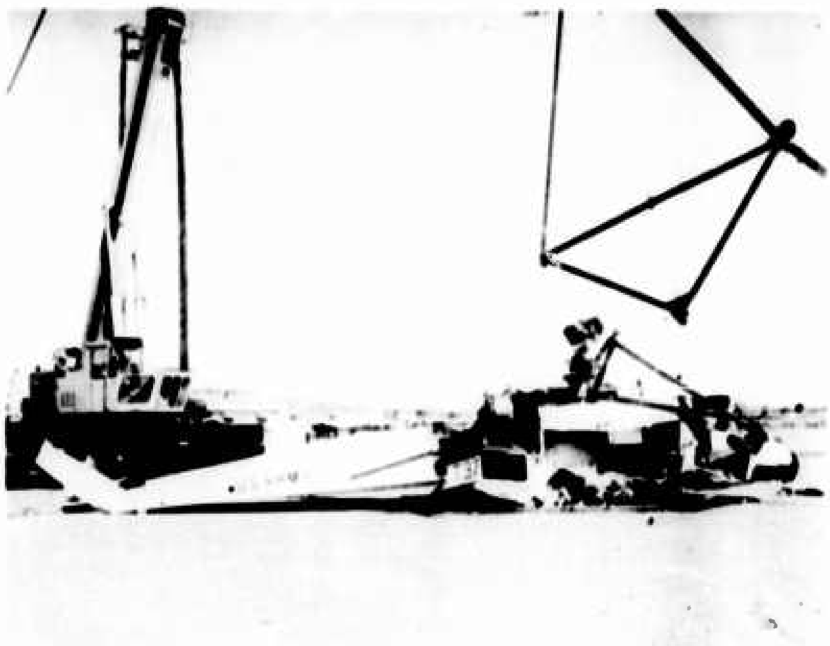

Figure 38. Posttest Attitude of Helicopter (Test 3).

Complete roll-over was probably prevented by three factors: (1) the cocking of the tail boom, (2) the contact of the yaw stabilizer boom with the ground, and (3) the bending moment applied by the stump in the right side of the fuselage. Both the engine and transmission remained with the helicopter.

Transmission

The transmission mounts were still intact. Although the rotor hub moved approximately 8 inches to the right and 6 inches forward during the impact, it had returned to its normal position after the test.

Engine

The left side engine mounts were buckled, and those on the right side were broken off. The engine had shifted forward about 3-1/3 inches, and the aft end was 5 inches below its original access position through the aft firewall (see Figure 39).

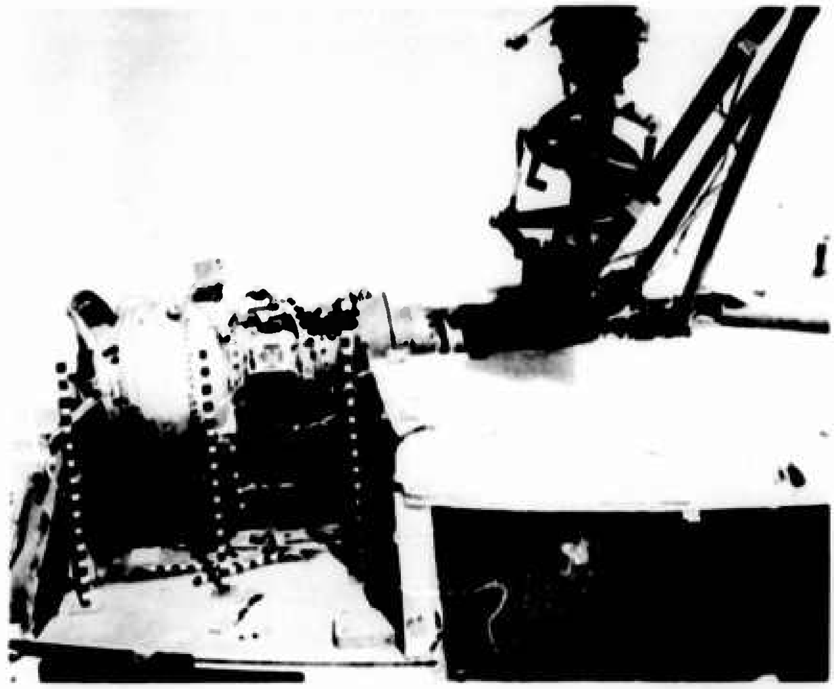

Figure 39. Posttest Position of Engine and Transmission (Test 3).

## Initial Fluid Spillage Assessment

Right after impact, a gurgling noise indicated fuel was still flowing, so the left skid was raised high enough to obtain a damage assessment of the bottom before the fluid drained out. The high-speed film analysis conducted later showed some spurts of fuel coming from the left side of the aircraft in the aft landing gear cross-tube area. Figures 40 and 41 show the aircraft in the elevated position. Examination revealed that the aft cross-over line had been severed when a boulder intersected it. This failure occurred immediately adjacent to the in-line breakaway valve. The valve had not separated, and both halves of the line were leaking fluid. The total leakage rate was estimated at about 1 gallon per minute (see Figure 42). This rate may have been higher during the initial stages because the flow gradually diminished due to the lack of venting (both vent valves were sealed) or drainage from the aft cells.

Figure 40. Aft Underside View Immediately
After Test 3.

Figure 41. Left Side Overall View Immediately
After Test 3.

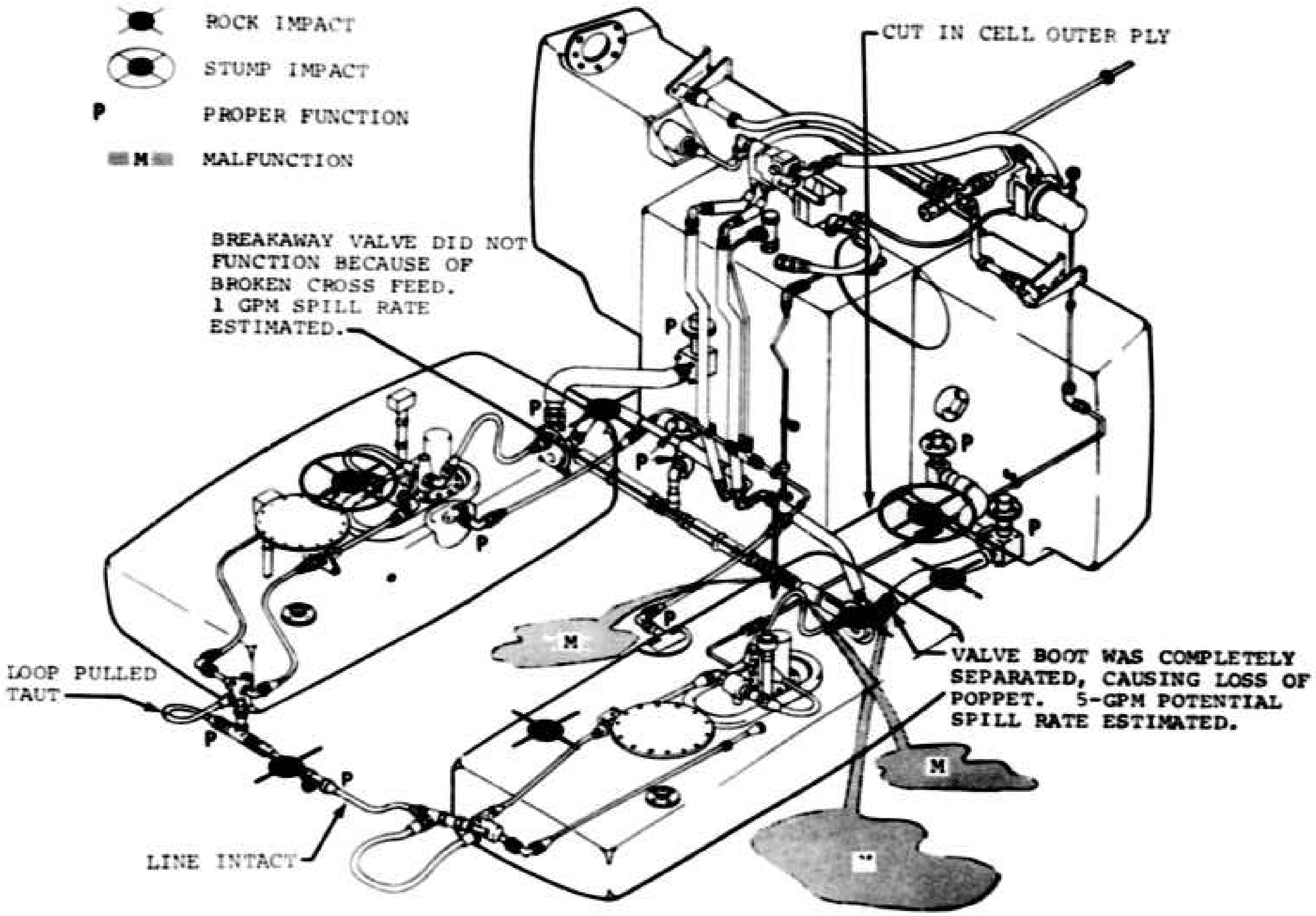


Figure 42. Fuel System Impact Reaction (Test 3).

TEST 3 FUEL SYSTEM DAMAGE ASSESSMENT

After the initial leakage assessment of the bottom was made, a damage evaluation was made on the top side of the system. The entire right-hand underfloor fuel cell cavity was displaced upward by the stump to a level approximately 20 inches from the ceiling. It then returned to a level about 15 inches above its original position (see Figure 43). This, coupled with the boulder impact on the landing gear cross tube, caused the aft inlet/outlet breakaway valve to separate. Both halves sealed. The boost line and aft cross-over outlets were still intact. The inboard side of the deck panel covering this underfloor cell separated from the bulkhead while the outboard seam held its rivets, carrying the entire outboard structure with it as it was thrust upward (Figure 43).

Figure 43. Deflection of Aft End of Right-Hand Underfloor Cell (Test 3).

Left-Hand Underfloor Cell

The deck panel above the left-hand underfloor cell was still in place and did not permit a view of the damage. Since no

further data could be collected from the top side, the aircraft was rolled onto its right side and the damage assessment continued. The underside of the cell had received a glancing blow from a boulder on its very inboard edge. The only reaction from this was the separation of the frangible connector of the forward drain line. Figure 44 shows this and other impact points on the bottom of the fuselage. Another boulder struck the inboard side of the aft inlet/outlet fitting of this cell. This and/or the rock directly behind it caused the inlet/outlet breakaway valve to separate. The forward half of the valve sealed, but the aft half lost its poppet. The line connected to this valve was not draining because both aft drain valves on this side had functioned and sealed. A close inspection of the inlet/outlet breakaway valve showed that the boot had failed at the seat, allowing the poppet unimpeded ejection.

Figure 44. View Showing Impact Points on Underside of Fuselage (Test 3).

As in the case of the right-hand underfloor cell, the boost line remained intact, as it was missed by the impact which

separated the breakaway valve. The aft cross-over connection to the inlet/outlet fitting remained intact but was separated (by the same boulder that struck the fitting) at its interface with the in-line breakaway valve. Figure 45 shows the separated line.

Figure 45. Separated Aft Cross-Feed Line (Test 3).

Left Vertical Cell

The left vertical cell remained virtually untouched by the impact. The stump placed to strike the rear of the aft cross tube made a direct hit on the tube. The stump was splintered, but segments were driven rearward into the structure directly between the left vertical drain valve and the center drain valve. The left drain valve was partially separated, apparently by the pull of the hose when it was driven upward by the cross tube. The valve boot had been cut at its forward end, but the poppets had closed.

## Forward Cross-Feed Line

The forward cross-feed line was struck by a boulder which protruded 8 inches into the aircraft at its point of maximum deflection. The line did not fail in this test as it did in Test 1. The 6-inch difference in height of the boulders (the Test 1 forward boulder intruded about 14 inches) apparently was the difference between success and failure of this point.

## Structural Damage

The bottom edges of the fuel cell cavities were torn and separated by rivet failure in several areas, exposing the fuel cells to jagged metal and possible cutting (only minor nicking actually occurred).

## TEST 3 HAZARD ASSESSMENT

## Structural Deformation

Neither the engine nor the transmission represented a hazard in this test. The right side of the aircraft above the stump impact point would have been a major hazard. An occupant sitting above the right-hand underfloor cell probably would have been smashed against the ceiling.

## Electrical Ignition Sources

The main electrical bundle which passes over the aft cross-feed line was driven upward by impact of the landing gear cross tube. One of the high-amperage lines was cut to its core, either by a torn edge of the landing gear cross-tube housing or by the hose connection of the in-line breakaway valve. Whatever the cause, the result was that the broken end of the fuel line was probably in direct contact with a broken electrical wire. Thus, the probability of ignition in this area was very high.

## Fuel Spillage

The actual fluid spillage rate from the severed aft cross-feed line probably did not exceed 2 gallons per minute at any time after the initial pulse. This rate gradually diminished as a function of the increasing negative pressure inside the tanks caused by isolation (sealed vent valves and drain lines) of the forward cell from the rest of the system. It is questionable whether this spillage would have caused a major hazard to the aircraft or its occupants, despite the fact that the structure was opened up into the cargo compartment, thereby eliminating the factor of isolation.

## TEST 3 HAZARD ANALYSIS

Table II lists the components under study in Test 3 and gives the impact reaction of each. The last column in Table II provides a hazard rating for each component based only on individual performance in Test 3.

| TABLE II. TEST 3 COMPONENT REACTIONS AND HAZARD RATINGS | | |
|---|---|---|
| Component | Reaction | Rating* |
| Forward cross-feed | Contoured around rock | Low Hazard |
| Forward cross-feed loops | Right hand stretched | Low Hazard |
| Left-hand forward drain | No damage | Safe |
| Left-hand inlet/ outlet fitting | No damage from direct impact on rock | Safe |
| Left-hand inlet breakaway valve | Poppet came out from rock impact | Moderate Hazard |
| Left-hand vent valve | Sheared and sealed | Safe |
| Right-hand vent valve | Sheared and sealed | Safe |
| Right-hand inlet valve | Separated and sealed | Safe |
| Right-hand boost pump | Registered shear load on edge by stump | Safe |
| Aft right-hand vertical cell drain valve | Partial separation and probable poppet closure | Safe |
| Aft left-hand vertical cell drain valve | Partial separation and probable poppet closure | Safe |
| Center vertical cell forward drain valve | Partial separation and probable poppet closure | Safe |

| TABLE II. CONTINUED | | |
|---|---|---|
| Component | Reaction | Rating* |
| Center vertical cell aft drain valve | Partial separation and probable poppet closure | Safe |
| Cell-to-cell interconnects | Remained intact | Low Hazard |
| Center vertical cell tank wall | aluminum skin cut through outer ply | Safe |
| Aft cross-over | Line broken adjacent to breakaway valve | Moderate Hazard |
| Fire wall to filter fuel line | Remained intact | Safe |
| Filter to engine fuel line | Stretched but intact | Safe |
| Right-hand boost line outlet | Narrowly missed by rock. Remained intact | Low Hazard |
| Left-hand boost line outlet | Narrowly missed by stump. Remained intact | Low Hazard |

*Values in Column 3 are based on experience of one test and do not necessarily represent a statistically supported hazard rating.

An additional potential hazard occurred in the same area in the form of the broken aft inlet/outlet breakaway valve. Had not both the left-hand aft drain valves sealed, the fluid loss would have approached 5 gallons per minute. Since the probability of both of these aft drain valves functioning was low, it must be assumed that this represented a sizeable potential hazard.

## DISCUSSION OF GENERAL HAZARD POTENTIAL

The following is a general discussion of the hazards representative of the cumulative data from all three tests. It is primarily devoted to fuel spillage, but also deals with structural hazards. Some extrapolations are made in that it not only treats the test results but also delves into probability based on realistic rough-terrain landing conditions. Each of the potential hazards is covered with respect to its relative hazard level in the aircraft.

All components are viewed with respect to their relationship to the total aircraft system as it would be performing in actual flight. This also assumes that the helicopter is descending within the following flight envelope:

| | |
|---|---|
| Angle of impact | 90 - 60 Degrees Forward |
| Yaw | 0 - 30 Degrees |
| Pitch | 15 - 15 Degrees |
| Roll | 15 - 15 Degrees |

### HIGHEST HAZARD - UNDERFLOOR CELLS INLETS/OUTLETS

The highest hazard rating is assigned not just to a specific component but to a general area, or, more specifically, to two general areas: the left- and right-hand inlets/outlets of the underfloor cells. Data from both Test 1 and Test 3 attest to a wide array of potential failure points clustered around these inlet/outlet fittings. These are as follows (not necessarily in order of their individual contribution to the overall hazard):

1. Boost line outlet
2. Inlet/outlet casting
3. Cross-feed outlet
4. Breakaway valve

### BOOST-LINE OUTLET

The boost-line outlet represents a sizeable hazard because of the possibility of fuel being sprayed from the broken fitting if the boost pump continues to run. This line is easily overloaded because of its lack of free length. Although it possesses some slack beyond the buttline 14 bulkhead, the

probability of its movement being restricted by the bulkhead is very high. The underfloor fuel cell also has a tendency to be thrown upward and forward at the same time the line is being held fast by the collapsing bulkhead. This suggests the need for more slack in the boost line before it passes through the buttline or, better, a breakaway valve.

INLET/OUTLET CASTING

The inlet/outlet casting indicated a very high hazard rating when loaded in bending as shown in Figure 22. The casting is a 356 aluminum alloy with a rated ultimate tensile strength of 33,000 psi, a yield stress of 25,000 - 28,000 psi, and a shear strength of 25,000 psi. A simple failure analysis of this fitting based on beam bending indicates that a 4,000-pound load applied between the top two bolts is sufficient to initiate failure. The actual load is probably somewhat lower due to stress concentration at the sharp transition between the flange and boost line exit cylinder. This appears to be the only real weakness in the casting. High impact loads applied to the base of the casting in three other tests (boulder impact on the left fitting in Test 1 and on both fittings in Test 3) showed no evidence of failure. Thus, it appears that the problem lies in impact on the boost pump plate. This drives the cell upward, putting the entire load on the casting.

To cope with this situation, the fitting should be strong enough to tear through the structure which surrounds it without damage to itself. This would necessitate a change to a forging, preferably of a fairly ductile material (2024-T-3), or a redesign of the transition of the flange to reduce the bending load.

CROSS-FEED OUTLET

Separation of only one cross-feed outlet (right-hand outlet, Test 1) would seem to indicate a relatively low hazard for this fitting; however, close inspection showed incipient failure (evidenced by collapse or buckling of the fitting end) of both the Test 1 left-hand cross-feed outlet fitting and of the Test 3 right-hand fitting. The only fitting of this group that did not show evidence of excessive loading was the Test 3 left-hand fitting, probably because the cross-feed line failed only 6-1/2 inches away (at its juncture to the in-line breakaway valve).

The effect on the boost line restriction from bulkhead collapse also pertains to the cross-feed line, indicating that the breakaway valve placed between the buttline 14 bulkheads is not particularly effective in preventing line fitting failure at the tank exit.

INLET/OUTLET BREAKAWAY VALVE

The breakaway valve connecting the underfloor cells to the outboard vertical cells malfunctioned in Test 1 and Test 3. The more serious of these two malfunctions was the loss of the poppet from the left-hand Test 3 valve, leaving the valve wide open. The problem in this valve design appears to be twofold: (1) the throat diameter of the valve is larger than the poppet, and (2) the rubber boot which doubles as a sleeve and a valve seat is the only restraint to keep the valve in place. In both malfunctions, at least part of the seat was torn out of the valve. When the entire seat is removed (as was the case in Test 3), the poppet is driven out through the open throat.*

AFT CROSS-OVER TUBE BREAKAWAY VALVE

The breakaway valve located toward the left terminus of the aft cross-over tube represents a hazard in that its strength appears to be too high when compared to the strength of the hose attached to it. This was especially evident in Test 3, where the line separated at its juncture to the breakaway valve. This condition probably existed largely because of the side loading of the line, which prevented axial separation of the valve. The fact that this valve can only separate axially is probably its major weakness.

Evidence of excessive valve separation strength also appeared in Test 1, in which the valve appeared to have been loaded axially. Even though the valve separated, the right-hand cross-feed hose terminus was broken. There was no structural collapse on the right side of buttline 14 to cause a major restriction of line movement, again indicating excessive valve strength. As mentioned earlier, the left-hand cross-feed terminus of Test 1 also showed signs of overload, again pointing to this valve as a potential problem. One of the main causes for concern with respect to malfunction in this area is that the breakaway valve is immediately adjacent to the power cable system. In Test 3 this would have represented a major ignition hazard; fuel was probably spilling directly onto the high-amperage cable during the crash pulse. At least two deep gouges in the cable demonstrated the potential for arcing.

CELL-TO-CELL INTERCONNECTS

The cell-to-cell interconnects represent a hazard from the standpoint that massive spillage occurs if struck by a ground

*When informed of this situation, the valve manufacturer indicated that the problem of seat failure had been corrected in all valves subsequent to this lot.

protuberance higher than 14 inches. Fortunately, the probability of a direct strike in this area is relatively low, especially if there is a forward component in the striking attitude. The reason is that the relatively small critical impact area of the fuel cells is hidden behind the landing gear cross tube (Figure 46). Impact on this cross tube would be sufficient to transmit the concentrated impact load uniformly to both cells, thus greatly diminishing the hazard. This is not to say that cell-to-cell breakaway valves are not desirable. The threat still remains that failure of one of these fittings would greatly increase the probability of catastrophic fire.

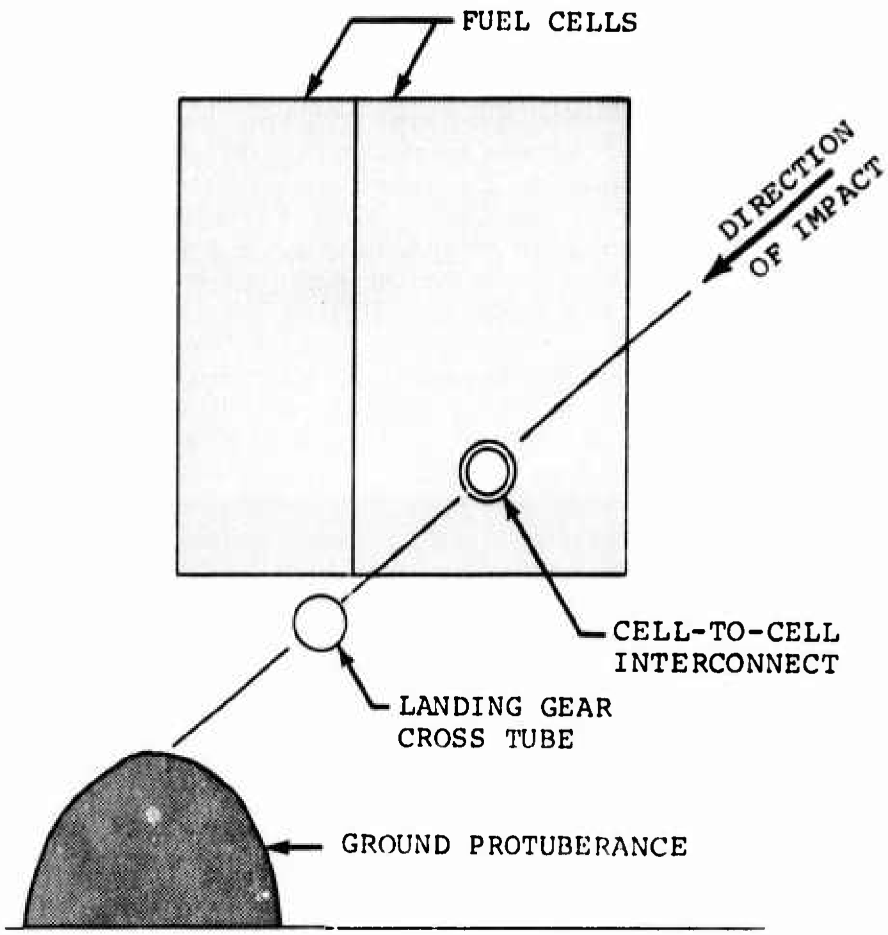


Figure 46. Relationship of Landing Gear Cross Tube and Aft Cells.

BOOST PUMP ACCESS PLATES

The boost pump access plates represent a hazard, not from their spillage potential but from their ignition potential as mentioned in the results discussion of Test 1.

FORWARD CROSS-FEED LINE

The forward cross-feed line represents only a minor hazard because of the low probability of impact damage as demonstrated in Test 3. Even if the line were separated as in Test 1, the fluid loss would not pose a major threat to survival of occupants. The loops in the line appear to be long enough to cope with fuel cell displacement.

AFT BREAKAWAY DRAIN VALVES

All four drain valves in the vertical cells performed satisfactorily. While the design of the valve suggests a potential hazard due to partial separation and boot failure causing minor leakage, there was no evidence in either Test 1 or Test 3 to give cause for concern.

FUEL-FILTER-TO-ENGINE LINE

In none of the three tests was there evidence which would cause any concern about the integrity of the line connecting the fuel filter to the engine. (USABAAR data also substantiates the low probability of complete engine separation in a survivable crash). While it appears desirable to have a breakaway valve in this line, the data does not substantiate any great urgency for its being pressed into operational use.

VENT LINE

The only leakage in Test 2 came from the vent line. This is a common occurrence in roll-over accidents, and the vent line must be considered a hazard. The installation of vent valves in the system would greatly increase its resistance to postcrash fire.

FUEL CELLS

Based on the three tests, there is no evidence of weakness in any part of the fuel cells. The one suspected weak point (the space between the boost pump fitting and the inlet/outlet fitting) proved to be sound, both when subjected to direct impact on the boost pump and when the impact load was applied from the direction of the inlet/outlet fitting.

## EFFECTS OF ACCELERATIONS ON FUEL SYSTEM

Acceleration data from Test 3 revealed a profile of peak accelerations ranging from 14 to 200G. Figure 47 presents a profile of peak acceleration taken from accelerometers mounted on the solid structure of the aircraft. The resultant accelerations seen by the underfloor ranged between 70 and 200G. It is assumed that direct rock or stump impact on components (such as the aft inlet/outlet valve) would have resulted in an acceleration load near the maximum, whereas the acceleration transmitted through the structure probably would have been somewhat lower. Even assuming the maximum G level and disregarding the direction of the load or the mass of the hose supported by the fitting, it is doubtful that any of the breakaway valves would have been functioned by accelerations alone.

The results of Test 2 also suggest that this is true (no valves functioned), although there were no acceleration data obtained in this test to support such an assumption.

A single bi-response pressure transducer was installed during each test. During the first test, the lead was broken at impact. Tension in the lead wire was the triggering cause in the second test. A continuous record was obtained throughout the impact sequence during the third test, but no apparent change in pressure was observed. There was a very minor pulse (<10 psi maximum) at the instant of impact. It is concluded that the data obtained are probably not representative and that no conclusions can realistically be made.

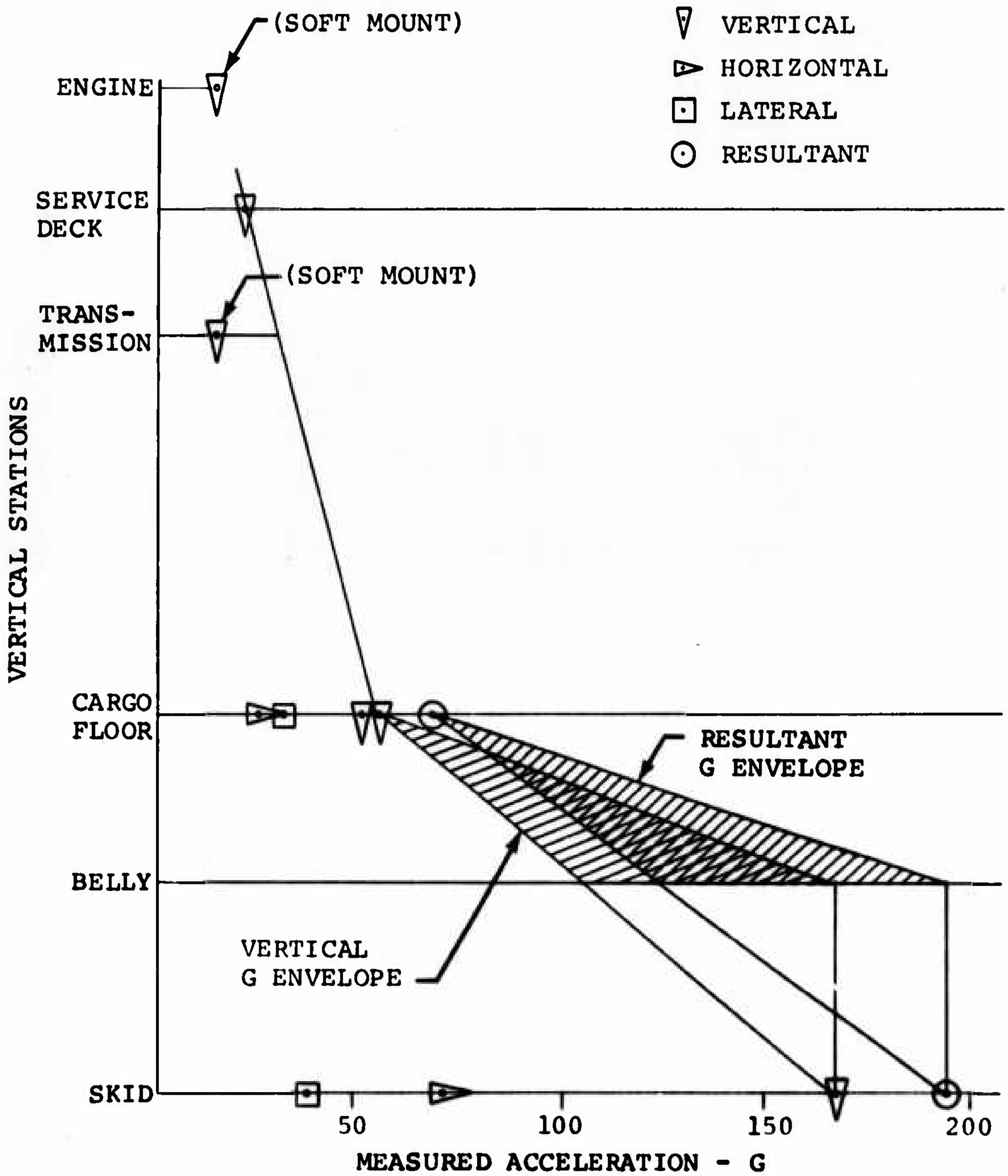


**Figure 47. Test 3 Peak Acceleration Profile.**

## CONCLUSIONS

Based on the results of this test program, the following conclusions were drawn:

### FUEL SYSTEM

1. The UH-1D/H helicopter crashworthy fuel system is highly resistant to failure in any survivable accident.

2. The fuel cells have a very high resistance to failure, even from concentrated loads imposed by ground protuberances.

3. The fuel cell fittings are highly resistant to concentrated loading; the only minor weakness discovered in this program was the boost pump access fitting. Direct impact on a ground protuberance will induce some minor leakage and simultaneously create an ignition hazard with the arcing of damaged boost pump lead wires.

4. The casting attached to the underfloor inlet/outlet fitting represents a significant hazard, as it is highly susceptible to breakage when impact is made on the boost pump fitting. The hazard is amplified by the addition of an electrical ignition source at the boost pump.

5. The inlet/outlet breakaway valves used in these tests are not reliable and deserve further attention.

6. The lack of a main vent valve is an ignition hazard.

7. The lack of a breakaway valve in the fuel line from the fuel filter to the engine is a minor hazard.

8. The underfloor vent valves and aft drain valves are considered safe.

9. The forward cross-feed line constitutes a very minor hazard. The cross-feed slack loops are an adequate substitute for cell-to-line breakaway valves in this area.

10. The recessed sump drain valves are adequate.

11. The boost line outlets are a sizeable hazard because of their tendency to pull out of the underfloor cells, or to fail before the in-line breakaway valve separates.

12. The aft cross-feed line constitutes a sizeable hazard because of its tendency to pull out of the underfloor cells.

## FRANGIBLE CONNECTORS

The frangible connectors performed satisfactorily in all areas of tank-to-structure displacement.

## ENGINE

The engine will invariably buckle its mounts in an upper-survivability level impact, but the engine tends to remain with the aircraft. The engine fuel line is subject to some elongation, but the probability of its being severed is not extremely high.

## TRANSMISSION

The transmission tends to stay in place in dead drop tests. A dead load is not an adequate substitute for the inertial loading induced by rapidly rotating rotor blades.

## STRUCTURE

In a rough-terrain landing, the probability of structural failure of the floor above the underfloor cells is an extreme impact hazard to occupants above them.

## RECOMMENDATIONS

Based on the results of this test program, it is recommended that:

1. The aft inlet/outlet casting be redesigned to include a change from a casting to a forging and/or to eliminate the sharp angle of transition between the top flange and the exit ports.

2. The inlet/outlet breakaway valves currently being placed in the systems be sampled for seat failure. If the problem persists, consideration should be devoted to replacing the present valve with an omnidirectional breakaway valve.

3. A review be made of current breakaway valve designs which would permit their replacement in the boost line outlets from the fuel cells.

4. A review be made of current breakaway valve designs which would permit their placement in the boost line outlets from the fuel cells in the aft cross-feed line outlets.

5. Samples of the aft cross-feed in-line breakaway valves be strength tested to determine if the breakaway strength is actually too high for the line. If this is the case, the strength should be reduced, or (better) the valve should be replaced with an omnidirectional breakaway valve.

6. A breakaway valve be placed in the filter-to-engine fuel line.

# APPENDIX I

## STATIC TESTING OF MIL-H-58089(Av) HOSE AND SEVERAL HOSE END-FITTING COMBINATIONS

### OBJECTIVE

The objective of this test series was to determine the failure method and ultimate separation load for various hose and hose end-fitting combinations which had not been previously tested.

### TEST ITEM

The test item consisted of medium-pressure hose with an end fitting attached to one end. Twelve inches of hose was permitted to extend beyond the end fitting. The hose had a seamless inner tube made of synthetic compound. This tube was reinforced with a partial stainless-steel wire braid impregnated in the outer surface of the tube wall. A sheath made of tightly braided stainless-steel wire encased the reinforced inner tube. The end fittings tested were of three types: (1) straight, (2) 90-degree tube elbow, and (3) 90-degree forged elbow. The sizes tested were 1/4 inch, 1/2 inch, 5/8 inch, 3/4 inch, 1 inch, and 1-1/4 inch. All end fittings were made of anodized aluminum except for the nut and nipple of the 1/4-inch fittings, which were made of cadmium-plated steel.

Figure 48 illustrates the various hose and end-fitting combinations which were tested. Figures 49 through 61 present pretest and posttest views of the test items.

### TEST METHODOLOGY

All tests performed in this test series were static tests in which a 10,000-pound tensile test machine was used to apply the failure loads. The end fitting of each test item was attached to the movable crosshead of the test machine by a suitable attachment fixture. This fixture used a steel adapter fitting for the attachment of the hose end fitting in all sizes. The upper end of each test hose was retained by a special clamping fixture which provided a firm grip on the hose and also prevented fluid leakage. Each test specimen was kept filled with water from a pressurized reservoir to provide a visual means of leakage detection. Figures 49, 51, 53, 55, 57, and 59 illustrate the test setups.

All loads were applied at a rate of 1 inch per minute. Prior to and during load application, an internal fluid pressure of 5 psig $\pm 1$ psig was maintained on the test item. Load application was maintained until the test item failed or until fluid

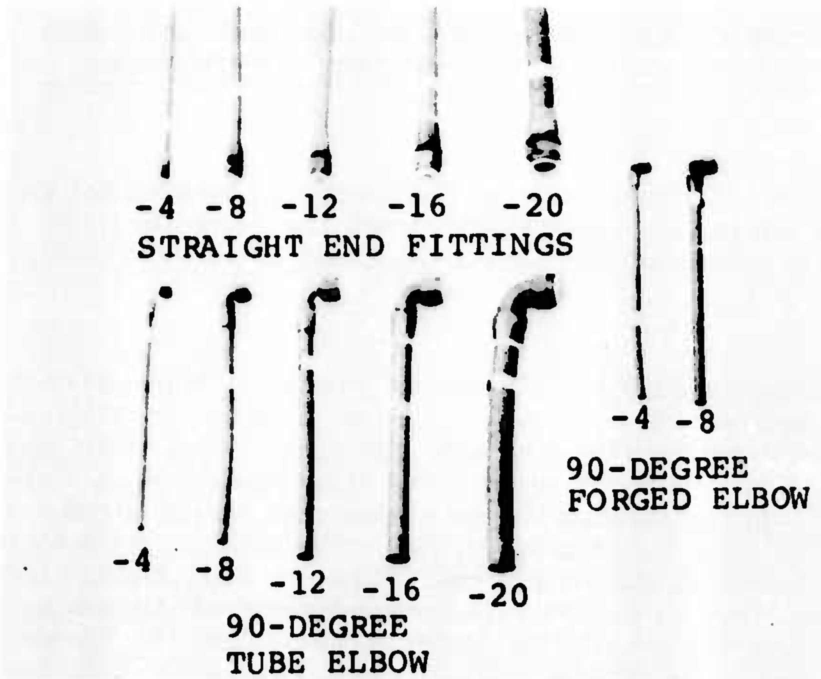


Figure 48. Typical MIL-H-58089 Hose and End-Fitting Combinations.

loss rate reached a steady stream. At that point, the applied load was recorded. If complete separation had not occurred, loading was continued until failure and additional load values were recorded, if greater than the original value. The lowest value obtained was used in the specification data. The total elongation of the test specimen was measured and recorded. All tests were performed at room temperature.

All tests were conducted on the hose and end-fitting configurations exactly as supplied by the manufacturer.

## INSTRUMENTATION

The loads applied to the test items were measured by a load cell located between the upper clamping fixture and the top of the test machine. For the smaller test items where failure loads were anticipated below 1,000 pounds, a 0- to 1,000-pound load cell was used. The other test items used a 0- to 4,000-pound load cell.

The load cell data were recorded on a light spot recording oscillograph. Chart speed was 1/2 inch per second.

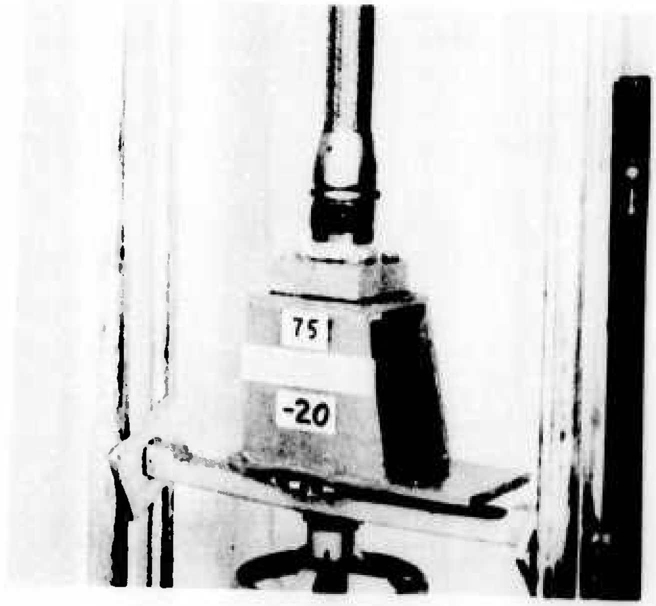


Figure 49. Typical Tension Load Application Method on Hose and Straight End-Fitting Combination.


Figure 50. Typical Straight End-Fitting Combination Following Tension Load Application.

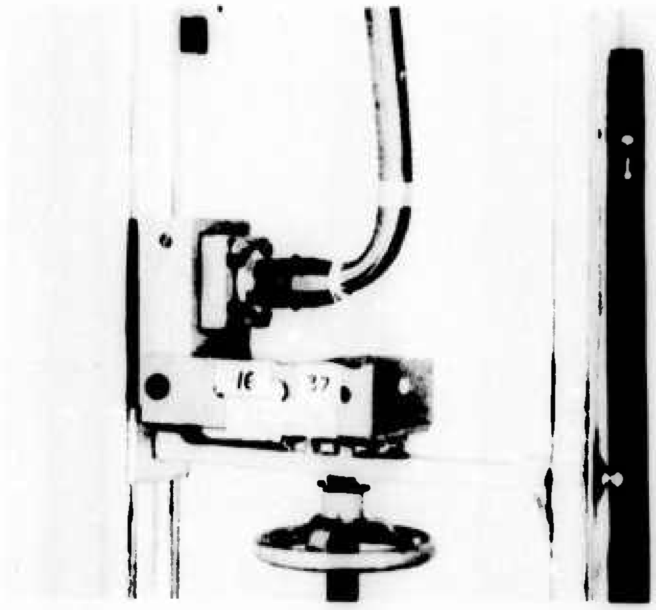

Figure 51. Typical Bending Load Application Method on Hose and Straight End-Fitting Combination.

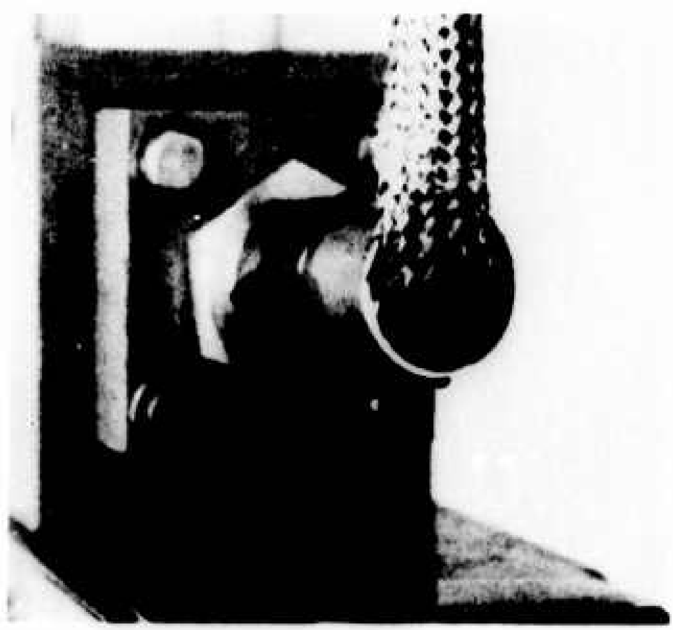

Figure 52. Typical Straight End-Fitting Combination Following Bending Load Application.

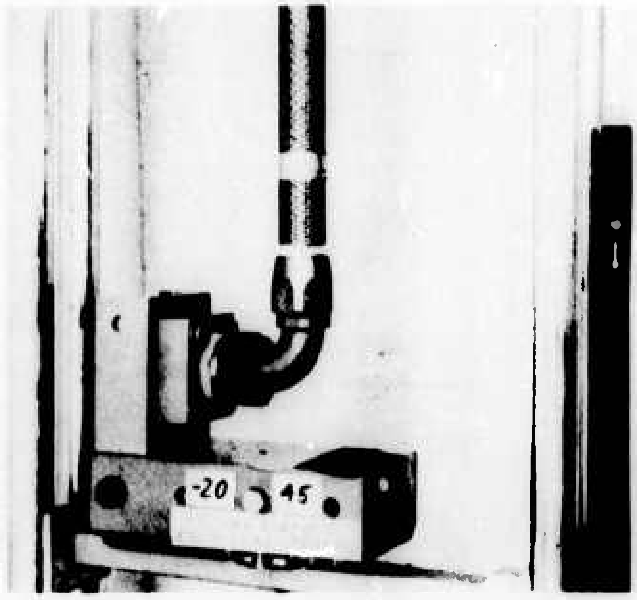

Figure 53. Typical Tension Load Application Method on Hose and Tube Elbow End-Fitting Combination.

Figure 54. Typical Tube Elbow End-Fitting Combination Following Tension Load Application.

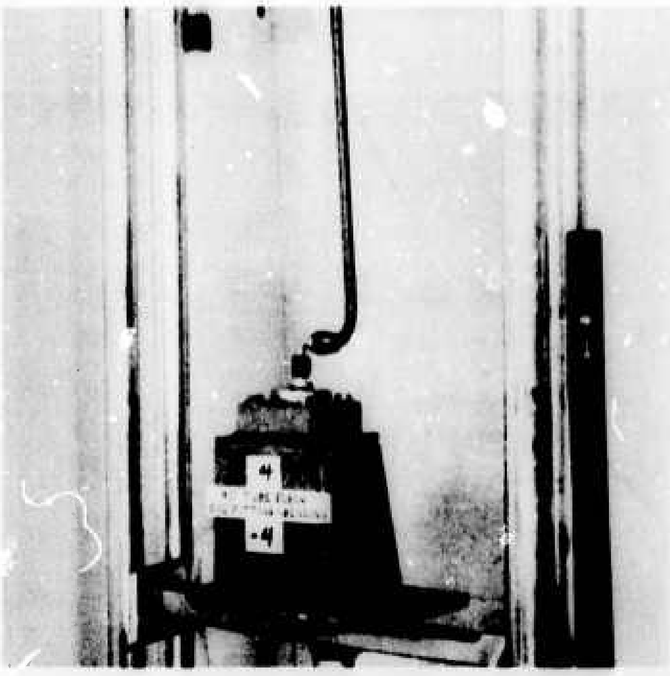

Figure 55. Typical Bending Load Application Method on Hose and Tube Elbow End-Fitting Combination.

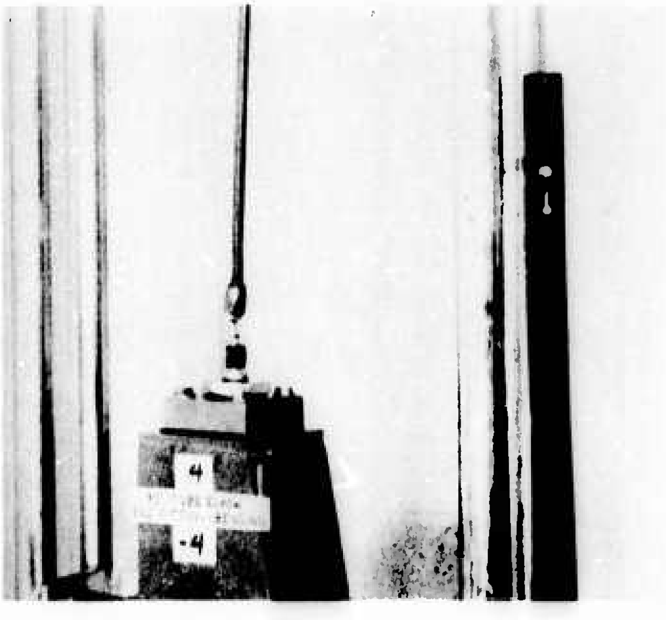

Figure 56. Typical Tube Elbow End-Fitting Combination Following Bending Load Application.

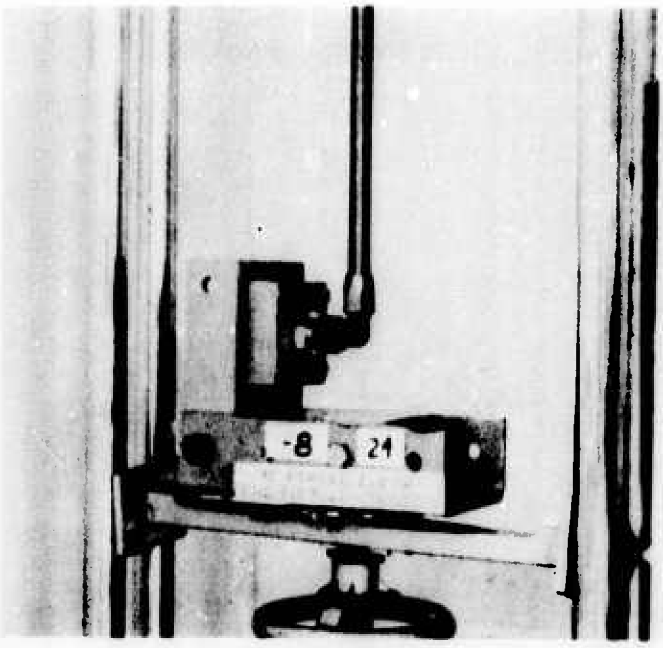


Figure 57. Typical Tension Load Application Method on Hose and Forged Elbow Combination.

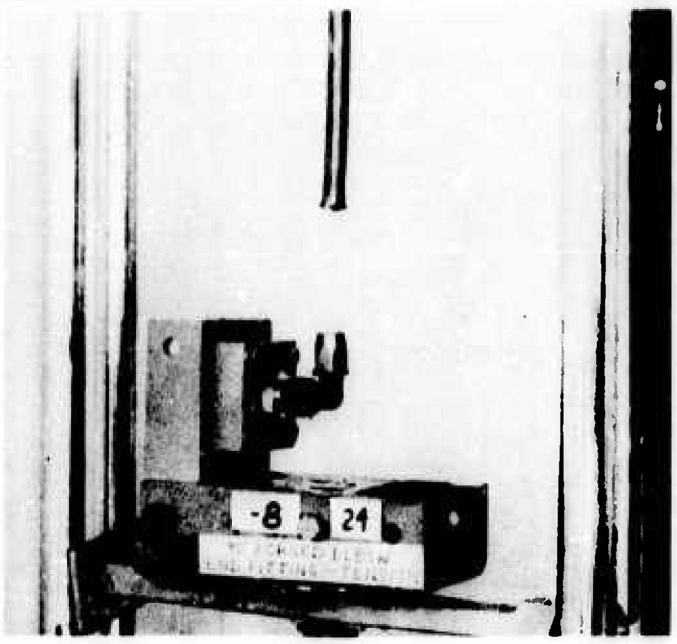


Figure 58. Typical Forged Elbow End-Fitting Combination Following Tension Load Application.

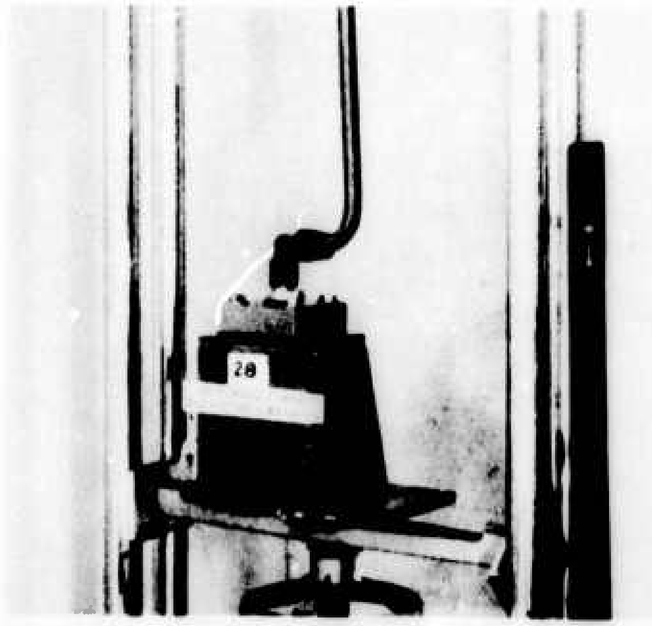


Figure 59. Typical Bending Load Application Method on Hose and Forged Elbow Combination.

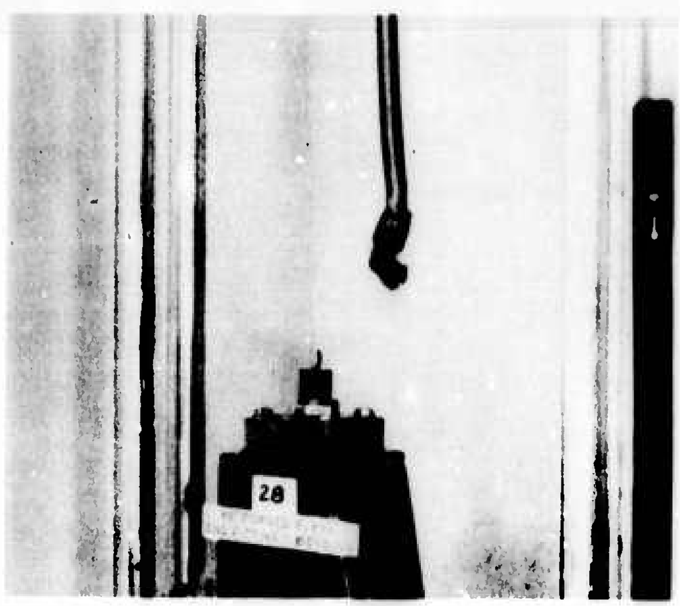


Figure 60. Typical Forged Elbow End-Fitting Combination Following Bending Load Application.


Figure 61. Typical Varied Angle Load Application Method on Straight End-Fitting Combination Just Prior to Fluid Spillage.

Black and white 35mm photographs were taken of typical test items and each setup before and after each test.

RESULTS

The test specimens were subjected to a total of 81 static loading tests: 37 in straight tension, 24 in 90-degree bending, and 20 at varying degrees of bending. Typical test items following load application may be seen in Figures 50, 52, 54, 56, 58, and 60.

None of the three types of fittings tested experienced any spillage prior to hose pullout when loaded in a tension mode. Spillage occurred prior to ultimate load in only two of the 90-degree elbow configurations tested. The hose end-fitting configuration most affected by fluid loss prior to ultimate load was the straight end fitting when tested in the bending mode.

Tension and bending test data are presented in Tables III, IV, and V. Table VI contains data obtained when the angle of load application was varied.

The data generated from this test series compare favorably with existing static test data on the subject hose, i.e., hose tests conducted in 1966 and in 1968. The 1966 test series used hose with only one end fitting attached. No fluid pressure system was used, and the load rate was 20 inches per minute. The 1968 test series used complete hose assemblies (end fittings on both ends) loaded at a rate of 1 inch per minute. Fluid pressure was not used in the 1968 test series.

The combined results of all three test series (1966, 1968, and the series reported herein) may be found in Tables VII, VIII, and IX. It should be noted that, since fluid pressure was used in only one test series, all values given are for ultimate loads. Based on the results of the test series reported herein, the only configuration which would be expected to have its values lowered if fluid spillage values were used would be the straight end fittings when loaded in the bending mode (Table III).

In general, the test results complemented existing test data. Hose sizes which had not been previously tested produced values compatible with existing data with two exceptions: (1) -4 (1/4 inch) 90-degree tube elbows and (2) -8 (1/2 inch) straight end fittings. The -4 90-degree tube elbows, when subjected to a bending load, failed at values only 50 percent of those of a previous test series. Tension loads on five -8 straight end fittings resulted in widespread values.

TABLE III. MIL-H-58089 HOSE AND STRAIGHT END-FITTING STATIC TEST RESULTS

| TENSION* 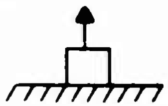 | | | BENDING 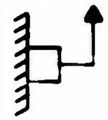 | | | |
|---|---|---|---|---|---|---|
| | | | **Fluid Spillage** | | **Ultimate** | |
| **Fitting Size** | **Individual Loads (lb)** | **Average Loads (lb)** | **Individual (lb)** | **Average (lb)** | **Individual (lb)** | **Average (lb)** |
| -4 | 780<br>800<br>810 | 797 | 450<br>482<br>580 | 504 | 450<br>525<br>600 | 525 |
| -8 | 600<br>710<br>750<br>1160<br>1275 | 899 | 740<br>880<br>680 | 769 | 750<br>900<br>1190 | 947 |
| -10 | 1760 | 1760 | - | - | - | - |
| -12 | 2075 | 2075 | 1060 | 1060 | 1475 | 1475 |
| -16 | 2025<br>2250 | 2138 | 1460<br>1720 | 1590 | 2050<br>2050 | 2050 |
| -20 | 2700<br>2780<br>3140 | 2873 | 1600<br>1835 | 1718 | 2100<br>2125 | 2112 |

***Tension loadings pulled hose out of end fitting, resulting in fluid spillage** simultaneous with ultimate load or immediately following ultimate load.

TABLE IV. MIL-H-58089 HOSE AND TUBE ELBOW STATIC TEST RESULTS

| TENSION* 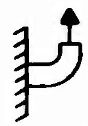 | | | BENDING 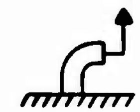 | | | |
|---|---|---|---|---|---|---|
| | | | **Fluid Spillage** | | **Ultimate** | |
| **Fitting Size** | **Individual Loads (lb)** | **Average Loads (lb)** | **Individual (lb)** | **Average (lb)** | **Individual (lb)** | **Average (lb)** |
| -4 | 430<br>475<br>575<br>750 | 557 | 180<br>200<br>210<br>250 | 210 | 180<br>200<br>210<br>250 | 210 |
| -8 | 1210<br>1260<br>1340 | 1270 | 350<br>375<br>425 | 383 | 350<br>375<br>425 | 383 |
| -12 | 1960<br>1975<br>2050 | 1995 | - | - | - | - |
| -16 | 2570<br>2660<br>2690 | 2640 | 860 | 860 | 1150 | 1150 |
| -20 | 2300<br>2340<br>2620 | 2420 | 1200 | 1200 | 1250 | 1250 |

***Tension loadings pulled hose out of end fitting, resulting in fluid spillage simultaneous with ultimate load or immediately following ultimate load.**

TABLE V. MIL-H-58089 HOSE AND FORGED ELBOW STATIC TEST RESULTS

| TENSION* 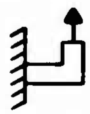 | | | BENDING** 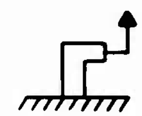 | | | |
|---|---|---|---|---|---|---|
| | | | Fluid Spillage | | Ultimate | |
| Fitting Size | Individual Loads (lb) | Average Loads (lb) | Individual (lb) | Average (lb) | Individual (lb) | Average (lb) |
| -4 | 525<br>570<br>1000 | 698 | 260 | 260 | 260 | 260 |
| -8 | 760<br>870<br>920 | 850 | 660<br>825<br>825 | 770 | 660<br>825<br>825 | 770 |

*Tension loadings pulled hose out of end fitting, resulting in fluid spillage simultaneous with ultimate load or immediately following ultimate load.
**All failures occurred when "B" nut snapped.

TABLE VI. EFFECT OF VARYING LOAD ANGLE ON HOSE AND STRAIGHT END FITTING

| Fitting Size | Load Angle and Value (Pounds) | | | | | | | | | | | | | |
|---|---|---|---|---|---|---|---|---|---|---|---|---|---|---|
| | TENSION 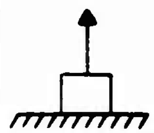 | | 15° 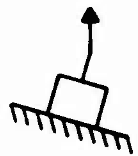 | | 30° 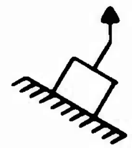 | | 45° 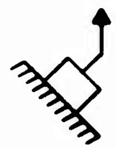 | | 60° 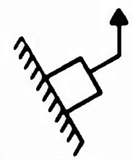 | | 75° 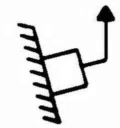 | | 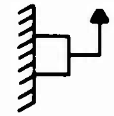 90° BENDING | |
| | Spillage | Ultimate | Spillage | Ultimate | Spillage | Ultimate | Spillage | Ultimate | Spillage | Ultimate | Spillage | Ultimate | Spillage | Ultimate |
| -4 | 797 | 797 | 675 | 675 | 675 | 675 | 755 | 800 | 795 | 860 | 630 | 875 | 504 | 525 |
| -8 | 899 | 899 | 1300 | 1360 | 1300 | 1300 | 1150 | 1400 | 845 | 1310 | 890 | 1160 | 769 | 947 |
| -12 | 2075 | 2075 | 1975 | 1975 | 1300 | 1740 | 1385 | 1510 | 1235 | 1750 | 910 | 1410 | 1060 | 1475 |
| -20 | 2873 | 2873 | 2620 | 2750 | 2225 | 2345 | 1585 | 2115 | 1875 | 2420 | 1255 | 1900 | 1718 | 2112 |

TABLE VII. COMBINED TEST DATA FROM STATIC TESTS OF MIL-H-58089 HOSE AND STRAIGHT END FITTINGS

| Fitting Size | TENSION 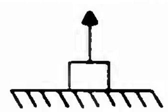 | | | | | | | | BENDING* 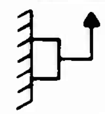 | | | | | | | |
|---|---|---|---|---|---|---|---|---|---|---|---|---|---|---|---|---|
| | Test Series | | | | | | | | Test Series | | | | | | | |
| | 1966 | | 1968 | | Current | | Total | | 1966 | | 1968 | | Current | | Total | |
| | 20"/Min No Fluid | | 1"/Min No Fluid | | 1"/Min With Fluid | | | | 20"/Min No Fluid | | 1"/Min No Fluid | | 1"/Min With Fluid | | | |
| | **No.** | **Avg. Load (lb)** | **No.** | **Avg. Load (lb)** | **No.** | **Avg. Load (lb)** | **No.** | **Avg. Load (lb)** | **No.** | **Avg. Load (lb)** | **No.** | **Avg. Load (lb)** | **No.** | **Avg. Load (lb)** | **No.** | **Avg. Load (lb)** |
| -4 | 0 | - | 0 | - | 3 | 797 | 3 | 797 | 0 | - | 2 | (550) | 3 | 525 | 5 | 535 |
| -6 | 8 | 752 | 1 | 800 | 0 | - | 9 | 757 | 2 | 555 | 2 | 686 | 0 | - | 4 | 620 |
| -8 | 0 | - | 0 | - | | 899 | 5 | 899 | 0 | - | 0 | - | 3 | 947 | 3 | 947 |
| -10 | 12 | 1720 | 0 | - | 1 | 1760 | 13 | 1723 | 12 | 927 | 0 | - | 0 | - | 12 | 927 |
| -12 | 0 | - | 1 | 1790 | 1 | 2075 | 2 | 1932 | 0 | - | 2 | 1385 | 1 | 1475 | 3 | 1415 |
| -16 | 4 | 2597 | 0 | - | 2 | 2138 | 6 | 2922 | 1 | 1770 | 0 | - | 2 | 2050 | 3 | 1957 |
| -20 | 0 | - | 1 | 3070 | 3 | 2873 | 4 | 2922 | 0 | - | 2 | 2175 | 2 | 2112 | 4 | 2144 |
| Total Tests | 24 | | 3 | | 15 | | 42 | | 15 | | 8 | | 11 | | 34 | |

*All data are ultimate loads (loads at point of spillage, if lower than ultimate, are not included).

TABLE VIII. COMBINED TEST DATA FROM STATIC TESTS OF MIL-H-58089 HOSE AND 90-DEGREE TUBE ELBOW END FITTINGS

| Fitting Size | TENSION 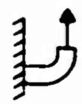 | | | | | | | | BENDING* 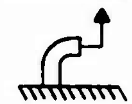 | | | | | | | |
|---|---|---|---|---|---|---|---|---|---|---|---|---|---|---|---|---|
| | Test Series | | | | | | | | Test Series | | | | | | | |
| | 1966 | | 1968 | | Current | | Total | | 1966 | | 1968 | | Current | | Total | |
| | 20"/Min No Fluid | | 1"/Min No Fluid | | 1"/Min With Fluid | | | | 20"/Min No Fluid | | 1"/Min No Fluid | | 1"/Min With Fluid | | | |
| | **No.** | **Avg. Load (lb)** | **No.** | **Avg. Load (lb)** | **No.** | **Avg. Load (lb)** | **No.** | **Avg. Load (lb)** | **No.** | **Avg. Load (lb)** | **No.** | **Avg. Load (lb)** | **No.** | **Avg. Load (lb)** | **No.** | **Avg. Load (lb)** |
| -4 | 0 | - | 0 | - | 4 | 557 | 4 | 557 | 0 | - | 3 | 500 | 4 | 210 | 7 | 340 |
| -6 | 4 | 701 | 0 | - | 0 | - | 4 | 701 | 4 | 171 | 3 | 126 | 0 | - | 7 | 152 |
| -8 | 0 | - | 0 | - | 3 | 1270 | 3 | 1270 | 0 | - | 0 | - | 3 | 383 | 3 | 383 |
| -10 | 6 | 1541 | 0 | - | 0 | - | 6 | 1541 | 6 | 503 | 0 | - | 0 | - | 6 | 503 |
| -12 | 0 | - | 0 | - | 3 | 1995 | 3 | 1995 | 0 | - | 3 | 539 | 0 | - | 3 | 539 |
| -16 | 1 | 2200 | 0 | - | 3 | 2640 | 4 | 2530 | 2 | 1150 | 0 | - | 1 | 1150 | 3 | 1150 |
| -20 | 0 | - | 0 | - | 3 | 2420 | 3 | 2420 | 0 | - | 3 | 1200 | 1 | 1250 | 4 | 1212 |
| Total Tests | 11 | | 0 | | 16 | | 27 | | 12 | | 12 | | 9 | | 33 | |

*All data are ultimate loads (loads at point of spillage, if lower than ultimate, are not included).

TABLE IX. COMBINED TEST DATA FROM STATIC TESTS OF MIL-H-58089 HOSE AND 90-DEGREE FORGED ELBOW END FITTINGS

| Fitting Size | TENSION 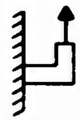 | | | | | | | | BENDING* 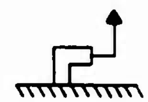 | | | | | | | |
|---|---|---|---|---|---|---|---|---|---|---|---|---|---|---|---|---|
| | Test Series | | | | | | | | Test Series | | | | | | | |
| | 1966 | | 1968 | | Current | | Total | | 1966 | | 1968 | | Current | | Total | |
| | 20"/Min No Fluid | | 1"/Min No Fluid | | 1"/Min With Fluid | | | | 20"/Min No Fluid | | 1"/Min No Fluid | | 1"/Min With Fluid | | | |
| | No. | Avg. Load (lb) | No. | Avg. Load (lb) | No. | Avg. Load (lb) | No. | Avg. Load (lb) | No. | Avg. Load (lb) | No. | Avg. Load (lb) | No. | Avg. Load (lb) | No. | Avg. Load (lb) |
| -4 | 0 | - | 0 | - | 3 | 698 | 3 | 698 | 0 | - | 3 | 278 | 1 | 260 | 4 | 274 |
| -6 | 0 | - | 0 | - | 0 | - | 0 | - | 0 | - | 3 | 389 | 0 | - | 3 | 389 |
| -8 | 0 | - | 0 | - | 3 | 850 | 3 | 850 | 0 | - | 0 | - | 3 | 770 | 3 | 770 |

*All data are ultimate loads (loads at point of spillage, if lower than ultimate, are not included).

## APPENDIX II

## STATIC AND DYNAMIC TESTING OF A 90-DEGREE ELBOW-TYPE SELF-SEALING BREAKAWAY VALVE

### OBJECTIVE

The objective of this test series was to evaluate the functional characteristics of a 90-degree, elbow-type, self-sealing breakaway valve during the most likely loading conditions anticipated in an upper-limit survivable crash.

### TEST ITEM

The test items consisted of eight aluminum, 90-degree, elbow-type, self-sealing breakaway valves. The valves were supplied in two sizes. Six were 3/4-inch (-12) valves weighing 9.0 ounces each, and two were 1-1/4-inch (-20) valves weighing 17.3 ounces each.

One end of the valve containing a spring-loaded poppet and seat assembly was designed for insertion in a fuel cell through a crash-resistant fitting. The flange portion of the valve body was then bolted to the outside of the fitting. The other half of the valve also contained a spring-loaded poppet and seat assembly. The two portions of the valve body were joined with a frangible section which provided the breakaway feature of the valve. The two poppets were held open through the use of a two-piece rod which passed through the frangible section. As the valve was subjected to a crash load, these rod sections distorted and released the spring-loaded poppets.

Each valve was supplied with approximately 12 inches of aircraft-type steel-braid-reinforced hose incorporated as part of the valve assembly.

### TEST METHODOLOGY

Static tests were conducted to determine the loads required for triggering in the shear and bending modes. Dynamic testing subjected the valve assemblies to various anticipated crash loads.

### Static Tests

The static tests were performed on a tensile test machine using special test fixtures to properly support the test items. Test loads were obtained in a static bending configuration as illustrated in Figure 62 and in a shear configuration as shown in Figure 63.

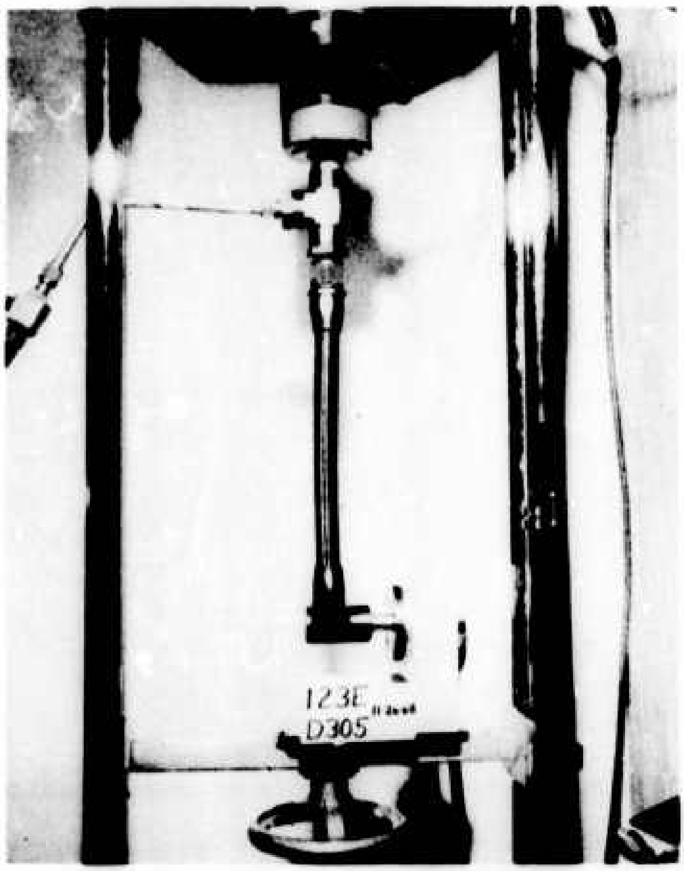


Figure 62. Static Bending Load Application.

The assembly was pressurized to 4 psig with water to permit evaluation of the flexible boot's sealing ability during valve body movement and to show the effectiveness of the valve sealing mechanism. An end cap was used on the tank half of the valve. All air was bled from the system prior to each test. Liquid flow was maintained through the valve during each test to denote when valve actuation had occurred.

## Dynamic Tests

The dynamic tests were conducted on a high-speed sled capable of reaching speeds up to 75 fps at the time of impact with arresting honeycomb. The test valves were subjected to bending, shear, and direct-impact loading conditions. The valves were pressurized to 4 psig during and for 5 minutes following each dynamic test.

Figure 63. Shear Bending Load Application.

The valves were installed on a sled-mounted aluminum panel which simulated the honeycomb aircraft structure. The installations and loading configurations are described below.

Dynamic Bending

This loading configuration simulated the impact of an object on the hose which attaches to the drain valve in the outboard vertical tanks of the UH-1D helicopter. The end of the hose was attached to a cable which was suspended below the sled to engage a fixed retaining hook attached to a concrete pad. The cable was snagged by the hook just prior to honeycomb stack impact and delivered the dynamic load to the test valve at peak sled velocity. A load cell positioned between the hook and the concrete pad measured the load. Figure 64 illustrates the dynamic bending test method.

Dynamic Peel

This test configuration simulated a dynamic loading in which the tank liner material is displaced away from the fuel cavity structure in an area adjacent to a valve.

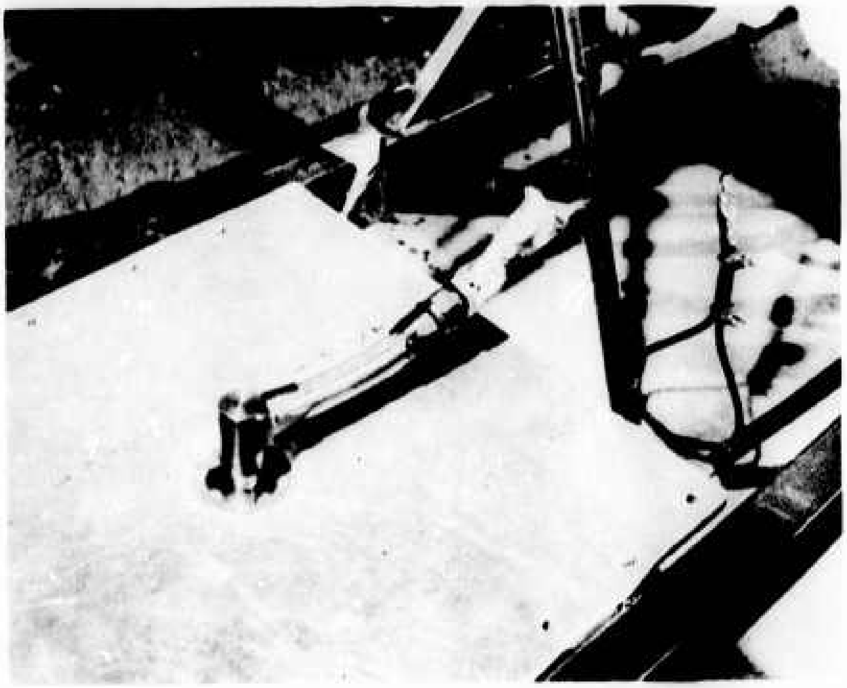

Figure 64. Dynamic Bending Test Method.

For this test series, the -12 test valve was bolted to the metal center insert of a crash-resistant tank section fitted with an aluminum plate which simulated the crash-resistant fitting. The opposite side of the valve mounting flange was then attached to the aluminum panel with frangible screws. This panel was then mounted vertically on the sled. The dynamic load was delivered to the valve through the use of the cable, hook, and load cell snagging system used in the dynamic bending test method. The cable in this case was attached to one side of the simulated tank fitting, which caused the fitting and attached valve to peel from the simulated aircraft structure. The frangible screws permitted the valve body to separate from the aircraft structure. As the hose assembly contacted the opposite side of the structure, the frangible section of the valve body separated and permitted the poppets to actuate. Figure 65 illustrates this test method.

Dynamic 45-Degree Impact

This loading configuration simulated an impact on the portion of the valve body which protrudes outside the tank cavity. For this test sequence, the valve was

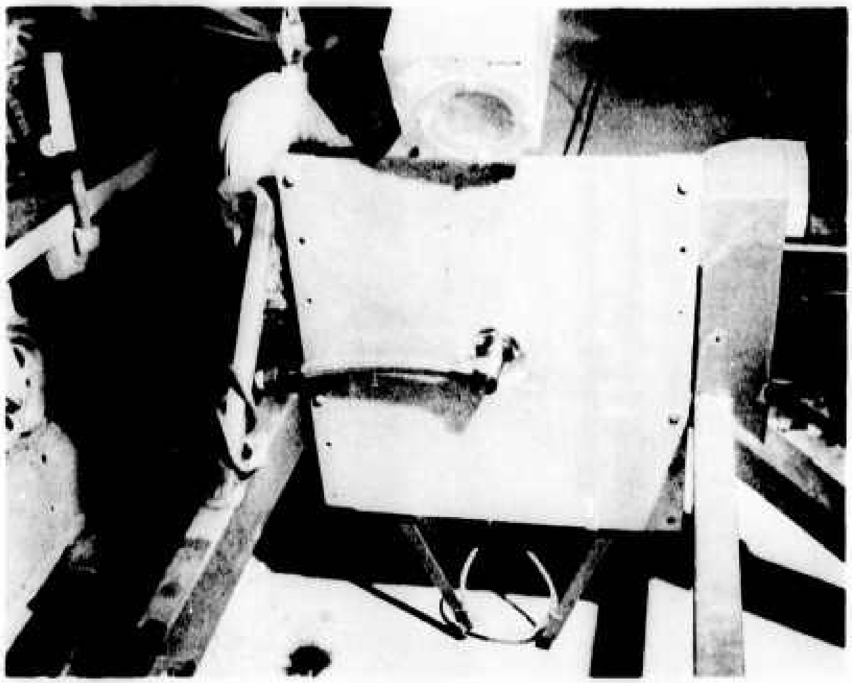

Figure 65. Dynamic Peeling Test Method.

mounted in the simulated aircraft structure with steel screws. Steel screws were used to insure that the frangible section of the valve would receive the full load. This panel was then attached to the sled at a 45-degree angle as shown in Figures 66 and 67.

The impact mechanism consisted of a steel plate, a steel rod, and a load cell. The plate was positioned 1.5 inches in front of the sled. Upon impact with the arresting barrier, the steel plate and rod drove the end of the load cell into the valve body.

## INSTRUMENTATION

The static test loads were obtained with 0- to 1,000-pound and 0- to 10,000-pound load cells. The dynamic test loads were obtained with a 0- to 4,000-pound load cell. All load data were recorded on a direct-writing oscillograph. The oscillograph chart speeds were 0.25 inch per second for the static tests and 64 inches per second for the dynamic tests. The dynamic test velocities were obtained through the use of an electronic counter used in the time interval measurement mode.

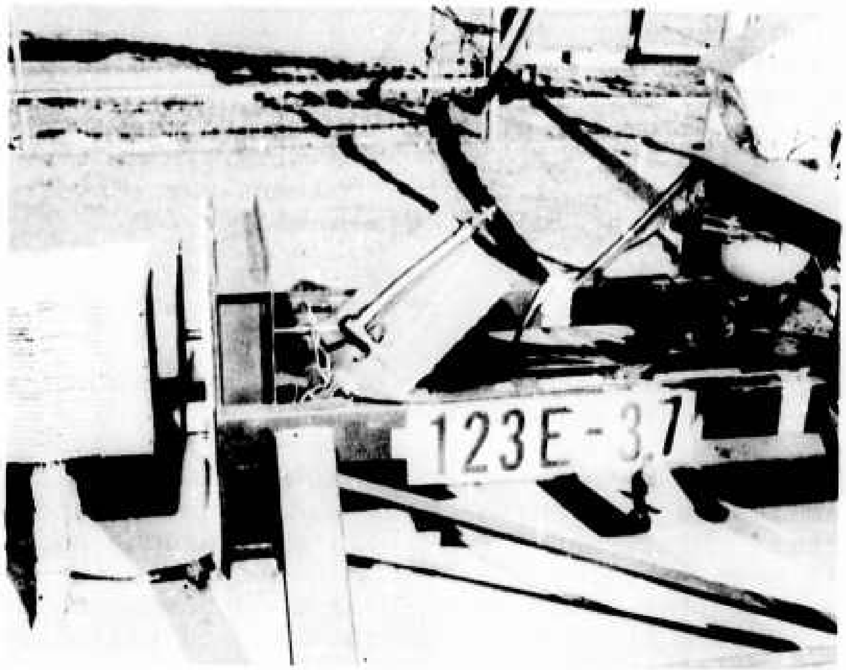


Figure 66. Side View of Dynamic 45-Degree Test Method.

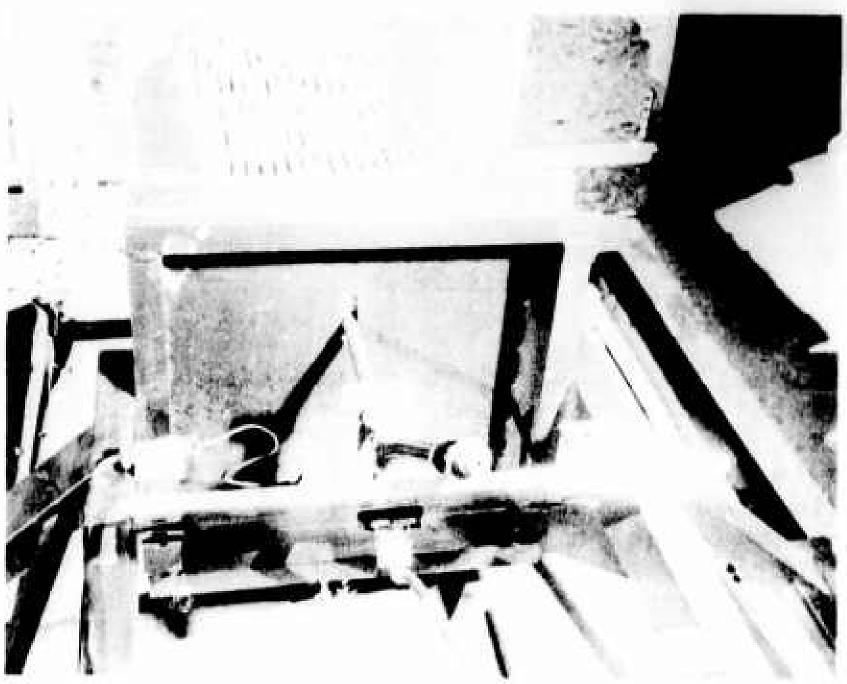

Figure 67. Sled-to-Barrier View of Dynamic 45-Degree Test Method.

The start-stop triggering was achieved through the use of a voltage hold-off circuit. An arm on the moving sled sheared graphite columns placed 2 feet apart. The first column removed the voltage from the start trigger, and the second column actuated the stop trigger. The millisecond time interval between the shearing of the two columns was converted to the sled velocity in the following manner:

$$V(\text{fps}) = \frac{2\ (\text{ft})}{t\ (\text{ms})}$$

A 0- to 25-psig pressure gauge was used to measure the water pressure prior to each dynamic test run.

Black-and-white and color high-speed film coverage was provided by cameras located on the sled and on the ground at the impact barrier. Black-and-white still photographs and 35mm color slides were taken of the static and dynamic test setups and of each test item before and after each test. Color documentary movies were taken to illustrate the installation and removal of the test items during selected tests.

## RESULTS

The valves were subjected to five static and six dynamic tests. Six 3/4-inch valves (-12) and five 1-1/4-inch valves (-20) were tested. (Only two 1-1/4-inch valves (-20) were supplied; however, these were rebuilt by the manufacturer for the three additional tests.) Table X provides a listing of all pertinent data.

### Static Tests

A discussion of the results of the five static tests follows:

#### Static Bending

Static loads were applied at a rate of 1 inch per minute. The initial valve subjected to bending loading exceeded the design load values. The valve separated through the frangible section at 1,500 pounds. The outermost edge of the valve body deflected upward 0.60 inch. Posttest examination revealed that the wall thickness in the frangible section was approximately twice that called out on the manufacturer's drawing. The five remaining -12 valves were modified by the manufacturer to conform to the drawing prior to further testing.

The test was repeated on the modified valve, with separation occurring through the frangible section at 400 pounds

| TABLE X. TEST DATA, 90-DEGREE ELBOW-TYPE BREAKAWAY VALVE | | | | |
|---|---|---|---|---|
| Dynamic Science Test Number | Valve Size | Test Configuration | Load Rate | Separation Load (pounds) |
| D304 | -12 | Static Bending | 1 in/min | 1500* |
| D305 | -12 | Static Bending | 1 in/min | 400 |
| D306 | -12 | Static Shear | 1 in/min | 1075 |
| D312 | -20 | Static Bending | 1 in/min | 378** |
| D313 | -20 | Static Shear | 1 in/min | 1030** |
| 123E-35 | -12 | Dynamic Bending | 83.0 fps | 1825 |
| 123E-36 | -12 | Dynamic Peel | 67.5 fps | 3000 |
| 123E-37 | -12 | Dynamic 45-Degree Impact | 68.4 fps | 817 |
| 123E-44 | -20 | Dynamic Bending | 73.4 fps | 3330 |
| 123E-45 | -20 | Dynamic 45-Degree Impact | 60.5 fps | 1270+*** |
| 123E-46 | -20 | Dynamic Peel | 68.6 fps | 1000 |

*Higher load due to thicker wall section than called out on drawing.
**Hose-half poppet leaked slightly if tipped back and forth.
***Load cell failed at 1270 pounds.

and an upward deflection of 0.33 inch. The valve body distorted approximately 45 degrees from its original position as loading continued.

The -20 valve when subjected to the same loading conditions separated at 378 pounds. Both poppets of the valve sealed; however, the hose half of the valve could be made to leak if tipped back and forth.

### Static Shear

The -12 valve reached a value of 1,075 pounds prior to frangible section separation, and the -20 valve required 1,030 pounds for separation. The -12 valve functioned well with no leakage other than the small amount trapped in the boot at time of closure. The -20 valve required a small amount of additional movement to result in poppet closure after the frangible section released. More fluid than normal was lost. The hose half of the valve could also be made to leak by tipping the valve body back and forth.

## Dynamic Tests

A discussion of the results of the six dynamic tests follows:

### Dynamic Bending

The loads were applied to the end of the connecting hose at a rate of 83.0 feet per second for the -12 valve and at a rate of 73.4 feet per second for the -20 valve. The force applied through the hose caused frangible section separation and triggered the poppets. The peak forces recorded were 1,825 pounds for the -12 valve and 3,330 pounds for the -20 valve. All poppets sealed properly, and no leakage was observed other than of the fluid which was trapped in the boot during valve closure. Figure 68 illustrates the -12 valve after removal from the sled.

Figure 69 illustrates the line half of the -20 valve following load application. The entire boot portion of the -20 valve remained in the flange half of the valve. This boot was cut in two places prior to pulling free of the hose half of the valve (Figure 70).

### Dynamic Peel

The loads were applied to the simulated tank sections at a rate of 67.5 feet per second for the -12 valve and a rate of 68.6 feet per second for the -20 valve.

The frangible screws which retained the valve and simulated fitting to the simulated aircraft structure released at 401 pounds and 319 pounds for the -12 and -20 installations, respectively. This then permitted the hose sections to bear against the simulated structure, resulting in frangible section separation loads of 3,000 pounds and 1,000 pounds, respectively.

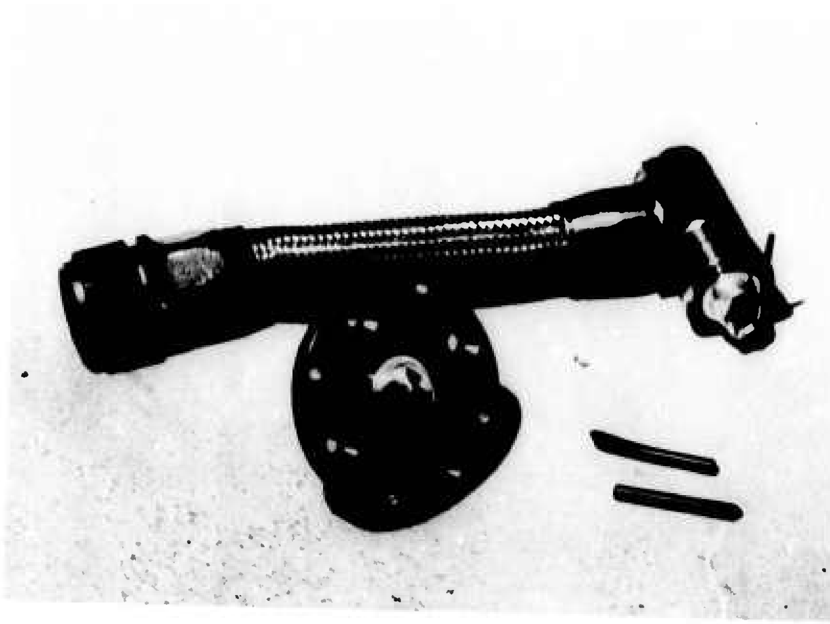

Figure 68. View of -12 Valve After Dynamic Bending Test.

Figure 69. View of Line Half of -20 Valve After Dynamic Bending Test.

Figure 70. Cut Boot in -20 Valve.

All valve sections sealed properly in both tests, resulting in no leakage of fluid other than that which was trapped in the boots during poppet closure. Figure 71 shows the -20 valve and hose assembly after the tests.

Dynamic 45-Degree Impact

The impact loads were applied through the impact mechanism at a rate of 68.4 feet per second for the -12 valve and 60.5 feet per second for the -20 valve. The loads recorded during impact were 817 pounds for the -12 valve and 1,270+ pounds for the -20 valve. The latter figure is not a peak load due to load cell failure at that value. Both valves functioned properly. Separations were made at the frangible sections, and no leakage was observed other than of the fluid entrapped in the boot during actuation. The -20 hose assembly and valve section were thrown over the impact barrier following impact. Figure 72 illustrates the -20 valve following dynamic impact.


Figure 71. View of -20 Valve After
Dynamic Peel Test.

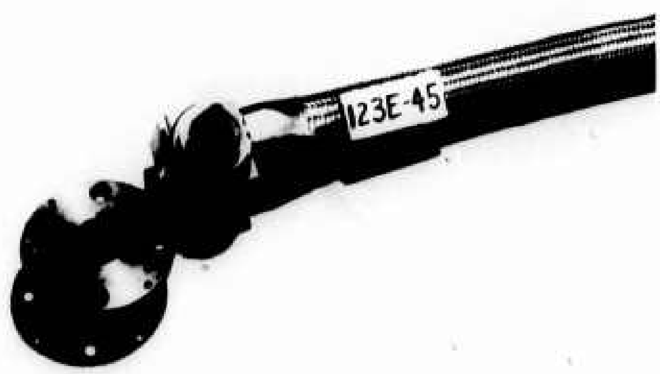


Figure 72. View of -20 Valve After Dynamic
45-Degree Impact Test.

As a result of this test series, it was concluded that the valve design is capable of separation and of providing efficient sealing under various loads which are typical of the crash environment. Other pertinent comments are:

1. It is possible to fail the frangible section statically without closing the valve. While the rubber boot prevents spillage during this condition, the boot is vulnerable to cutting by the valve and other jagged structure.

2. The rods which hold the poppets apart did not interfere with valve sealing during any of the tests.

3. The basic boot design was good.

4. Incorporating the fitting as part of the hose assembly is a good design approach; it permits a short, stiff section.

5. The valve design may possibly restrict flow; however, no flow tests were performed.

6. The design is simple and conducive to low-cost production.

## APPENDIX III

## STATIC AND DYNAMIC TESTING OF CELL-TO-LINE BREAKAWAY VALVES

### OBJECTIVE

The objective of this test series was to evaluate the crashworthy functional characteristics of a cell-to-line, self-sealing, breakaway valve during the most likely loading conditions anticipated in an upper-limit survivable crash.

### TEST ITEM

The test item consisted of five aluminum cell-to-line, self-sealing, breakaway valves weighing 2 pounds each (Figure 73). The valves featured an enlarged version of the frangible section, triggering, and sealing concept used in previous breakaway valves designed by the same manufacturer. One end of the valve protrudes inside the fuel cells, and the other incorporates a Marman clamp flange for hose attachments.

Figure 73. Cell-to-Line, Self-Sealing, Breakaway Valve.

The valve measures approximately 4-7/8 inches in diameter. Its attachment flange is 4-5/8 inches in diameter. The inside hose is 2-5/16 inches in diameter.

For some of the tests, an 18-inch-long section of -32 aircraft-type metal-braid-reinforced hose assembly was attached to the valve at the Marman flange.

## TEST METHODOLOGY

The test program used both static and dynamic testing. Static tests obtained loads required for triggering in the shear and bending modes. Dynamic testing subjected the valve assemblies to various anticipated crash loads.

### Static Tests

The static tests were performed on a tensile test machine using special test fixtures to properly support the test items. Test loads were obtained in a bending configuration as shown in Figure 74 and in shear configuration as shown in Figure 75.

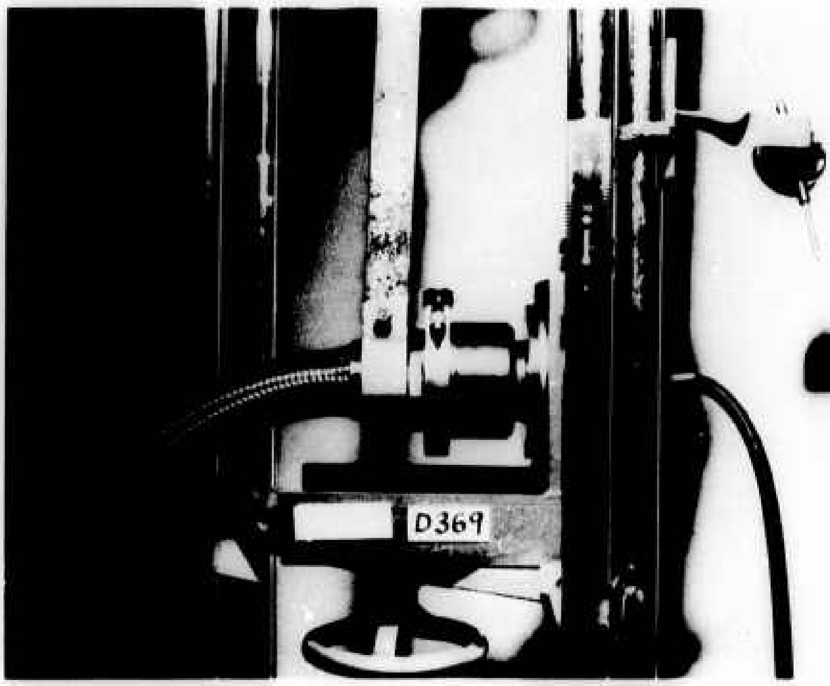


Figure 74. Static Bending Load Application Method.

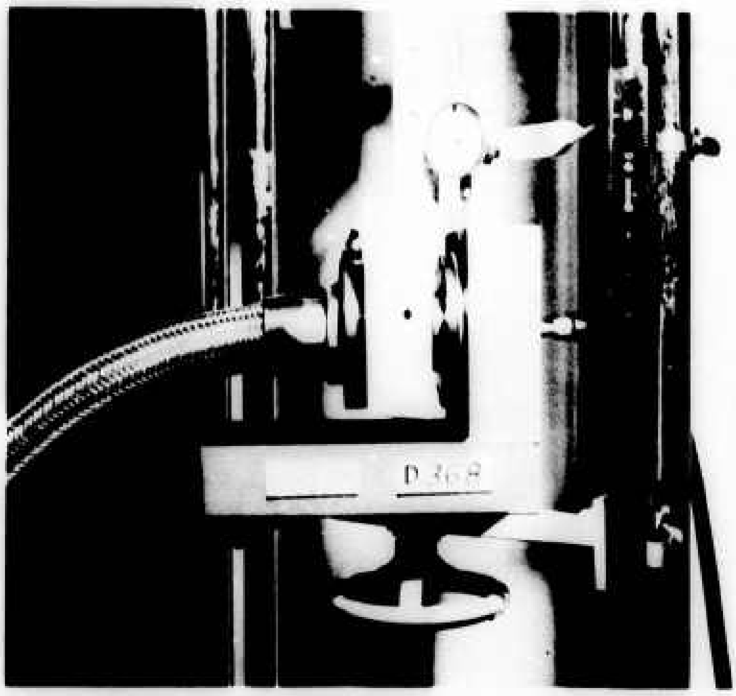

Figure 75. Static Shear Load Application Method.

The assembly was pressurized to 4 psig with water to permit evaluation of the flexible boot's sealing ability during valve body movement and to show the effectiveness of the valve sealing mechanism. All air was bled from the system prior to each test. Liquid flow was maintained through the valve during each test to denote when valve actuation had occurred.

Dynamic Tests

The dynamic tests were conducted on a sled capable of reaching a speed of 75 fps. Test valves were mounted on the sled and subjected to bending, shear, and direct-impact loading conditions. For two of the tests, the valves were pressurized to 4 psig during the test and for a period of 5 minutes following the test.

For all loading configurations, the valves were mounted on an aluminum panel which simulated the honeycomb aircraft structure.

A discussion of the three test installations and loading conditions follows:

## Bending

This loading condition simulated the impact of an object on the hose which attaches to a cell-to-line valve. The valve was oriented vertically by bolting it to horizontally mounted simulated structure (Figure 76).


Figure 76. Dynamic Bending Load Application Method.

The hose was gripped 1-1/2 inches above the attachment fitting with a circular clamp 1-1/2 inches in width. This clamp was attached to a cable which was routed over a roller at the rear of the sled and downward to the base of the sled. The cable was snagged just prior to impact by an arresting hook, which was attached through a load cell to a concrete slab.

## Direct Impact

This loading condition simulated an impact on the portion of a valve which protrudes inside the fuel tank by an object which has displaced the tank bottom upward. For

this test, the valve was positioned in the simulated aircraft structure with the tank side of the valve facing upward (Figure 77).

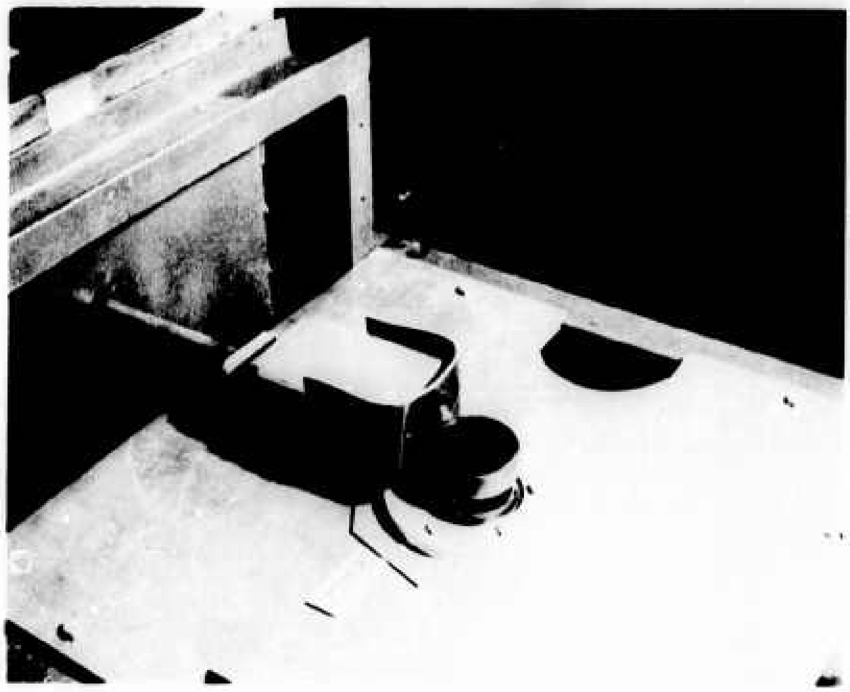

Figure 77. Dynamic Impact Load Application Method.

This was the only test in which the test item was not rigidly attached to the mounting plate. A frangible retainer (see Appendix V) identical to those tested for UH-1D helicopters was used to more realistically simulate the actual installation of the valve. This retainer was positioned on the lower side of the mounting flange and then bolted rigidly to the test item on the upper side of the mounting flange, thereby retaining the test item in position. The load was applied through the use of a rod which was attached to a plate in front of the sled and to a block of wood which was positioned on the rear of the rod. The plate made initial contact with the sled arresting honeycomb stack and, in turn, drove the wooden block into the valve body. The wooden block was covered with a section of tank wall material. No load-measuring equipment or pressurization system was provided for the test sequence.

Shear

This loading condition simulated the situation which occurs when the airframe structure is stopped suddenly and the tank and valve continue to move. For this test, the valve was rigidly attached to a simulated tank structure. The shearing action was obtained by pulling an actual section of the UH-1D airframe through the valve (Figure 78).


Figure 78. Dynamic Shear Load Application Method.

The honeycomb structure was attached to a cable which was routed over a roller at the rear of the sled and downward to the base of the sled. The cable was snagged just prior to sled impact by an arresting hook, which was attached through a load cell to a concrete slab.

## INSTRUMENTATION

The static test loads were obtained with a 0- to 10,000-pound load cell located in a tensile test machine. The dynamic shear and bending test loads were obtained with a 0- to 4,000-pound load cell. All load data was recorded on a direct-writing oscillograph. The oscillograph chart speed was 0.35 inch per second for the dynamic tests.

The dynamic test velocities were obtained through the use of an electronic counter used in the time interval measurement mode. The start and stop triggering was achieved through the use of a voltage hold-off circuit. An arm on the moving sled sheared two graphite columns placed 2 feet apart. The first removed the voltage from the start trigger and the second actuated the stop trigger. The millisecond time interval between the shearing of the two columns was converted to sled velocity in the following manner:

$$V(\text{fps}) = \frac{2\ (\text{ft})}{t\ (\text{ms})}$$

A 0- to 25-psig pressure gauge was used to measure the water pressure prior to each dynamic test run.

High-speed black-and-white (1000 frames per second) and color movies (500 frames per second) were taken of each dynamic test. Black-and-white still photographs and 35mm color slides were taken of each static and dynamic test setup and of each test item before and after the test. Color documentary movies were taken to illustrate the installation and removal of the test item during selected tests.

## RESULTS

The test valve was subjected to two static and three dynamic loading configurations. A listing of all pertinent data for this test series is presented in Table XI.

### Static Tests

A discussion of the results for the two static tests follows:

#### Static Bending

The test setup for this configuration loaded the valve with an effective moment arm of 4.6 inches. The static load was applied at a rate of 1.0 inch per minute. Slightly over 4 inches of head travel was necessary to completely actuate the valve and to fully stop the test

TABLE XI. CELL-TO-LINE VALVE TEST DATA

| Dynamic Science Test Number | Test Configuration | Load Rate | Separation Load | Amount of Fluid Spillage | UH-1 Crashworthy Criteria |
|---|---|---|---|---|---|
| D-368 | Static Shear | 1 Inch/ Min. | 3800 Pounds | 50 Drops/ Min. | Failed* |
| D-369 | Static Bending | 1 Inch/ Min. | 1530 Pounds | 6.5 Cubic Inches | Passed |
| 123M-80 | Dynamic Shear | 65 fps** | 4100 Pounds | 6.5 Cubic Inches | Passed |
| 123M-81 | Dynamic Bending | 62 fps | 2750 Pounds | 6.5 Cubic Inches | Passed |
| 123M-82 | Dynamic Impact | 64.3 fps | - | N/A | Failed*** |

*Boot was cut by sharp edge of frangible section, allowing drippage, prior to valve poppet closure.
**Approximation ±5 percent.
***This test mode not applicable if valve does not extend into tank past metal tank fitting.

fluid flow. The frangible section yielded at 1.3 inches travel, and the peak load recorded was 1,530 pounds. No seepage occurred. Figure 79 illustrates valve position at the time of flow stoppage. Figure 80 is a close-up of the valve body after removal from the test fixture.

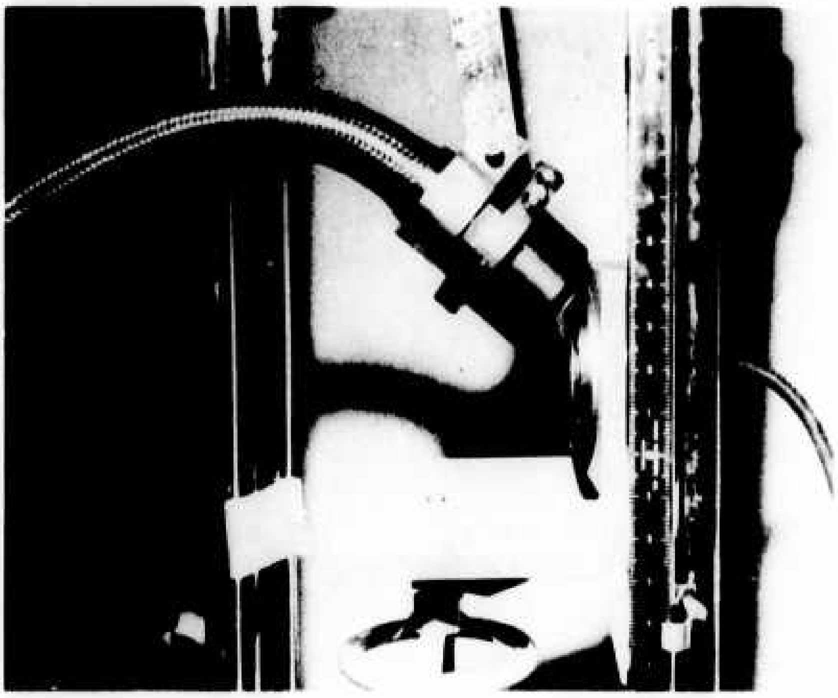

Figure 79. Valve Position at Time of Valve Closure During Static Bending Test.

As can be seen in Figure 79, the valve assembly bent approximately 45 degrees before closing. While the inner boot stretched and prevented fluid spillage during the valve displacement, an undesirably large amount of boot surface area was exposed. This exposed area could be cut by jagged metal or by the sharp edge of the torn frangible section.

The maximum allowable amount of exposed boot area was not previously specified; however, the need to do so is obvious. The valve manufacturer is studying the problem and is attempting to reduce the area.


Figure 80. Valve Body After Removal From Test Fixture. (Note uncut portion of boot still holding valve halves together.)

Static Shear

The test setup for this loading configuration subjected the valve to a shear loading with an effective moment arm of 0.57 inch. Static loading was applied at 1 inch per minute. Fluid dripped from the boot section at 0.9 inch head travel. Poppets closed at 0.2 inch travel and separation occurred at 1.8 inches travel. Peak load required to shear the frangible section was 3,800 pounds. Figures 81 and 82 show the test item after separation.

The fluid spillage which occurred at 0.9 inch valve displacement resulted because the jagged edge of the torn frangible section cut the boot. Upon disassembly, it was discovered that the boot was vulcanized to the inside of the frangible section. The adhesion tended to hold the boot against the cutting edge.

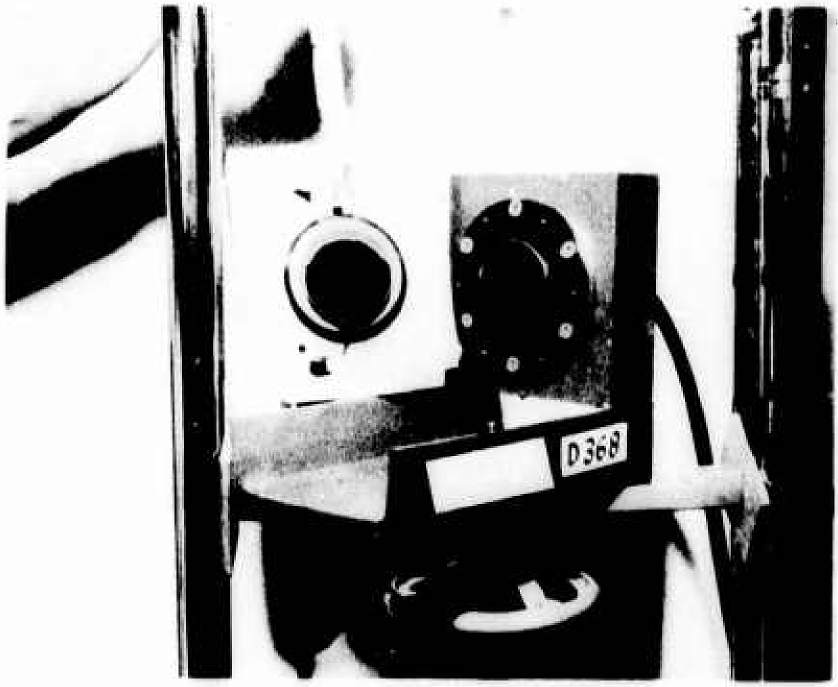


Figure 81. Valve Separation at Completion of Static Shear Test.

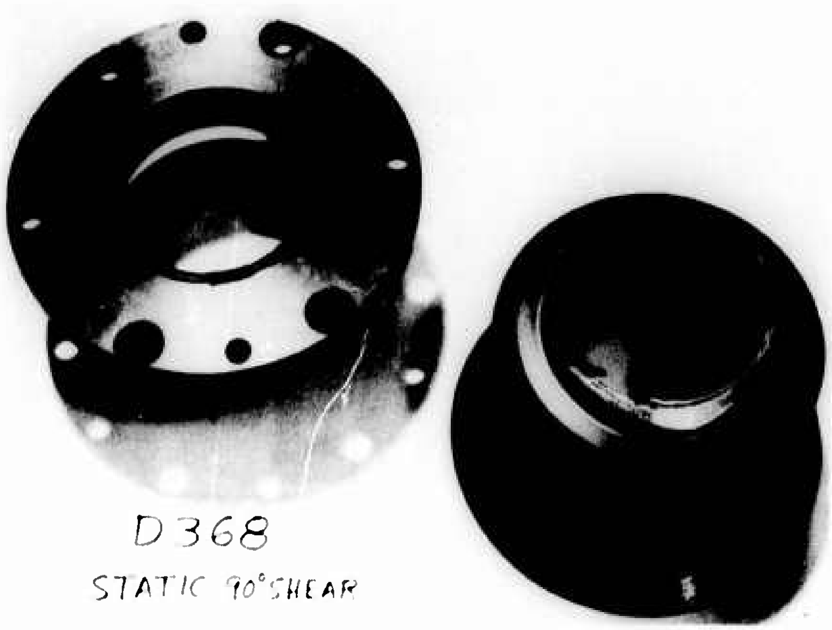


Figure 82. Valve Body After Removal From Test Fixture. (Note sharp edge on deformed shear section.)

## Dynamic Tests

A discussion of the three dynamic tests follows:

### Dynamic Bending

The load was applied to the connecting hose at 62 feet per second. The force caused the valve halves to separate at the shear pins rather than at the frangible section. Peak force required to break the valve in half was 2,750 pounds. Both sections of the valve sealed properly. The only fluid lost was that trapped in the boot after poppet closure. Figure 83 shows the valve sections following separation as well as the entrapped fluid spillage pattern. Figure 84 shows the valve body following separation.

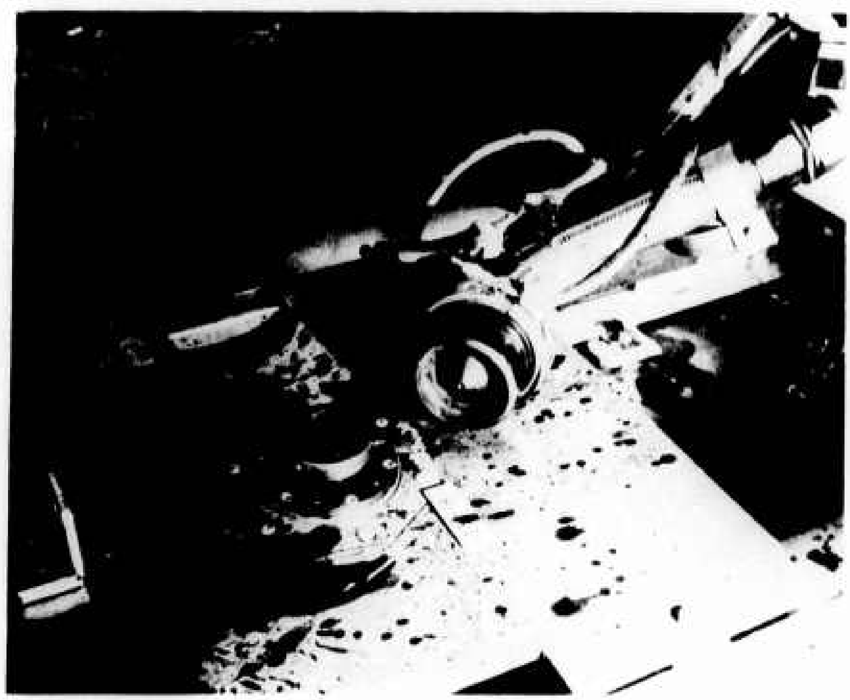

Figure 83. Valve Sections at Completion of Dynamic Bending Test.

### Dynamic Impact

As previously mentioned, no pressure system was used and no load measurements were recorded.

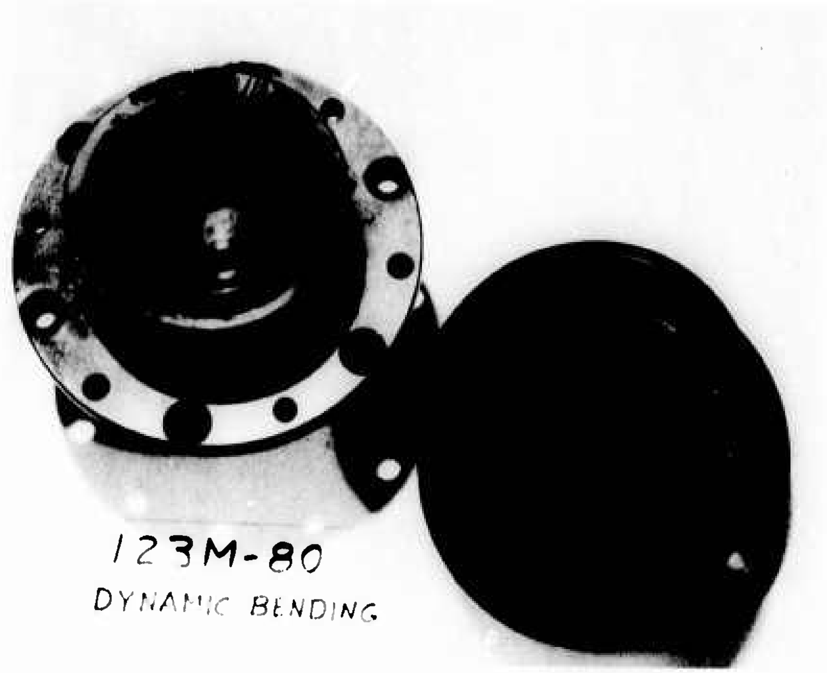


Figure 84. Valve Sections After Removal From Test Fixture Following Bending Test.

The wooden block covered with the tank material impacted the valve body at 64.3 feet per second. Upon impact, a portion of the valve body separated. The line half of the valve sealed as designed; however, the tank half could not seal because the valve body was torn free (Figure 85). A close-up view of the valve body after impact is shown in Figure 86.

Since this was the only "failure" with this valve during the entire test series, further discussion is in order. This type of loading -- a direct impact on a protruding valve half -- is realistic and can be expected during survivable crashes. The valve designer has several alternatives at his disposal to prevent this type of failure. He can "beef up" the valve body to the point where it will carry the direct impact load, or he can make the portion of the valve which protrudes into the tank short enough so that it will not extend into the tank past the dome nuts on the tank-mounted metal fitting. All future models of this valve design have been shortened. Consequently, this direct-impact test will no longer be applicable to this particular valve design.

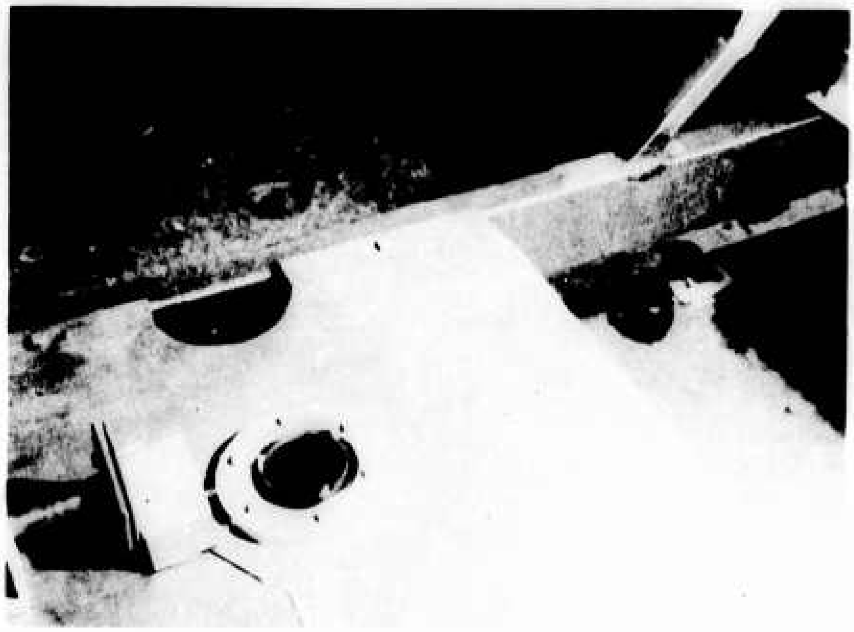

Figure 85. Valve Separation at Completion of Dynamic Impact Test.

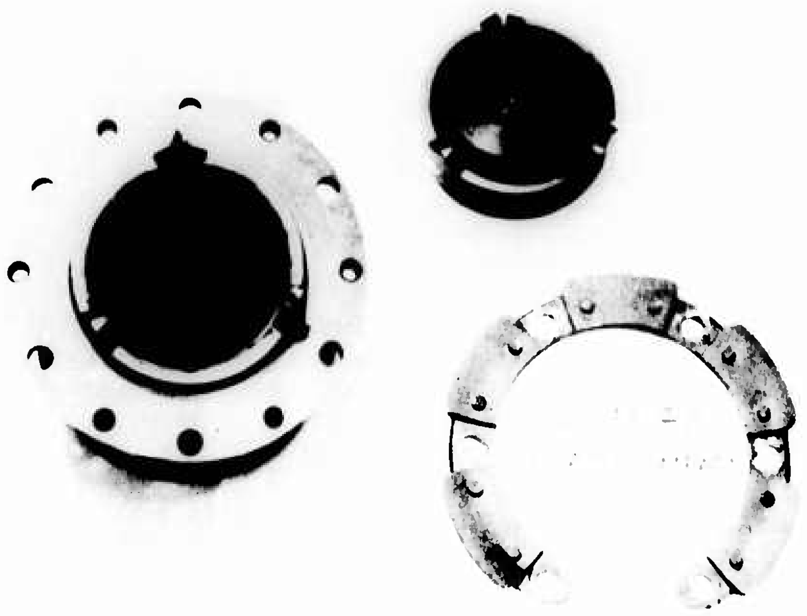

Figure 86. Valve Sections and Frangible Retainer After Removal From Test Fixture.

## Dynamic Shear

The honeycomb panel flange impacted the valve body at approximately 65 feet per second. The entire panel sliced through the frangible section of the valve at a load of 4,100 pounds. Both valve halves sealed, with no leakage other than of fluid trapped in the valve boot between the closed poppets. Exact velocity readings were not obtained due to a malfunction in the electronic counter. Figure 87 shows the valve sections and the honeycomb panel following impact. A close-up of the valve sections is shown in Figure 88.

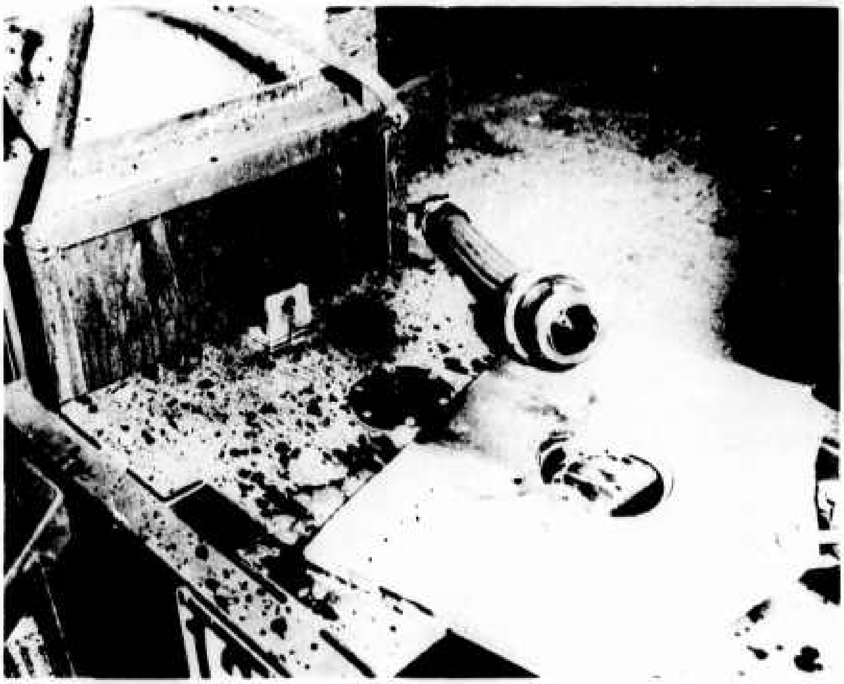

Figure 87. Valve Separation at Completion of Dynamic Shear Test.

As a result of this test series, it is concluded that the cell-to-cell, self-sealing valve design is capable of separation and of providing efficient sealing under various loads which are typical of the crash environment.

Other pertinent comments are:

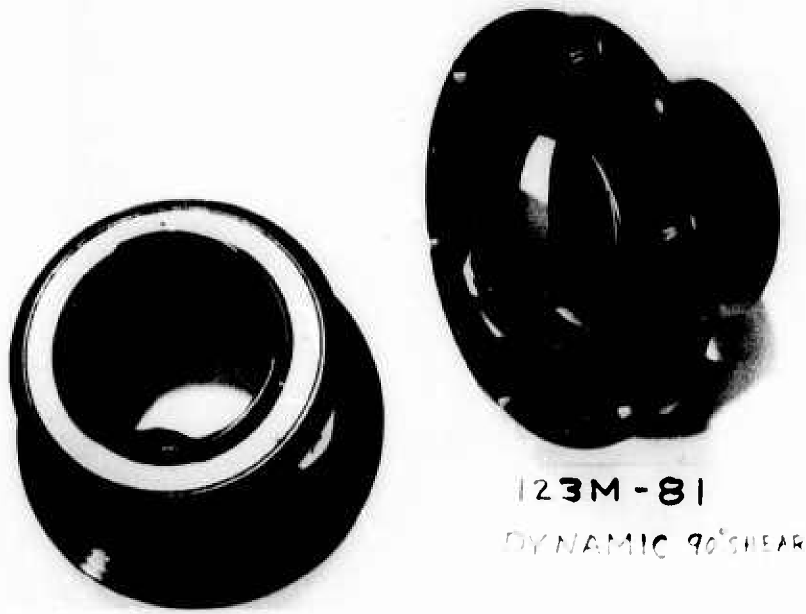


Figure 88. Valve Sections After Removal From Test Fixture Following Shear Test.

1. The valve assembly successfully passed two of the three dynamic failure modes anticipated during upper-limit survivable crashes.

2. The rod which holds the poppets apart did not interfere with valve sealing during any of the tests.

3. The valve assembly can be bent 45 degrees without valve closure. While the rubber boot prevents spillage during this condition, the boot is vulnerable to cutting by the valve and other jagged structure.

4. The present design does not permit installation in existing aircraft structure (UH-1A, B, and C) without modification of the aircraft. The Marman clamp flange on the valve is too large to pass through the airframe structure.

5. The valve assembly is a simple design and conducive to low-cost production.

## APPENDIX IV

## STATIC AND DYNAMIC TESTING OF SEVERAL CANDIDATE CHECK VALVES FOR THE UH-1 FUEL SYSTEM

### OBJECTIVE

The objective of this test series was to determine the strength of the candidate valves, the manner of failure of the valves or attached components, and the performance of the valves when subjected to various representative loads.

### TEST ITEMS

Twelve valves produced by two manufacturers were tested. Three 1/4-inch line-size (-4) and six 1/2-inch line-size (-8) valves were made by one manufacturer. The bodies of these valves were made of 303 stainless steel.* They were designed for a cracking pressure of 2 psi maximum within a temperature range of -20° to +350°F. The operating pressure range of the valve was 0-200 psi. The -4 valve weighed 0.07 pound and the -8 valve weighed 0.18 pound.

The bodies of the remaining three valves were made of 2024-T3 aluminum.** They operated with a cracking pressure of 8 inches $H_2O$ maximum at temperatures ranging from -65° to 180°F. These 1/2-inch line-size valves were used in the external auxiliary fuel supply lines of the UH-1B and C helicopters. A potential modification relocated the valve inside the underfloor fuel tank of the UH-1B with the bulkhead nipple extending below the boost pump plate. The valve weighed 0.25 pound.

### TEST METHODOLOGY

#### Static Tests

The purpose of the static tests was to determine the loads required to fail the valves in a 90-degree bending mode. All tests were performed with a 10,000-pound tensile test machine. The valves were mounted in text fixtures with the center line of the valve perpendicular to the direction of load application as shown in Figure 89. This fixture was then secured to the movable crosshead of the test machine. A steel "B" nut which had been welded to a steel attachment yoke was then firmly attached to the test item. The length of the moment arm from the valve flat surface to the center line of load application was 1-1/2 inches. The yoke was then attached

*These valves are identified herein as S.S.-1/4 and S.S.-1/2.
**These valves are identified herein as Al-1/2.

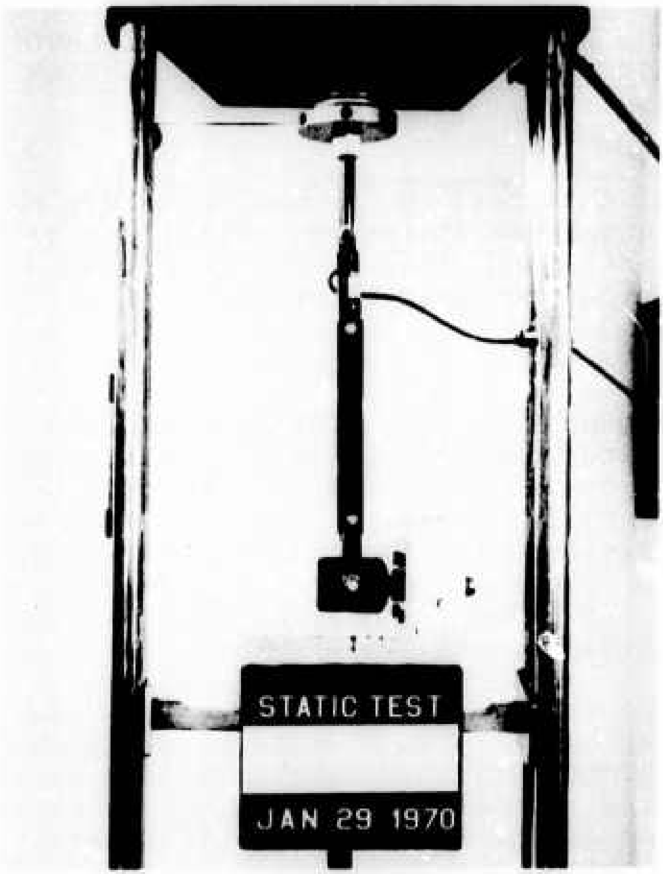


Figure 89. Tensile Machine Setup for Static Tests.

through the load cell at the top of the test machine. No fluid pressure was used during the static tests.

All loads were applied at a rate of 1 inch per minute. Load application was maintained until the valve nipple and/or threads distorted or until the valve pulled out of the attachment fixture.

Dynamic Tests

The purpose of the dynamic tests was to simulate typical loading conditions that the check valves might be subjected to when installed in the UH-1 fuel system. A drop tower and horizontal test track with a high-speed sled were used for this test series. This sled (Figure 90) is capable of reaching a speed of 75 fps at the time of impact with the arresting honeycomb barrier. The valves were mounted on the sled in

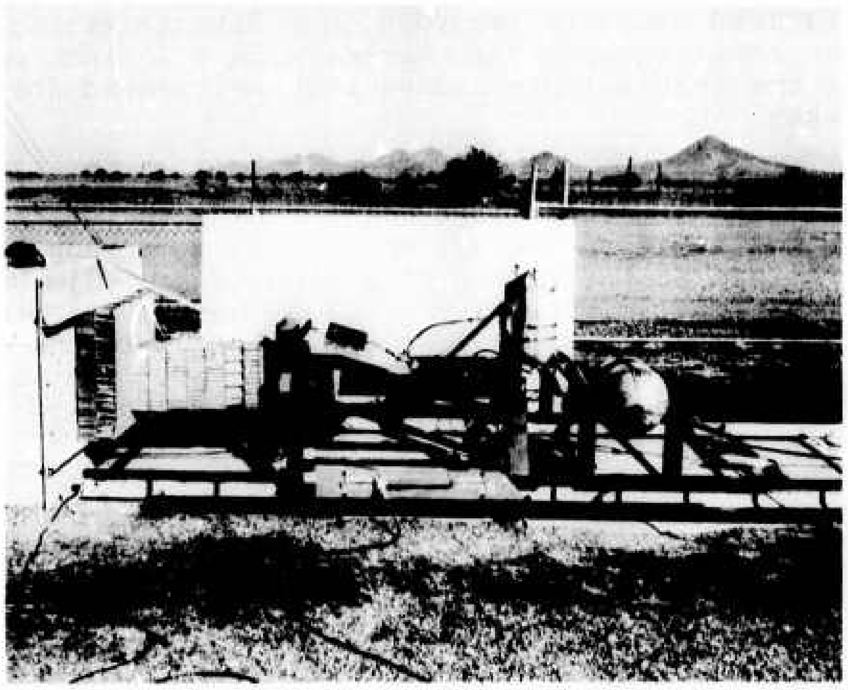

Figure 90. Horizontal Sled Setup
for Dynamic Tests.

fixtures which simulated their installation in the helicopter. A pressure system which simulated the aircraft fuel system was used for each test to evaluate the sealing capabilities of the valves both prior to and immediately following the dynamic load application. This pressure system delivered fluid pressure to the upstream side of the test item at 5 ±0.5 psi. The opposite side of the test item was attached to a drain line and bleed valve. All entrapped air was bled from the system prior to testing.

All dynamic loads were applied at a rate of 65 ±5 feet per second. The valve operation was checked both prior to and immediately following load application. An internal fluid pressure of 5 ±0.5 psig was maintained on the test item during load application.

INSTRUMENTATION

The static test loads were measured by a 0- to 4,000-pound load cell located between the top of the tensile test machine and the load application linkage. The tensile and bending dynamic test loads were measured by a 0- to 4,000-pound load

cell positioned between a snag hook and a concrete pad under the sled. Loads were not recorded during the dynamic impact tests. All load data was recorded on a direct-writing oscillograph. The oscillograph chart speeds were 0.25 inch per second for the static tests and 64 inch per second for the dynamic tests.

The test velocities were obtained with an electronic counter used in the time interval measurement mode. The start-stop triggering was achieved through the use of a voltage hold-off circuit. An arm on the moving sled sheared graphite columns placed 2 feet apart. The first graphite column removed the voltage from the start trigger, and the second column actuated the stop trigger. The millisecond time interval between the shearing of the two columns was converted to the sled velocity in the following manner:

$$V(\text{fps}) = \frac{2\ (\text{ft})}{t\ (\text{ms})}$$

A 0- to 25-psig pressure gauge was used to measure the water pressure prior to each dynamic test.

High-speed (1,000 frames per second) black-and-white movies were taken of each dynamic test. Black-and-white still photographs and 35mm color slides were taken of each dynamic test setup before and after each load application. Close-up photographs were also taken of each test item after removal from the test fixtures.

## RESULTS

Three check valve types from two manufacturers were subjected to a total of ten dynamic tests and two static tests. A breakdown of the tests is given in Table XII. A discussion of the individual tests results follows (referenced to the test numbers as listed in Table XII).

### Valve Type A1-1/2

Dynamic Bending - Test No. 80-150K-5: The valve and hose assembly were positioned on the sled as shown in Figure 90. A dynamic load was applied to the hose assembly at a rate of 65.5 feet per second. The force applied caused the hose to pull free of the elbow end fitting attachment at a peak load of 958 pounds. The valve was not damaged and performed properly following the test load application. A posttest view of this test may be seen in Figure 91.

TABLE XII. ONE-WAY CHECK VALVE STATIC AND DYNAMIC TEST DATA

| Test Number | Valve Model | Test Type | Loading Method | Impact Velocity (fps) | Applied Load (lb) | Leakage Rates Before Load | Leakage Rates After Load | Leakage Rates After Recyling |
|---|---|---|---|---|---|---|---|---|
| 80-150K-5 | Al-1/2 | Dynamic | Bending | 65.5 | 958 | None | None | None |
| 80-150K-6 | S.S.-1/2 | Dynamic | Bending | 65.2 | 1190 | None | None | None |
| 80-150K-7 | S.S.-1/4 | Dynamic | Bending | 65.2 | 650 | None | 34 cc/min | None |
| 80-150K-8 | Al-1/2 | Dynamic | 45° Impact | 64.7 | - | None | Partial Flow | None |
| 80-150K-9* | Al-1/2 | Dynamic | 45° Impact | 65.5 | - | None | 102 cc/min | None |
| 80-150K-10 | S.S.-1/2 | Dynamic | 45° Impact | 66.2 | - | None | 100 cc/min | None |
| 80-510K-11 | S.S.-1/4 | Dynamic | 45° Impact | 63.4 | - | None | None | None |
| 80-150K-13** | Al-1/2 | Dynamic | 75° Impact | 63.5 | - | Almost Full Flow | None | None |
| 80-150K-12 | S.S.-1/2 | Dynamic | Tension | 65.1 | 1015 | Partial Flow | None | None |
| 80-150K-14 | S.S.-1/2 | Dynamic | Tension | 65.8 | 846 | Partial Flow | None | None |
| SK-17 | S.S.-1/2 | Static | Bending | 1 in./min | 2550 | None | None | None |
| SK-18 | Al-1/2 | Static | Bending | 1 in./min | 2640 | None | None | None |

*Reused valve from Test 80-150K-5.
**Reused valve from Test 80-150K-8.

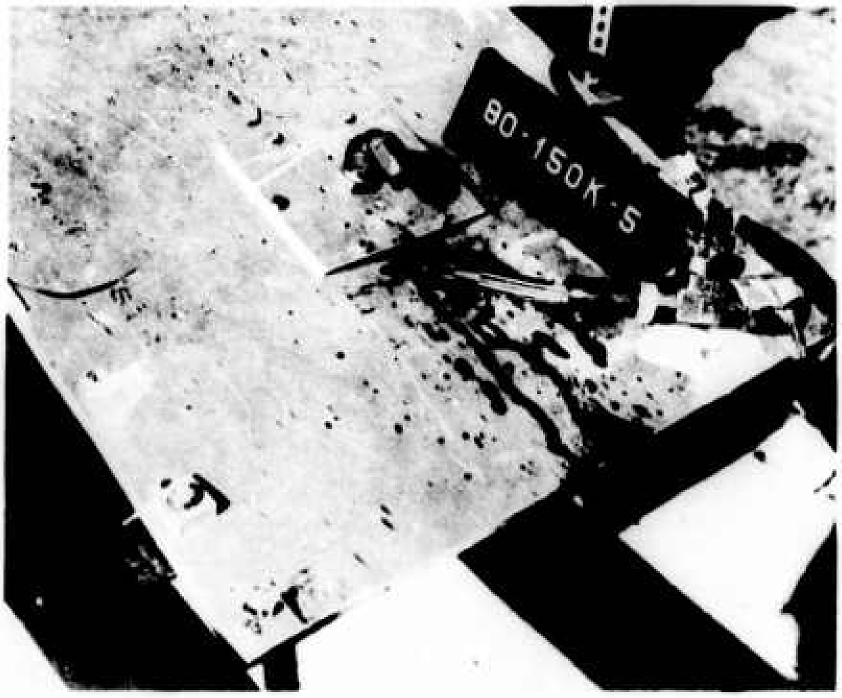


Figure 91. View of Valve A1-1/2 After Dynamic Bending Test.

45-Degree Dynamic Impact - Tests Nos. 80-150K-8 and 80-150K-9: A valve and hose assembly were positioned on the sled as shown in Figure 92. This test configuration was run twice, once using a hardwood block as an impact head and once with a cast lead impact head. The impact velocities were 64.7 and 65.5 feet per second, respectively. The first impact shattered the hardwood block, and the second distorted the lead impact head. The bulkhead nipple of the second valve was distorted 5 degrees off centerline. Both valves permitted some test fluid to flow in the reverse direction following load application. Leakage was measured for the second test at approximately 102 cc/min under a 5-psi line pressure. However, after several changes of flow direction, the valves functioned normally.

75-Degree Dynamic Impact - Test No. 80-150K-13: The test setup was similar to the one shown in Figure 92 except that the angle of the plate with the horizontal was reduced to 15 degrees. This produced the desired 75-degree angle between the valve centerline and the direction of force application. The valve used for this test permitted fluid leakage prior to the test load application. The valve was removed from the test fixture and was found to permit free flow of fluid in both directions.

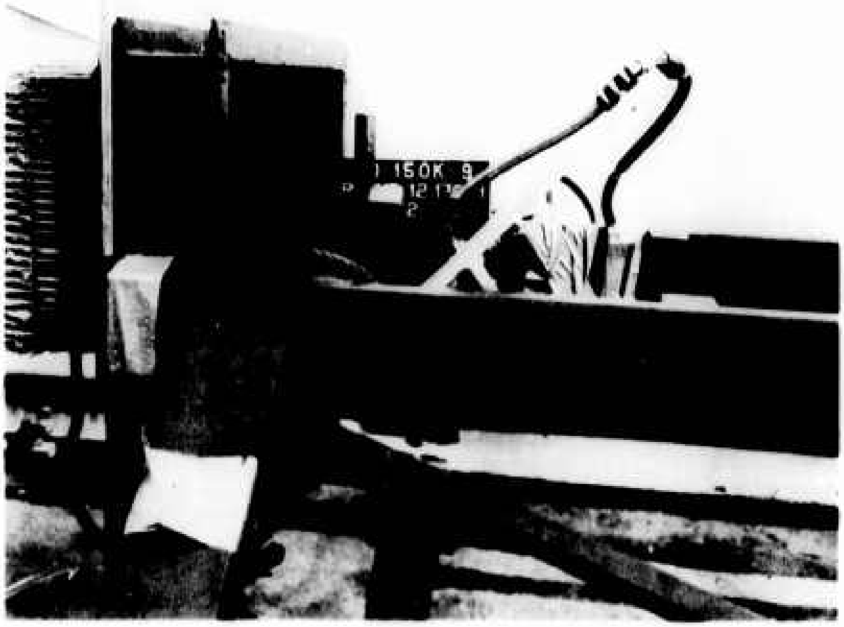


Figure 92. Typical Test Setup for 45-Degree Impact Tests.

After manual actuation, the valve was then rechecked and found to function properly. The valve was reinstalled on the sled, the flow was checked, and the valve was subjected to a 75-degree impact load at 63.5 feet per second. The valve nipple yielded in bending but did not fail. The valve permitted only a few drops of fluid leakage following impact load application and then sealed completely. The "B" nut and elbow hose end fitting did not fail (Figure 93).

Static Bending - Test No. SK-18: The A1-1/2 valve was positioned on the rear of the vertical plate of the test fixture with the bulkhead nipple protruding through the vertical plate. The attachment fitting and "B" nut were then installed on the valve nipple. This configuration subjected the valve to a static load with an effective moment arm of 1-1/2 inches.

The valve resisted an applied bending load of 2,640 pounds prior to failure of the threads on the valve nipple. The valve nipple was distorted upward prior to failure. The valve performed properly when checked both prior to and following the static test. Figure 94 shows the valve after removal from the test fixture.

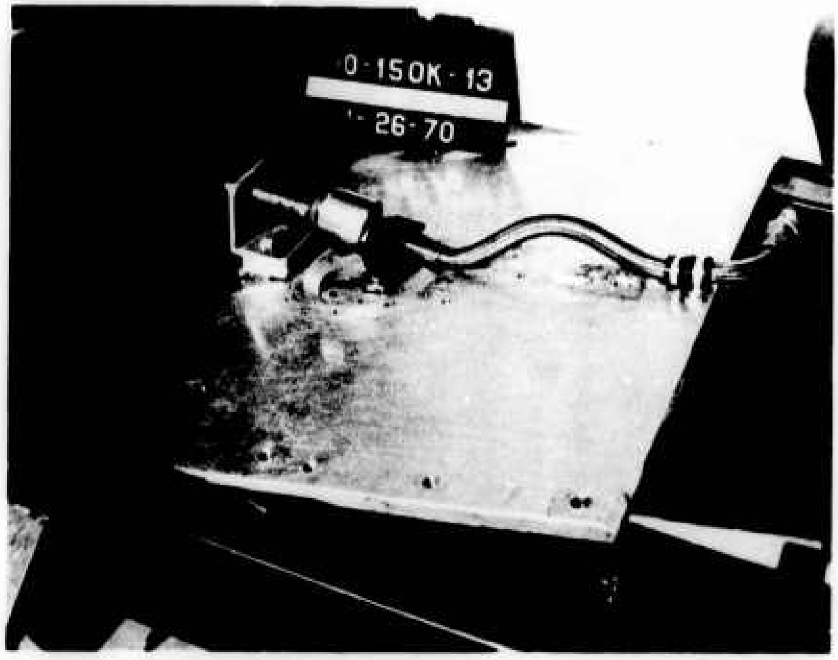


Figure 93. View of Al-1/2 Valve After Dynamic 75-Degree Impact Test.

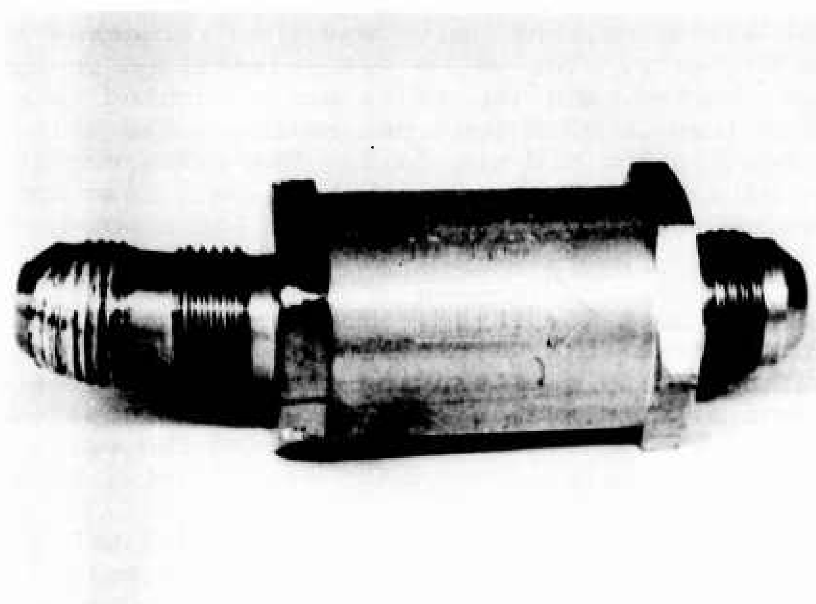

Figure 94. View of Al-1/2 Valve After Static Bending Test.

Valve Type S.S.-1/2

Dynamic Bending - Test No. 80-150K-6: The valve and hose assembly were positioned on the sled in a manner similar to the setup shown in Figure 90. A dynamic load was applied to the hose assembly at a rate of 65.2 feet per second. The force applied caused the straight end fitting of the hose to fail at a peak load of 1,190 pounds. The snap ring in the "B" nut failed and permitted the remainder of the hose end fitting to pull free of the "B" nut and valve nipple. The valve was not damaged and performed normally following the test. A posttest view of the test setup is shown in Figure 95.

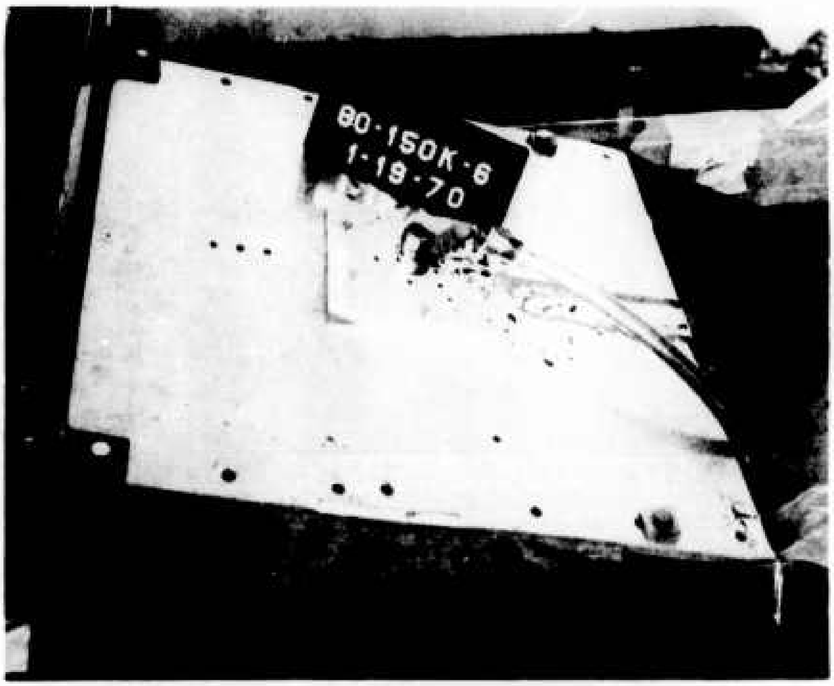


Figure 95. View of S.S.-1/2 Valve After Dynamic Bending Test.

45-Degree Dynamic Impact - Test No. 80-150K-10: The valve and hose assembly were positioned on the sled as shown in Figure 92. The straight hose end fitting installed on the valve nipple was impacted with a lead impact head at a rate of 66.2 feet per second. The "B" nut failed and permitted the remainder of the hose end fitting to break free of the "B" nut. A posttest pressure check of this valve indicated a fluid

leakage rate of approximately 100 cc/min. A view of the failed "B" nut is shown in Figure 96.


Figure 96. View of S.S.-1/2 Valve After Dynamic 45-Degree Impact Test.

Dynamic Tension - Tests Nos. 80-150K-12 and 80-150K-14: The valve and hose assemblies were positioned on the sled as shown in Figure 97.

The first valve leaked at a high rate when tested prior to load application. This leakage stopped when the valve seated while being tapped.

A dynamic load was applied to the hose assembly at a rate of 65.1 feet per second. This dynamic loading resulted in a hose pull-out from the end fitting located opposite the valve end of the hose assembly (Figure 98); the pull-out load reached 1,015 pounds. The valve did not permit any leakage in the reverse direction following load application.

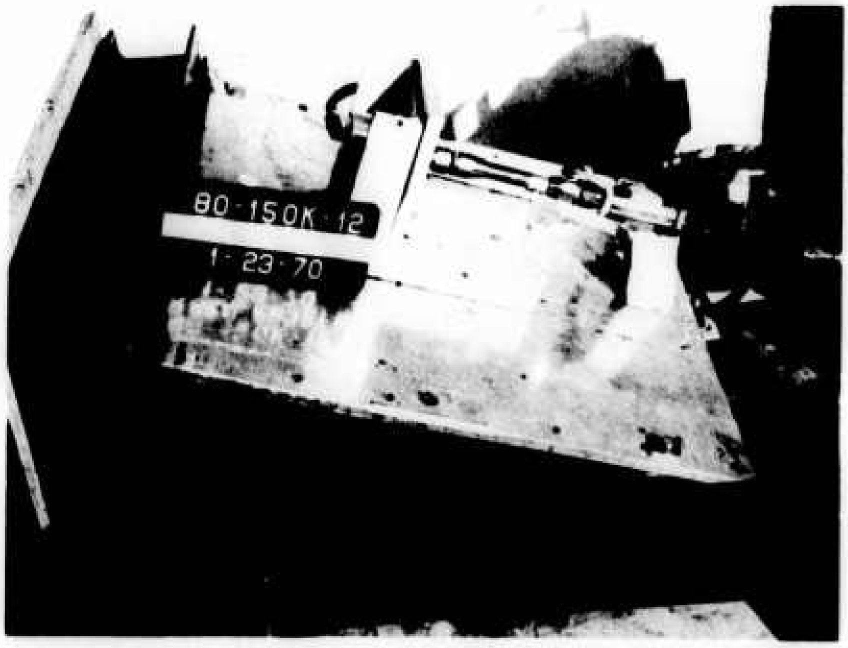


Figure 97. Setup for Dynamic Tension Tests.


Figure 98. View of S.S.-1/2 Valve After Dynamic Tension Test.

Another valve and hose assembly were then subjected to the same dynamic loading (Test No. 80-150C-14). This valve also leaked prior to the test when fluid pressure was applied in a reverse flow direction after being subjected to flow in the normal direction. The valve sealed after the mounting plate was rapped smartly. This failure to seat was repeatable.

The valve and hose assembly were subjected to dynamic loading at a velocity of 65.8 feet per second. The hose end fitting pulled off the hose at 846 pounds (Figure 99). The valve remained sealed and did not leak.


Figure 99. View of S.S.-1/2 Valve After Dynamic Tension Test.

Static Bending - Test No. SK-17: The valve was positioned on the tensile test machine as shown in Figure 89. The static bending load was applied with an effective moment arm of 1-1/2 inches and at a rate of 1 inch per minute. The valve resisted an applied bending load of 2,550 pounds prior to the attachment linkage "B" nut pulling off the valve nipple. A view of this valve following removal from the test fixture is shown in Figure 100.

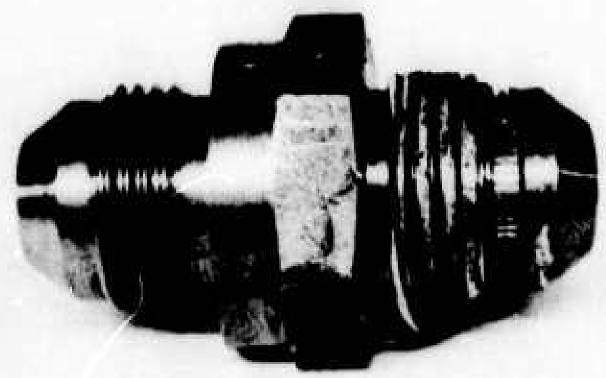

Figure 100. View of S.S.-1/2 Valve After
Static Bending Test.

<u>Valve Type S.S.-1/4</u>

Dynamic Bending - Test No. 80-150K-7: The mounting setup for the valve and tube assembly was similar to that shown in Figure 101. A load was applied to the 1/4-inch hose assembly at a rate of 65.2 feet per second. The force applied caused the tube to fail in tension at the top of the "B" nut as shown in Figure 102. The peak load recorded was 650 pounds. This dynamic load caused the valve to permit a leakage of 34 cc/min following the dynamic load application. The valve was then subjected to a flow in a normal direction and, when rechecked in the reverse direction, leakage still occurred. The direction of flow was again changed and, upon return to reverse direction, the valve sealed completely.

45-Degree Dynamic Impact - Test No. 80-150K-11: The valve and tube assembly were positioned on the sled as shown in Figure 99. The tube and "B" nut installed on the valve nipple were struck with a lead impact head at the rate of 63.4 feet per second. The impact head distorted across the top of the "B" nut and completely flattened the tube, resulting in tube failure (Figure 103). A posttest pressure check of the valve

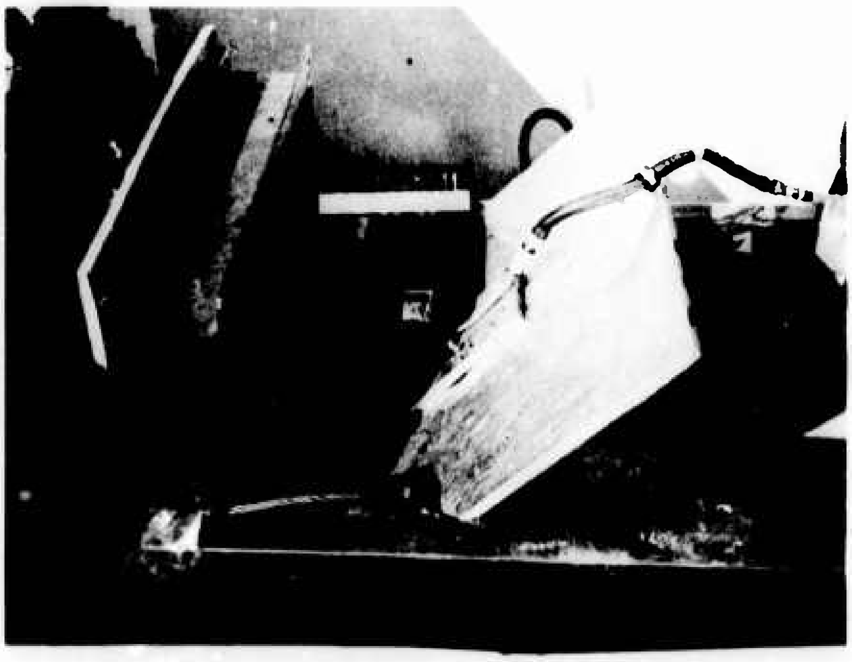

Figure 101. Setup for S.S.-1/4 Valve Tests.


Figure 102. View of S.S.-1/4 Valve After Dynamic Bending Test.

Figure 103. View of S.S.-1/4 Valve After Dynamic 45-Degree Impact Test.

revealed that the valve was not damaged by the impact and performed normally.

## DISCUSSION

The operating mechanisms of the Al-1/2 check valves which were subjected to the various dynamic and static applied loads in this test series received no permanent damage. However, the aluminum bulkhead nipple of the valve was bent, and the threads were damaged in the dynamic 75-degree impact and static bending tests.

The operating mechanisms of the S.S.-1/4 and S.S.-1/2 check valves also received no permanent damage as a result of the applied loads. The continued load application on the static bending test did, however, begin to distort the cone point (end plug) of the nipple which was installed in the aluminum test fixture. As the aluminum threads failed, the valve was pulled from the fixture.

Two of the Al-1/2 valves and one each of the S.S.-1/4 and S.S.-1/2 valves did permit leakage following the dynamic load application. This leakage was stopped by cycling the valve either manually (shaking) or with pressure and letting it reseat.

Two of the S.S.-1/2 valves permitted flow during a functional check prior to load application. These were new valves and had been installed in the test fixture and subjected to a flow in a normal direction prior to the reverse flow check. This leakage may have been caused by contamination of the test fluid (no filter was installed and the leakage occurred only on the last test runs). Each of the malfunctioning valves sealed upon cycling.

## CONCLUSIONS

1. Minor damage was sustained on all the valves, and all of them permitted some fluid loss after impact.

2. None of the valves represents a serious hazard even when subjected to direct impact.

3. Hose fitting failure adjacent to the valve represents a much greater hazard than impact on the valve.

## RECOMMENDATIONS

1. No changes are indicated for the intended applications.

2. All hose fittings to the valves should be analyzed for probable load in a maximum survivable crash, and one or more of the following precautionary measures should be taken:

   a. Use steel fittings.

   b. Design ample slack in hose to accommodate distortion.

   c. Relocate component.

# APPENDIX V

## DYNAMIC TESTING OF FRANGIBLE RETAINERS FOR USE IN UH-1D/H HELICOPTER CRASH-RESISTANT FUEL SYSTEM

### OBJECTIVE

The objective of this test series was to evaluate the functional characteristics of frangible retainers under what was estimated to be the three most extreme loading conditions that would be experienced under actual crash conditions.

### TEST ITEMS

Both of the two frangible retainer designs tested in this series use the frangible clip concept but differ slightly from each other in design. They are identified in this report by the numbers -648 and -669.

The -648 retainer is designed for the aft inlet on the underfloor tank in the UH-1D helicopter. This retainer consists of an aluminum (7075-T6), 0.063-inch-thick, horseshoe-shaped ring that has six bolt holes for attachment to the crash-resistant tank fitting. Five 0.050-inch aluminum clips (2024-T3) are attached to this base ring with 1/8-inch-diameter aluminum rivets (2117-T3). Two rivets are used per clip. These clips have a greater diameter than the base ring that provides the retaining feature of the part. As these clips are loaded dynamically, they tend to be pried from the ring section and distort, thereby providing the frangible feature of the design. Figure 104 illustrates the -648 retainer.

The -669 retainer is designed for the filler cap of the UH-1D and uses two horseshoe-shaped aluminum parts. The mounting base is also made of 0.063-inch aluminum stock (7075-T6). This section has 12 mounting holes for attachment to the crash-resistant tank fitting. The second part is made of 0.032-inch aluminum (2024-T3) and is of similar horseshoe shape except for the larger diameter and oversize bolt holes. These oversize holes pass over the heads of the bolts that attach the mount rings. This 0.032-inch-thick ring is attached to the mounting with 11 aluminum rivets (1/8 inch). The combination of the overhanging 0.032-inch ring and the aluminum rivets provides the frangible feature of the retainer design. Figure 105 illustrates the -669 retainer.

Ten each of the two designs were fabricated for testing.

Figure 104. -648 Frangible Retainer.

Figure 105. -669 Frangible Retainer.

## TEST METHODOLOGY

The dynamic tests were conducted with a cage dropped from a 50-foot drop tower. The test items were installed in a simulated honeycomb structure and subjected to three different loading conditions: tension, bending, and 90-degree shear (see Figure 106).

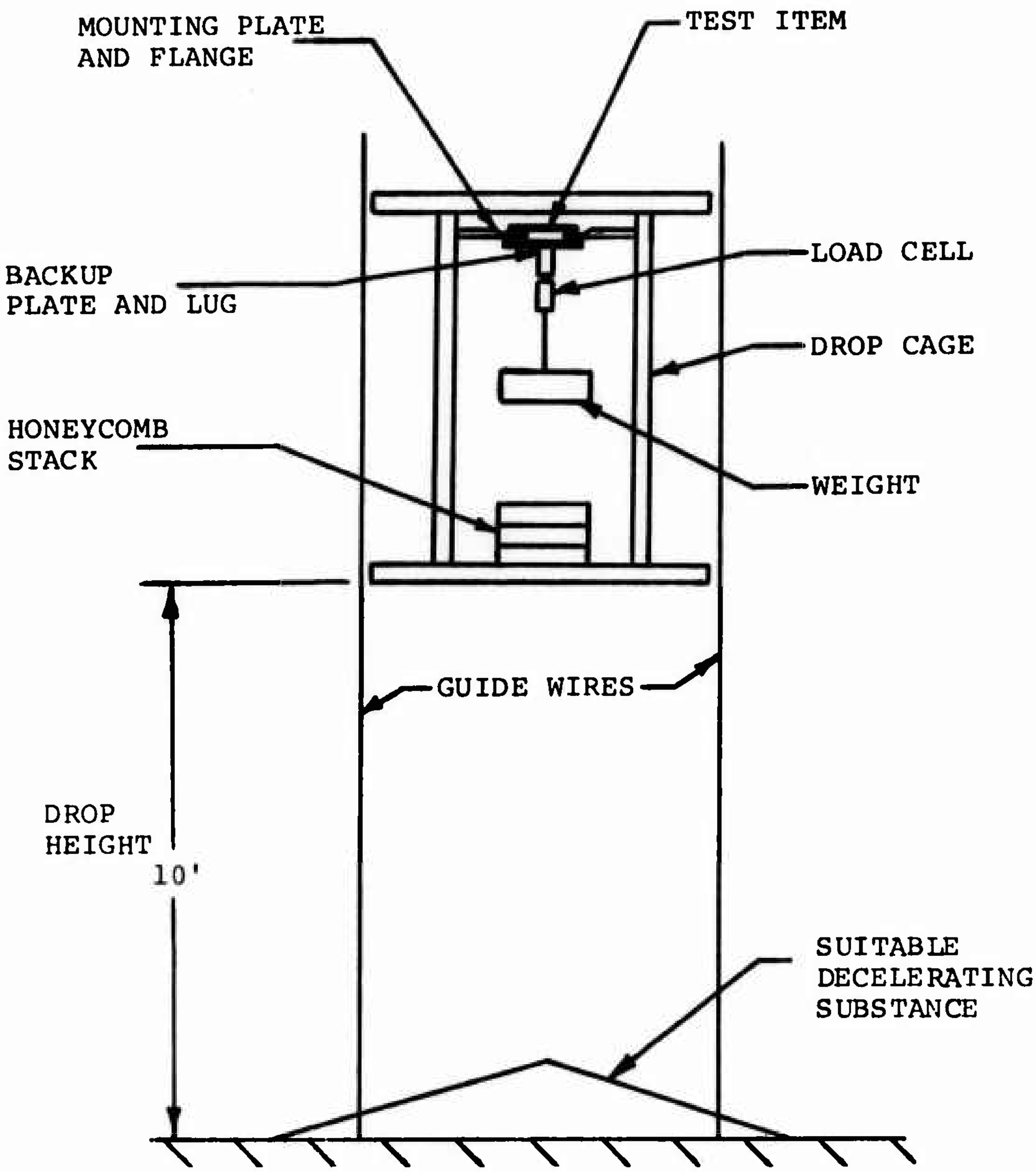


Figure 106. General Dynamic Test Setup.

The test items were positioned on one side of the mounting plate and bolted firmly to a 1/4-inch-thick aluminum backup plate positioned on the opposite side of the mounting plate. The overlapping tabs of the test items retained the assembly in position.

After each frangible retainer was in position, a load cell and weight were then attached to a lug protruding from the backup plate. This weight was allowed to move freely vertically but restrained from any lateral movement by the channels of the vertical I-beams.

The test item and backup plate were restrained after release by the use of a bungee cord. This bungee prevented any damage to the test item or load cell due to impact with drop cage structure. Figures 107 through 110 illustrate the three typical test setups for this test series.

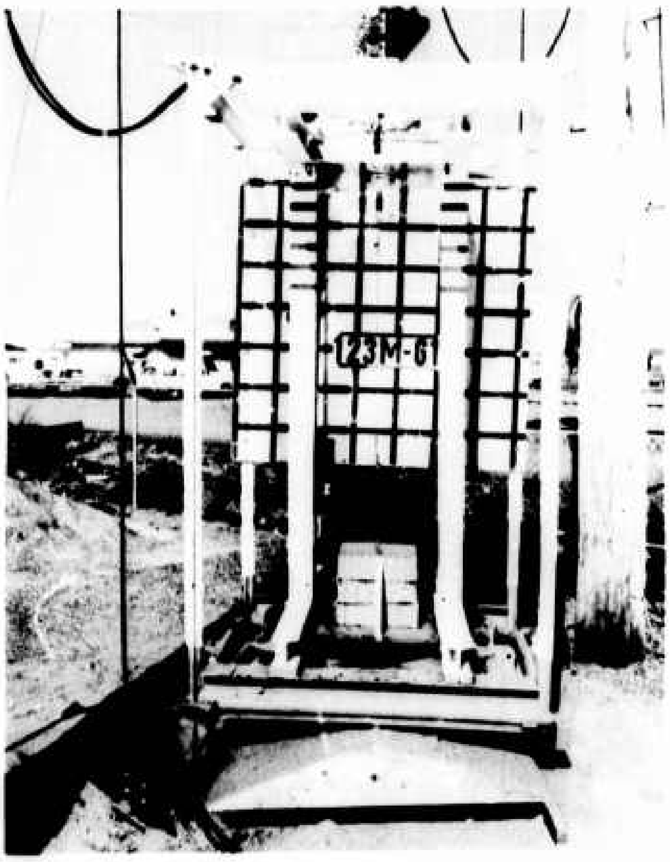


Figure 107. Typical Tension Test Setup.

Figure 108. Typical Tension Test After Release.

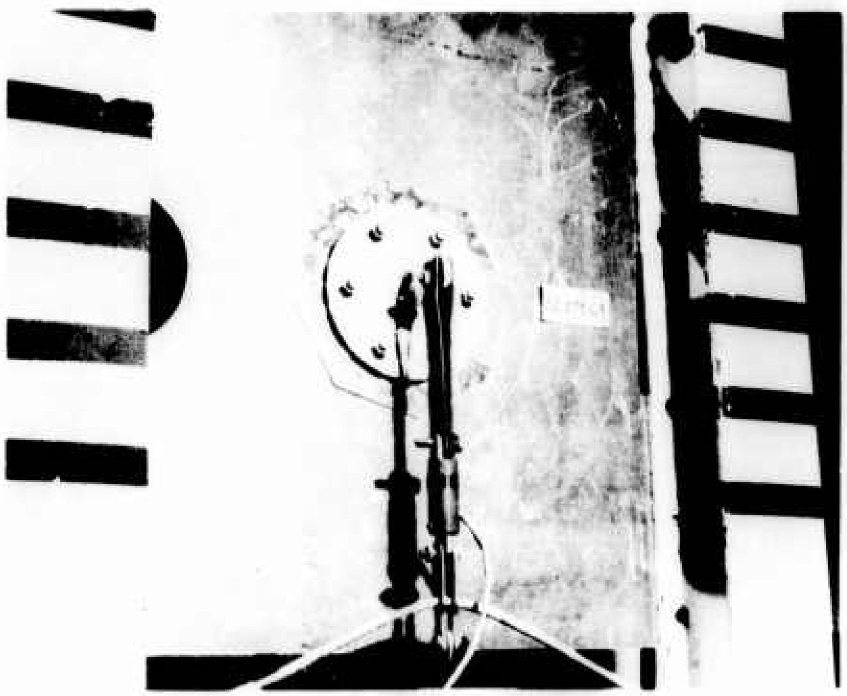

Figure 109. Typical Bending Test Setup.

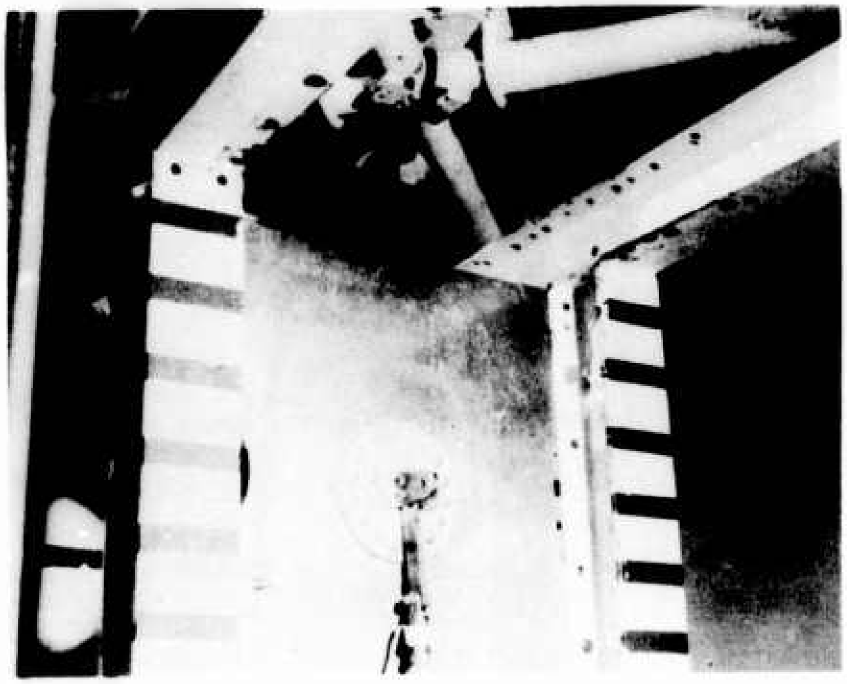

Figure 110. Typical Shear Test Setup.

INSTRUMENTATION

Release loads were obtained through the use of a 0- to 4,000-pound load cell located in the linkage between the test item and the attached weight.

An accelerometer (100G) was mounted on a horizontal I-beam at the top of the drop cage. These data as well as the load cell data were recorded on a direct-writing oscillograph at 64 inches per second.

High-speed black-and-white (1,000 frames per second) movies were taken of each test. Black-and-white still photographs and 35mm color slides were taken of each typical test setup, test item, and failed test hardware. High-speed color (500 frames per second) movies were taken of nine selected tests. Color documentary movies were taken to illustrate the installation and removal of the test item in each of the three typical test configurations.

## RESULTS

The frangible retainers were subjected to a total of 19 test drops. Of this total, nine involved the -648 retainer, three of which were in tension, three in bending, and three in 90-degree shear. The other 10 drops involved the -669 retainer, three of which were in tension, four in bending, and three in 90-degree shear.

All test drops were made from a height of 10 feet, and the cage was impacted on the decelerating material at a velocity of 25 feet per second.

The cage accelerations resulting from these drops ranged from 71.5 through 88.4G, with an average of 81.8G for the 19 drops.

Discussion of results by test mode is presented below.

### Dynamic Tension

The six tension drops of the two retainer designs resulted in average values that were very close. The -648 retainer averaged release loads of 1,068 pounds, and the -669 retainer averaged release loads of 1,065 pounds. The tension values for the -648 retainer were more closely grouped than those of the -669 retainer. Figure 108 illustrates a typical tension setup immediately following release. Figure 111 illustrates a typical -648 retainer and Figure 112 illustrates a typical -669 retainer following tension loadings. Detailed test results are presented in Table XIII.

### Dynamic Bending

Seven drops were made with the two retainer designs in the bending loading configuration. The loads were applied with a moment arm of 2.4 inches. The three drops with the -648 retainer resulted in an average release load of 995 pounds. Four drops were made in bending with the -669 retainer. The first drop of this series did not result in release due to fixture failure. The faulty fixture was replaced and the three additional bending drops were made. The average release load for the -669 retainer was 1,377 pounds. Release loads within each type were very consistent with the values for the -648, being very closely grouped.

In all probability, the spread between the average bending release values was due primarily to the manner in which the retainers were mounted. The -648 retainers were mounted for the bending tests with the opening facing upward, whereas the -669 retainers were mounted for the bending tests with the opening facing downward in the same direction as the load application.

Figure 111. -648 Retainer After Tension Loading.


Figure 112. -669 Retainer After Tension Loading.

| TABLE XIII. DYNAMIC TEST RESULTS | | | | | |
|---|---|---|---|---|---|
| Drop* Number | Test Type | Test Item | Cage (G) | Failure Load (lb) | Remarks |
| 123M-61 | Tension | -648 | 71.5 | 1025 | Average Failure Load - 1068 lb |
| 123M-62 | Tension | -648 | 84.5 | 1100 | |
| 123M-63 | Tension | -648 | 79.5 | 1080 | |
| 123M-64 | Bending | -648 | 79.2 | 1010 | Average Failure Load = 995 lb |
| 123M-65 | Bending | -648 | 79.2 | 978 | |
| 123M-66 | Bending | -648 | 87.0 | 997 | |
| 123M-67 | Shear | -648 | 84.0 | 2680 | Average Failure Load = 2543 lb |
| 123M-68 | Shear | -648 | 87.0 | 2450 | |
| 123M-69 | Shear | -648 | 88.4 | 2500 | |
| 123M-70 | Tension | -669 | 83.8 | 768 | Average Failure Load = 1065 lb |
| 123M-71 | Tension | -669 | 83.5 | 1063 | |
| 123M-72 | Tension | -669 | 81.8 | 1365 | |
| 123M-73 | Bending | -669 | 77.1 | (836) | Failed fixture, did not pull out - results discarded |
| 123M-74 | Bending | -669 | 76.6 | 1340 | Retest of -73 |
| 123M-75 | Bending | -669 | 78.3 | 1440 | Average Failure Load = 1377 lb |
| 123M-76 | Bending | -669 | 87.9 | 1350 | |
| 123M-77 | Shear | -669 | 86.0 | 1990 | Broke cable - results discarded |
| 123M-78 | Shear | -669 | 71.5 | 2580 | Average Failure Load = 2510 lb |
| 123M-79 | Shear | -669 | 87.0 | 2440 | |

*The drop height for all tests was 10 feet.

This method was used to subject the retainers to the most likely loading conditions. The test loading modes were intended to simulate a stump or other object impacting the tank through the bottom of the UH-1D. The -648 retainer was designed to be installed at the rear of the underfloor tanks with its mouth facing downward. The -669 retainer was designed to be installed at the filler cap location with the mouth facing upward. It was for this reason that the retainers were loaded in opposite directions with regard to their potential bending mode strength. Had both retainers been loaded in a similar orientation, the average release loads would probably have been much closer.

Figures 113 and 114 illustrate the positions of the -648 and -669 frangible retainers prior to the bending tests.

Figure 115 illustrates a typical -648 retainer and Figure 116 illustrates a typical -669 retainer following release from a bending loading mode.

Dynamic Shear

Six drops were made on the two retainer designs under simulated shear load. Each retainer design was subjected to three drops. The -648 retainer averaged release loads of 2,543 pounds, and the -669 retainer averaged release loads of 2,510 pounds. The values for the -648 were again more closely grouped. Both retainer types in this test series were loaded downward with the retainer mounted with the opening pointed upward.

Figure 117 illustrates a typical -648 retainer and Figure 118 illustrates a typical -669 retainer following release from a shear loading mode.

## DISCUSSION

Both retainers appeared to be usable for the purpose for which they were designed and superior to previous designs. However, modifications to improve the directionality should be investigated. A reasonable indicator of the directionality of the design is the ratio of the shear failure load to the tensile failure load. As the data in Table XIII show, this ratio is approximately 2.4 for both of the designs tested. However, since the radial cord fittings currently in use have a shear load capability which is about half of their tensile load ability, it would appear that the attachment should ideally approach this characteristic. Obviously, some modification to the current design would be required to achieve this objective. Also, the need and effect of the nonsymmetrical design (horseshoe shape) should be investigated.

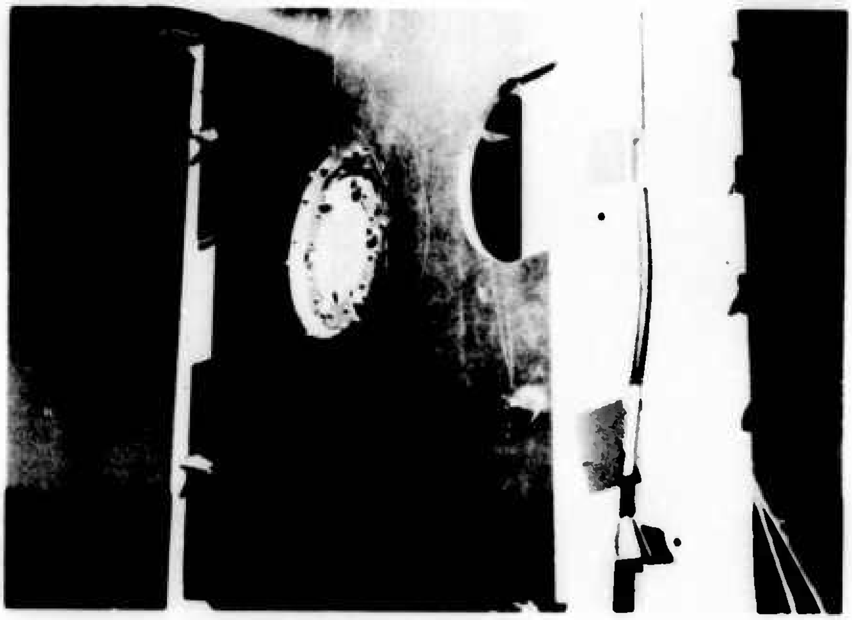

Figure 113. -648 Retainer Installed for Bending Test.

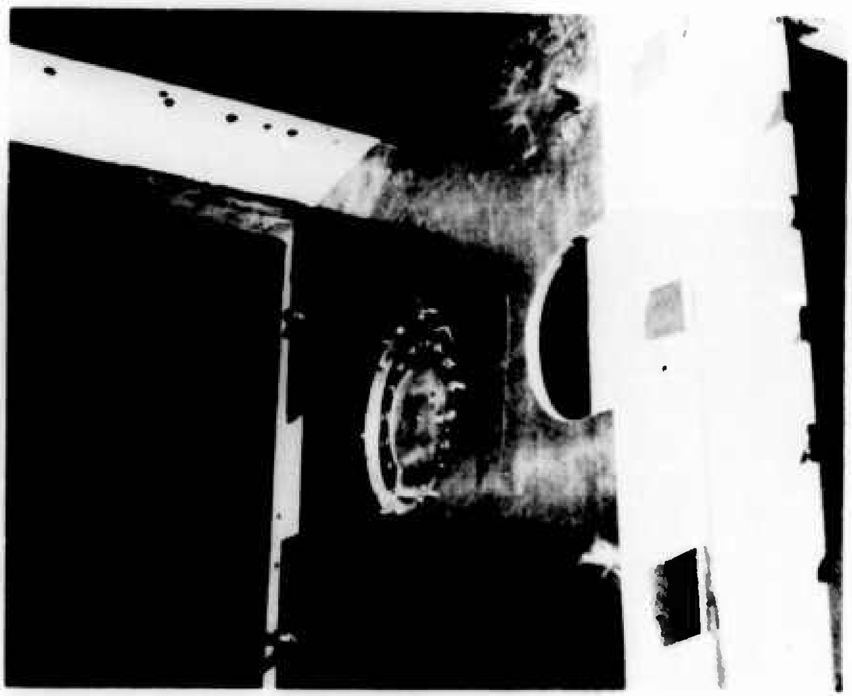

Figure 114. -669 Retainer Installed for Bending Test.

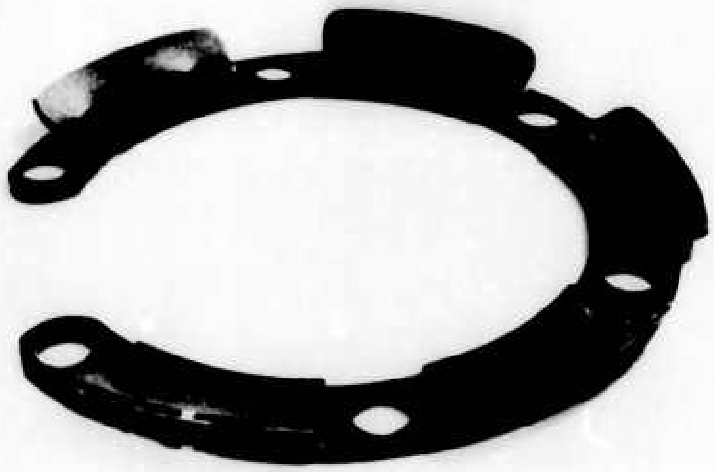

Figure 115. -648 Retainer After Bending Loading.


Figure 116. -669 Retainer After Bending Loading.

Figure 117. -648 Retainer After Shear Loading.

Figure 118. -669 Retainer After Shear Loading.

With the exception of the -669 fitting in tension, the results were very repeatable, with all data within ±5 percent of the average load. The grossly larger deviation of the -669 tensile test results suggests that a factor was present in these tests which was not present in all the remaining tests. One possibility is the orientation of the open end of the horseshoe-shaped fitting. The clock position of this end was closely controlled during the bending and shear tests because it obviously would have a first-order effect on these tests. On the surface, this orientation would appear to be unimportant during the tensile tests; it was therefore not controlled. However, it is quite possible that the loading during the tensile tests was not exactly uniaxial, especially at the onset, and, therefore, the orientation may have been a factor.

## APPENDIX VI

## STATIC TESTING OF SOCKET-HEAD FRANGIBLE SCREWS

### OBJECTIVE

The objective of this test series was to evaluate the functional characteristics of socket-head frangible screws under static tension and shear loading conditions.

### TEST ITEMS

The frangible socket-head test screws (Figure 119) were 1/4-20 aluminum screws with a thread length of 0.70 inch. The outer surface of each screw head was a smooth cylinder. A 1/8-inch hexagonal section is broached lengthwise entirely through the screw. This feature serves two functions: (1) it permits the installation and/or removal of the screw with a 1/8-inch Allen wrench, and (2) it reduces the strength of the screw to a desired value. The use of an Allen wrench prevents the application of excessive torque, thereby reducing the opportunities for possible mishandling.

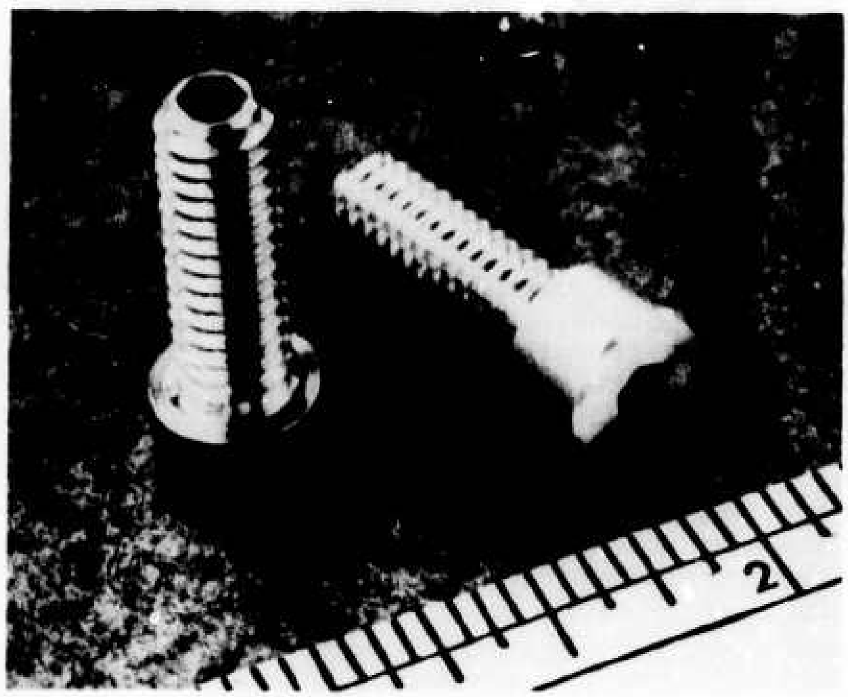


Figure 119. Allen Socket-Type Frangible Screws.

## TEST METHODOLOGY

The static tests were conducted on a tensile test machine. The frangible screws were installed in special test fixtures prior to load application.

Test loads were applied to one portion of each frangible screw for shear loading and to another portion for tensile loading. All loads were applied at a rate of 0.15 inch per minute. Figures 120 and 121 illustrate typical shear and tension test methods.

The frangible screws were subjected to a total of 26 tests: 12 in tension and 14 in shear.

As each test item was installed, it was torqued to a predetermined amount. Torque values used were: finger tight (1/2 inch-pound), 5 inch-pounds, 10 inch-pounds, 15 inch-pounds, and 20 inch-pounds.

## INSTRUMENTATION

A 0- to 1,000-pound load cell was used to measure the applied load. The data were recorded on a direct-writing oscillograph operated at a chart speed of 0.25 inch per second.

Black-and-white still photographs were taken of the test items and each typical test setup.

## RESULTS

The test results obtained were very consistent, and the amount of torque used had only a small effect on the breaking strength of the frangible screws. The average breaking load in shear was 290 pounds. The average breaking load in tension was 541 pounds. Table XIV lists the individual loads obtained for each frangible screw tested. The results for the screws which were torqued to 20 inch-pounds were not included in the above averages. It was determined that 20 inch-pounds was approaching the upper limit of the screw torsional strength. In fact, two shear specimens snapped at 19 inch-pounds, and one of the load values for the two tension specimens is questionable. The torque measurements in this test series were obtained by using a 0- to 120-inch-pound torque indicator.

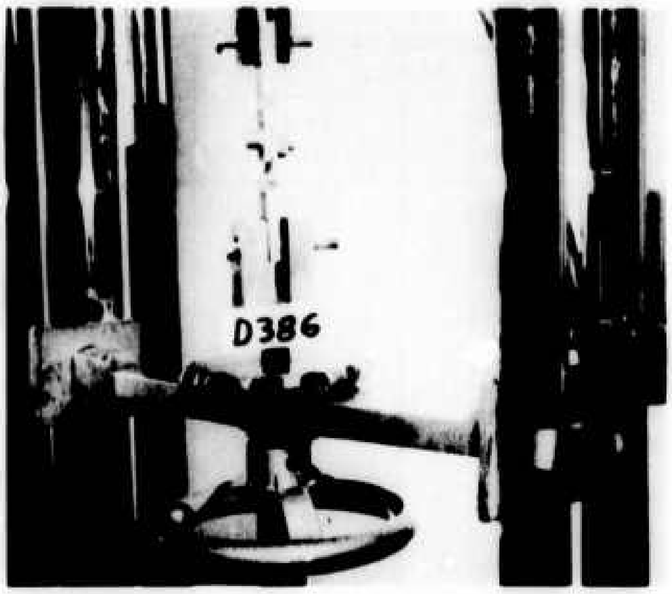


Figure 120. Static Shear Test Method Following Load Application. (Note distorted screw.)

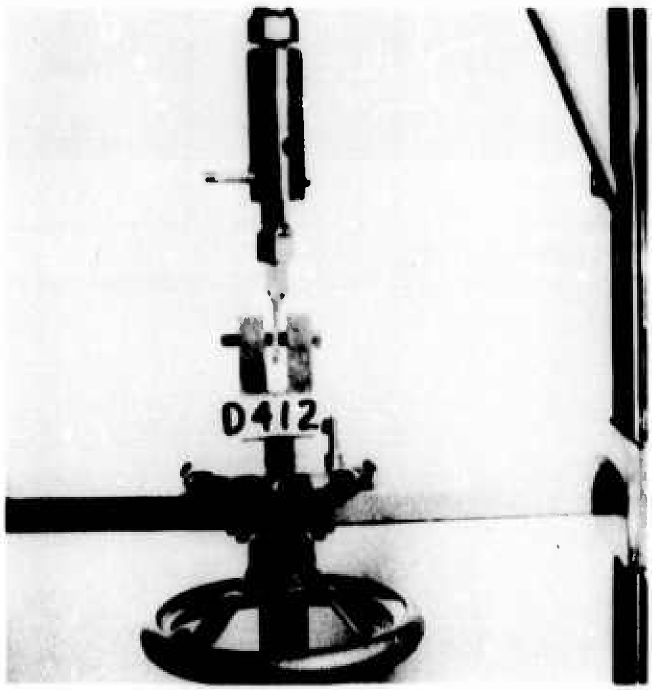


Figure 121. Static Tension Test Method Prior to Load Application.

| TABLE XIV. FRANGIBLE BOLT STATIC TEST RESULTS | | | | |
|---|---|---|---|---|
| | Shear | | Tension | |
| Applied Torque | Load (lb) | Avg. (lb) | Load (lb) | Avg. (lb) |
| Finger Tight | 332 | | 548 | |
| Finger Tight | 292 | 306 | 544 | 538 |
| Finger Tight | 294 | | 522 | |
| 5 Inch-Pounds | 332 | | 542 | |
| 5 Inch-Pounds | 280 | 307 | 544 | 543 |
| 5 Inch-Pounds | 310 | | 544 | |
| 10 Inch-Pounds | 286 | | 576 | |
| 10 Inch-Pounds | 266 | 273 | 490 | 540 |
| 10 Inch-Pounds | 268 | | 554 | |
| 15 Inch-Pounds | 266 | | 542 | |
| 15 Inch-Pounds | 268 | 271 | 526 | 543 |
| 15 Inch-Pounds | 280 | | 560 | |
| 20 Inch-Pounds | * | | 572 | 513 |
| 20 Inch-Pounds | * | | 454 | |

*Snapped at 19 inch-pounds.